Reply to Anonymous Referee #1

[Reviewer comment]
The paper describes a technical tool/technique to perform a dynamical down-scaling for the Mediterranean from a simulation with a global climate model. This is applied to a preindustrial/historical simulation and an early Holocene climate state. Whereas some aspects might be useful for other model systems as well, the focus lies on the models used at LMD: LMD atmosphere (global and regionally zoomed) and the Mediterranean setup of NEMO. The usefulness of the technique is mostly demonstrated for the early Holocene. The general approach (global AOGCM/ESM -> global AGCM driven with SST and SIC (sometimes with flux/bias corrections) -> regional ARCM -> regional Mediterranean OGCM) is fairly standard for evaluating future (and recent) climate changes for a regional ocean domain. However, this typically involves quite some handwork. The new aspect here is that there is an automatic procedure that simplifies the handling of this model chain. The authors apply this model chain also to the early Holocene, where a downscaling using a regional ARCM to my knowledge has not been attempted before. In general, the text reads well, there are, however, some problems with the figures, where a more thorough proofreading would have been useful.

[Reply]
We thank the reviewer for the careful and detailed review, and also for the numerous constructive advices. All of them were carefully implemented in the revised manuscript.

[Reviewer comment]
The nomenclature should be unified as well. As an example, in the text and the figures/captions sometimes LMD-global/regional, sometimes AGCM/ARCM (e.g. figs. 8/9 and 7) is used.

[Reply]
We agree that the initial manuscript was confusing for this aspect. In fact, we use AGCM / ARCM when we describe the general aspect of our approach, and we use LMDZ4-global / LMDZ4-regional when evoking the actual implementation of the modelling chain. We improved this aspect throughout the manuscript, including main text and figure captions.

[Reviewer comment]
From the description of the set up, it is not clear, whether the upper boundary conditions for the OGCM does include some restoring-term to a prescribed SST field in addition to the prescribed heat fluxes. This is important, as this seriously affects the interpretation of simulated SST signals. This needs to be clarified in the ms.

[Reply]
When the oceanic model NEMO is used alone, with prescribed surface fluxes, it is indispensable to implement a restoring term with a constant coefficient of 40 W/m2/K. This is a standard procedure for NEMO to prevent eventual run-away cases. In our modelling chain, the target temperature for the restoration is the surface air temperature from the regional atmospheric model.

[Reviewer comment]
The analysis of the Early Holocene simulation is a bit superficial, but this simulation acts rather as a proof of concept, so this is not a major problem.

[Reply]
Thanks, indeed we chose to publish our platform in GMD and to provide just an illustration. This is why we do not emphasize too much on this case study. Nevertheless, as also suggested by the second reviewer, we provide more information on the improvements obtained going from global to regional scales.

[Reviewer comment]
In some plots I had troubles to find the signals the authors were mentioning, some plots might even be wrong. In general, I believe that quite some revisions are necessary before the paper can reach a state sufficient for publication in GMD.

[Reply]
We believe that the revised manuscript is improved for this aspect. Many thanks to the reviewer for his/her careful reading of the manuscript We improved the plots, clarified most of them and corrected the errors raised by the reviewer.

[Reviewer comment]
Detailed comments:
Abstract Please explain to what extent this paper is useful to readers not using the LMD model system.

[Reply]

(All the lines mentioned hereafter refer to new version of the manuscript)

This manuscript is a compromise between a general concept of a sequential modelling platform from global to regional and an actual implementation with numerical tools available in IPSL. We hope that our manuscript can help to promote such an approach in dealing regional climate issues. The concept that we proposed can be easily extended to other groups with a similar background and a focus on high-resolution climate modelling

[Reviewer comment]
Line 32 'it' obviously is supposed to refer to Mediterranean basin, but this seems not to be backed by the structure of the sentence. ?seat? of civilizations.

[Reply]
We rephrased this sentence. By "seat of civilizations", we meant that the Mediterranean basin played an important historic role for human civilizations.

[Reviewer comment]
l55 'In this paper, we developed' -> Here we describe

[Reply]

We rephrased this sentence and a related sentence later in the paragraph.

[Reviewer comment]
l94 'surface fluxes and wind stresses from observations'
I am not aware of daily observational data for fluxes. You probably refer to reanalysis products. With respect to fluxes, these include the use of a model and its parametrisations. Please be correct. same in l115.

[Reply]
Yes, we agree, it is almost impossible to have good observation of fluxes at air-sea interface for daily frequency and for large extension in space. Such fluxes can only be obtained within a model (for climate simulation or meteorological analysis and re-analysis). We made the necessary modification accordingly (l100).

[Reviewer comment]
l101
'the method is not well adapted'
In fact it is, and superior to what you propose, the only problem is the computational effort for long simulations.
l120
it is possible but rather expensive. Please be more specific.

[Reply]
Yes, we agree. We recognize that our general framework of a sequential modelling chain is also a way to remediate the issue of computational resources. We made the necessary modification accordingly (l130).

[Reviewer comment]
l152 An alternative could be to rerun the coupled model with high frequency output for 30 years rather than to rerun an AGCM. please discuss.

[Reply]
Yes, we agree. The best way is to save the high-frequency 3-D outputs when running (or re-running) the paleo applications in their fully-coupled configuration. But this is not always possible or easily feasible. Our proposition of running only AGCM (the same one as in the coupled-mode application, or another independent one) is based on pragmatic consideration. Previous studies (references cited in the main manuscript), including some of our own studies, seem to validate this approach using AGCM with climate signals from SST and SIC in ocean-atmosphere coupled models.

[Reviewer comment]
l191 1.875◦x1.25◦ with 96x72 grid points (from Fig.1) does not result in a global domain! Please correct.

[Reply]
We apologize for the mistake. That should be 3.75 in longitude and 2.5 in latitude (l197).

[Reviewer comment]
l197 Please specify the frequency of the required AGCM output l201

[Reply]
We now provided these parameters: AGCM to ARCM every 2 hours; Fluxes from ARCM to ORCM every day; Atlantic buffer zone and discharges from rivers updated every month (l203).

[Reviewer comment]
L201 please specify in this section, whether any restoring of SST to prescribed values is involved. Is there any flux correction for P-E?

[Reply]
There is no flux correction in running our oceanic model NEMO: neither heat fluxes, nor water fluxes (P and E), nor wind stress. However, when the oceanic model NEMO is used alone, with prescribed surface fluxes, it is indispensable to implement a restoring term with a constant coefficient of 40 W/m2/K. This is a standard procedure for NEMO to prevent eventual run-away cases. In our modelling chain, the target temperature for the restoration is the surface air temperature from the regional atmospheric model. We made the necessary modification accordingly (l222).

[Reviewer comment]
l275 /Fig.2 caption define Mediterranean region/ Mediterranean-only. Does this mean only over the ocean?
l278 to what extent is the the response in 2m-air temperature over the ocean surprising if the SST is prescribed? Would you have gotten the same trend from the global AOGCM?

[Reply]
We apologize for the confusion. In fact, for both global average or Mediterranean average, we used surface air temperature at 2 m from land and water bodies. The Mediterranean average corresponds to the regional domain of LMDZ4-regional. We improved the caption to avoid any confusion. During the revision, we also added the global T2m from the ocean-atmosphere coupled model IPSL-CM5A, considered as a baseline, in order to appreciate the improvement that we made in our system (Figure 2 and l298).

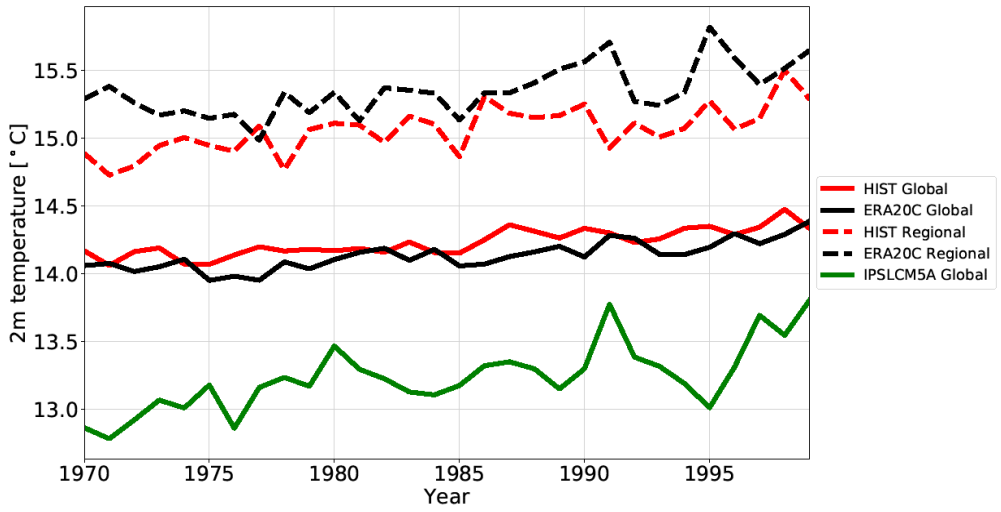

New figure 2: **Time series of annual mean surface air temperatures at 2 m in HIST (red) and ERA20C (black) and IPSLCM5A (green) for global average (solid lines) and Mediterranean-region (ocean and continent) average (dashed lines).**

[Reviewer comment]
Fig. 3b It seems that the anomalies HIST-OBS in panel b are not anomalies but the same fields as in 3a except with a different colour bar and masking over the ocean. Here you use HIST-OBs as anomalies, in Fig. 2 obviously as absolute values. Please stick to one definition. l293 BASIN MEAN 'P and E over the Med Sea ARE very close ...' please correct!

[Reply]
Thanks for your careful reading. Indeed, the initial panels in Fig. 3 were not very relevant for our purpose to illustrate the performance of our platform in simulating the rainfall. We finally changed Fig. 3 to a new illustration in the form of zonal and meridional averages (including more results). We also changed the description in the manuscript, accordingly (see section 3.3).

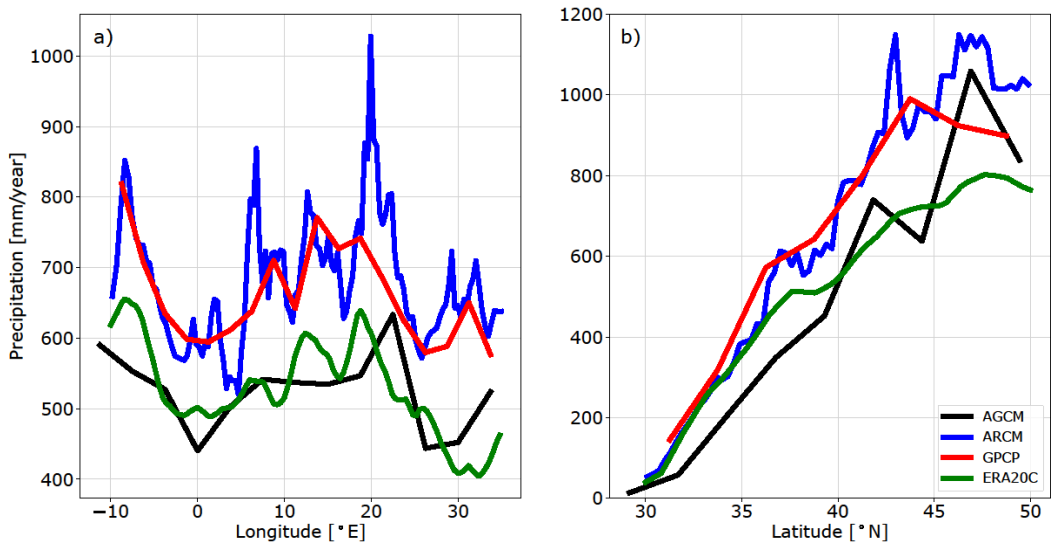

New Figure 3: Annual mean precipitation, a) meridionally averaged (30 to 50°N), b) zonally averaged (-10 to 35°E), in the historical simulations with AGCM (LMDZ-global) and ARCM (LMDZ-regional). Observation comes from GPCP (Global Precipitation Climatology Project, 1979 to 1999, blue line, ref: Adler et al., 2018). and ERA20C (green line, ref: Stickler et al., 2014).

[Reviewer comment]
Table 3 please include an extra column with the total freshwater budget of the Med (saves the reader from doing it him/herself).

[Reply]
Thanks. This is Table 1 now in the revised manuscript. We now completed it, including all terms of the fresh water budget over the Mediterranean Sea.

[Reviewer comment]
Figure 5 MLD averaged over the entire year is not very useful. Rather use annual max MLD or winter (Feb or March) MLD.This would indicate the depth of convection and thus the locations of deep water formation. This would fit to your use of this figure in l336. Table 1 bias of a simulation would be HIST-obs. From Fig. 4, I conclude that the model is too cold and salty. Here you seem to use a different sign for bias, which is confusing for the reader.

[Reply]
We apologize for the confusion. The figure caption was not appropriate. Our diagnostics were indeed the winter maximum value of the mixed layer depth. We corrected it accordingly in the revised manuscript. In Table 2 (initially labelled Table 1), we now corrected the sign of the convention.

[Reviewer comment]
l336 thicker -> deeper Please explain, why the simulated MLD is deeper in the EMed.

[Reply]

We think that a thicker MLD in the eastern basin is due to the salty conditions.

[Reviewer comment]
Fig. 6 why do we see in the ZOF deep cells both in EMed and WMed > 0.2 Sv but no corresponding water mass movement in the Gulf of Lions and the Adriatic? The deep branches seem to be < 0.1 Sv. Please explain this. Specify the longitudinal extent of the domains used to calculated the MOFs. The topography in the Adriatic MOF seems to be pretty deep, please check. You are using rows/columns in a wrong way. Where in Fig. 6 is the 3rd column from left, there are only 2 columns. (should be row from top) Please correct.

[Reply]
We firstly corrected the issue of row/column confusion and we also detailed the domain used for our calculation of the overturning stream function. The Adriatic MOF seems deeper, since our calculation includes the north of the Ionian Sea. But our MOF roughly corresponds to those of other similar studies (e.g. Somot et al. 2006 Fig. 11 and Adloff et al. 2016 Fig. 6). ZOF being integrated from the south coast to the north coast, and MOF from the west coast to the east coast for a particular semi-closed sector, we can observe different deep cells in the ZOF and MOFs. In fact, ZOF includes the circulation near the African coast which is in none of the MOFs

[Reviewer comment]
l348+ There must be more simulations than just the ones using the same ocean model setup. There are more models, e.g. the MIT model. Are there any estimates from observations? Please compare:

[Reply]
Under the Med-CORDEX framework, there are some initiatives for inter-comparison of models over the Mediterranean area. Results and publications are expected soon. In the recent literature, we also found an interesting work of Pinardi et al. (2019) who present ZOF derived from their reanalysis data (1987-2013). It seems that our ZOF in HIST is weaker than that from observation. We updated the text accordingly (l393): "The ZOF depicts in HIST simulation is consistent with the reanalysis (1987-2013) of (Pinardi et al., 2019) over the Western basin, but show a weaker Eastern deep cell compared to the reconstruction."

[Reviewer comment]
l350: "A large spread between the models for this pattern indicates that there is still a lack of modelling capacity to simulate the deep circulation of the Mediterranean Sea."
l367: "The thermohaline circulation is well captured by the oceanic model (compared to the simulations of Adloff et al., 2015 and Somot et al., 2006 for instance), which inspires confidence in our modelling platform for the investigations of past climate."
For me these two statements do not go together very well.

[Reply]
However, there is some uncertainties concerning the changes in deep circulation for the Mediterranean Sea. Our simulation is nevertheless in the range of circulation changes provided by different modeling studies. Therefore, the sensitivity for historical period is encouraging to go a step further and to investigate a larger

perturbation as the early Holocene one. To remove any confusion, we just deleted the first phrase and made some revisions for the second one (l410).

[Reviewer comment]
Figure 7 Please include labels a), b) etc. The top right panel looks like summer temperatures, but has a colour bar indicating mm/d. Inverse problem in bottom left panel. Please use same colour bar for summer and winter temps.
Compare Figs. 7 and 10! Assuming that LMD-Global is equal AGCM, why is Europe so much drier in Fig. 10 than in Fig. 7? Shouldn't these panels show the same signals? Please explain. Fig. 10 Please use the same colour bar in all panels!

[Reply]
We apologize for the wrong label in Figure 7b. We corrected it now. For the apparent difference between Fig. 7c and Figure 10c, it was mainly due to a small calendar shift, combined with a graphic problem in relation to "contour fill" with python matplotlib. The graphic was now plotted with "shading" option, which seems resolve the problem. We updated both Figs. 7 and 10.

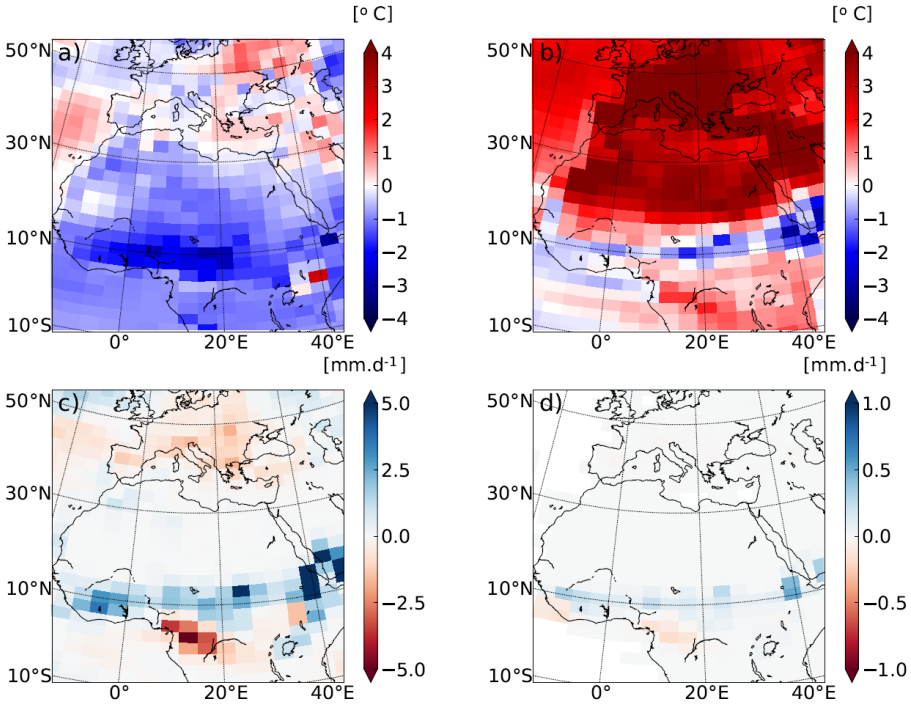

New Figure 7: Deviations between EHOL and PICTRL in the AGCM for a) winter temperatures at 2m, b) summer temperatures a, c) June to August precipitation, and d) July to September surface runoff (averaged over the entire simulation).

[Reviewer comment]
Fig. 9 Please add arrows in AGCM plots.

[Reply]
Ok, arrows added now in the revised plots.

[Reviewer comment]
Fig. 11 A mess! Split it up into 2 figs. and make sure that there is a clear relation between colour labels and displayed data panel. Why is the Nile shown in the west as well? If the Nile is flux corrected in EHOL, how can there be an anomaly of <-3000 during winter. Does this indicate a negative Nile runoff in EHOL winter? Please explain and discuss implications (deep convection in Nile plume?).

[Reply]
We apologize for any confusion in Figure 11, and we recognize that it was not an easy graphic to read and to understand. We entirely revised it and made text revisions in the "hydrological changes" subsection. We also split the graphic into two parts, as suggested. We keep only one part in the main text, and we put the second part into Supplementary materials. When we flux-corrected the river runoff there is no negative values, please see the sub section "River runoff to the Mediterranean Sea" of the section "Text S2 bias correction" in the supplementary. See also our response relative to your comment for the supplementary material.

[Reviewer comment]
l530 and Fig. 12c Please change consistent with Fig. 5!

[Reply]
Yes, we checked the consistency between Figure 12c and Figure 5. They are consistent. We added a phrase in this sense in the revised manuscript (l629).

[Reviewer comment]
l521 Please indicate in this section, how close the surface is to steady state. Please show time series of basin mean SSS during the EHOL and PICTRL simulations. Maybe in the supplement.

[Reply]
We believe that our simulation PICTRL and EHOL reached their stationary state, at least for surface properties. Figures S6 to S8 display the time series for the index of stratification, the zonal overturning stream-function and sea-surface salinity, which allow us to conclude the quasi-stationarity of the simulations. The following panel reproduces Figure S9 showing the evolution of SSS in PICTRL and EHOL.

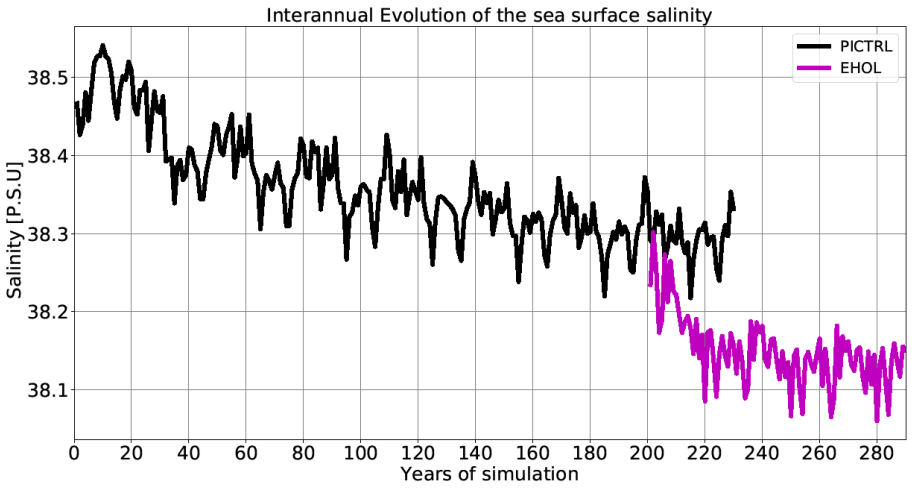

Figure S9: Interannual evolution of the sea surface salinity (SSS) for the Mediterranean Sea for the PICTRL and EHOL simulations (including the PTCRL spin-up phase).

[Reviewer comment]
Fig. 13 Please correct the caption Ionian should be Aegean.

[Reply]
Corrected

[Reviewer comment]
l530 Comparing Figs 6 and 13 it seems that the ZOF in EHOL is about as strong as in HIST. Compared to PICTRL it is indeed reduced. In the MOFs it is hard to see the reduction which is claimed to be obvious ('is followed by a general reduction in the thermohaline circulation compared to PICTRL'). Please make a careful and more detailed comparison. And include discussion of Fig. S7 which shows only a weak reduction.

[Reply]
We were limited to a visual inspection in the manuscript, since this GMD manuscript was mainly devoted to the introduction and presentation of the modelling platform. Detailed diagnostics will come in future works. Nevertheless, if we plot the difference EHOL-PICTRL and EHOL-HIST (as shown here in this review-reply text), we do clearly see the reduction of the Mediterranean overturning circulation.

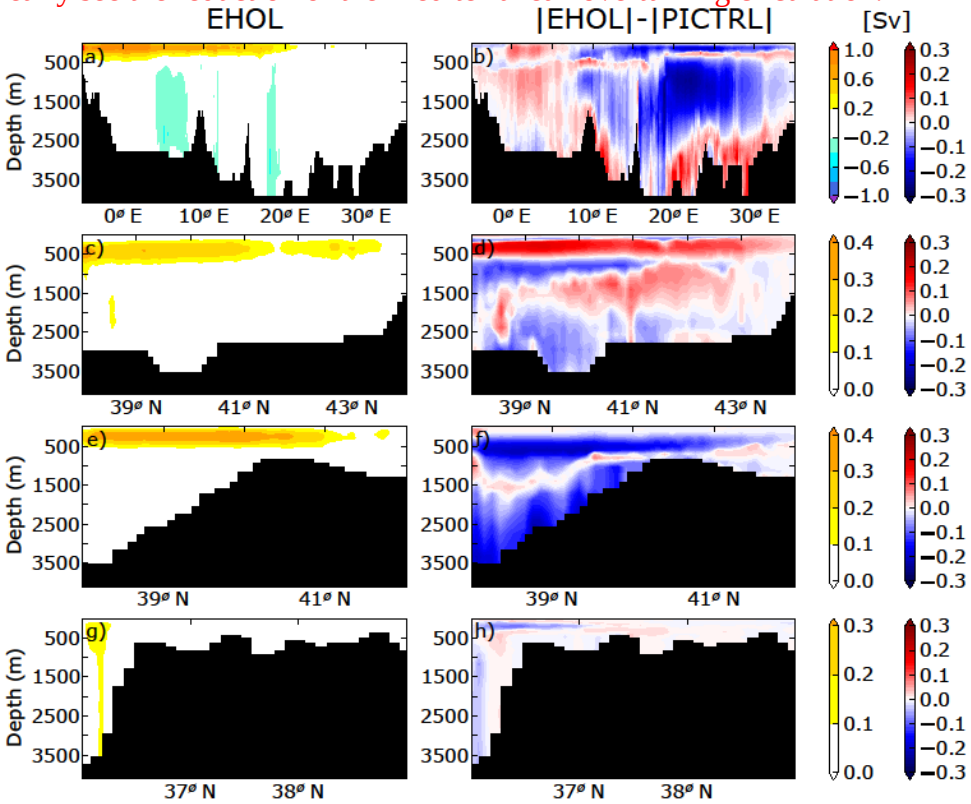

Additional figure 1: Overturning stream function. First column: EHOL, second column: EHOL minus PICTRL. From top to bottom are ZOF for the entire

Mediterranean, MOF for the Gulf of Lion, MOF for the Adriatic/Ionian Sea, and MOF for the Aegean Sea.

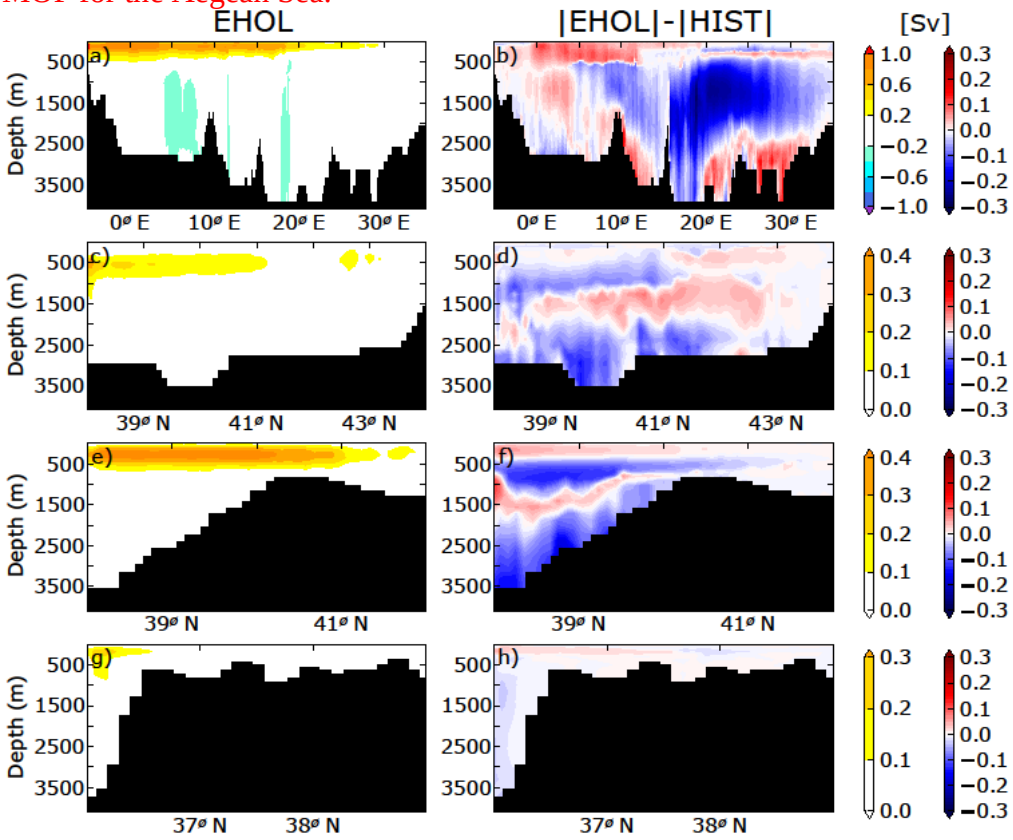

Additional figure 2: The same as in the precedent, but for EHOL-minus-HIST.

[Reviewer comment]
l579 you also used preindustrial pCO2 instead of early Holocene pCO2, which should be about 260 ppm. Please mention.

[Reply]
This comment is perfectly true. We should have changed in our case study the pCO2 value to 260 ppmv, as it is recommended by PMIP for mid-Holocene. Howerver our **goal in this paper was mainly to have a sensitivity to orbital parameters.** This is clearly stated in the supplementary information section Table S2.

[Reviewer comment]
supplement l180 'latest version' not a particular good description, especially in a few years from now. Specify the version.

[Reply]
Yes, that's right. We deleted the irrelevant words in the revised manuscript (l37 and l152).

[Reviewer comment]
supplement l260 Please mention that the method can lead to negative river runoff. Is this then effectively the same as a very strong local evaporation? Does this initiate salt driven convection at the mouth of the Nile?

[Reply]
Theoretically, a negative river runoff can happen with the water budget treatment in our modelling chain. It would be equivalent to a strong evaporation that can eventually induce a salt-driven convection. But in our case, EHOL shows a general increase of fresh water discharge in comparison to PICTRL, which prevents negative runoff from occurring.

[Reviewer comment]
supplement l299 Please compare the results shown in Fig. S2 with the bias corrected SST used to drive the global AGCM. Is there a real improvement or do you get more or less the same results? Compare with similar plots in Mikolajewicz (2011), who got almost no difference in the simulated climate signal.

[Reply]
We understand your concern and our results confirm your guess. What shown in Fig. S2 (now S3 in the revised manuscript) is the SST in the simulation EHOL, with comparison to a few reconstruction data. You asked if it is consistent with the bias-corrected SST (original SST from IPSL-CM5A, but with biases corrected) that was used to drive both AGCM and ARCM. The answer is Yes. The two fields are quite close to each other, although they do have different spatial resolutions and they differ in detailed structures. Uve Mikolajewicz, in 2011, published a similar study on the Mediterranean Sea climate during LGM (Climate of the Past, doi: 10.5194/cp-7-161-2011). He pointed out (Fig. 15, there) that the SST changes obtained in the regional ocean simulation is very close to those from the initial Earth System Model (MPI-ESM) serving as a driver with an AGCM in the intermediate step. We now cited this publication and mentioned the absence of ARCM in his approach.

Main changes

Article:

Figure 2: new curves (t2m IPSLCM5A).

Section 3.3: new descriptions of the new figure 3.

Figure 3: Annual mean precipitation, a) meridionally averaged (30 to 50°N), b) zonally averaged (-10 to 35°E), in the historical simulations.

Table 1: (former table 2) new column with the Black Sea values and the budget.

Figure 7: fix the contour/shading issues.

Figure 9: remove the difference (EHOL vs PICTRL)

Section 4.4: new description of the new figure 11

Figure 11: move the monthly Nile climatology to the supplements

Section 4.5: move the first paragraph of the conclusion to 4.5

SOM:

Addition of figure 1: climatological runoff of the Nile River

Figure S2: addition of IPSLCM5 SST (raw and corrected)

Figure S8: Interannual evolution of the sea surface salinity (EHOL and PICTRL)

Table S1: (former figure S1)

Reply to Anonymous Referee #2

[Reviewer comment]
Review of GMD-2019-196 Vadseria et al. present a sequential modelling tool to investigate (paleo-)climate change effects on Mediterranean Sea circulation. They first explain their set-up and validate for the present-day. Then an example of application, the Early Holocene, is given. It seems like a valid approach that is indeed of use for multiple (paleo-) applications. I would however suggest revision to make the paper clearer, both structurally and with respect to what exactly the added value of their sequential modelling tool is.

[Reply]
We thank the reviewer for his/her constructive comments that help to improve our work. We have implemented all of them in the revised manuscript.

[Reviewer comment]
So my main comments are:
- structurally the paper can improve to clear up some unclarities. For instance, Fig. 2 states "hist-obs" while the text only mentions "hist". I guess you mean the same simulation. Also, many citations seem to be absent from the reference list.

[Reply]
We apologize for such confusions. We made the necessary correction accordingly.

[Reviewer comment]
- content-wise, the authors seem to claim that high-resolution atmospheric forcing is needed to get correct Mediterranean Sea circulation. This needs to be better substantiated by results or discussion. For instance, can you show that your simulation yields better results than, say, a OGCM run forced directly with AGCM forcing rather than ARGCM?

[Reply]
We try to demonstrate this point by using results from literature. Lebeaupin Brossier et al. (2011) showed that high-resolution atmospheric forcing was crucial in triggering the Mediterranean deep-water formation. Increasing the spatial resolution produces finer and more intense wind stress over the north western Mediterranean area. It also slightly modified the precipitating systems representation. Li et al (2006) also showed that the 50-km resolution in the atmosphere seems a threshold to induce the right Mediterranean overturning circulation.

[Reviewer comment]
Please find more detailed comments below, followed by the GMD review criteria.
P2, line 67 "the localization of the ... of debate": true, and actually your set-up would allow for testing separate forcing sources for sapropel formation (i.e. only adding additional freshwater to a certain location, or only precipitation versus only river runoff). This would make your model setup even more useful than using it for overall Med-Sea circulation under paleo-climate-forcings.

[Reply]

(All the lines mentioned hereafter refer to new version of the manuscript)

We agree that we may perform a series of sensitivity experiments to test the response of the Mediterranean overturning circulation to different forcings. Actually, we are working on the impact of different hydrological perturbations during the deglaciation on the Mediterranean oceanic dynamics. We hope to be able to present these new results soon. However, we want to keep our initial objective for this manuscript, to build a coherent modelling chain, able to go to detailed regional oceanic features from simulations with coarser-resolution global models.

[Reviewer comment]
P3 lines 73-77. Please provide section numbers when outlining the paper.

[Reply]
Done

[Reviewer comment]
P4 lines 130-140: how about the exchange with the Black Sea? Is it common to deal with as if a river?

[Reply]
Yes, in most Mediterranean modelling studies, when the Black Sea is not explicitly simulated, it is often treated as a river. It is actually the case for all studies using the NEMO-MED platform.

[Reviewer comment]
P5 section 1.3: in my opinion this fits better in the methods section, where it can be merged with the specific LMDZ-NEMO set-up.

[Reply]
Yes, that's right. The current structure of the manuscript reflects our intellectual confrontation between generality and particularity. Our philosophy was to firstly propose a general concept, and then fill up different boxes by nominative models. So, we want to keep that structure

[Reviewer comment]
P6 lines 188-190: mention where it can derive boundary conditions from (SIC and SST).

[Reply]
Boundary conditions (in particular, SST and SIC) are derived from global coupled models, from IPSL-CM5A in our actual implementation. We detailed this description in the revised manuscript.

[Reviewer comment]
P6 lines 199-200: give a reference for ORCHIDEE and is it run at the same resolution?

[Reply]
Yes, ORCHIDEE (the land surface model) was integrated into LMDZ. The two components work at the same resolution (, reference added l208).

[Reviewer comment]
P6 line 208: which 'first dataset of river discharges' do you refer to? And does this represent the majority of discharge in the 192 ORCHIDEE river mouths?

[Reply]
We apologize for the confusion. We modified the manuscript accordingly (l216). In fact, we had the choice to use a dataset of climatological river discharges. This dataset divided the Mediterranean draining basin into 33 river mouths. However, when the ORCHIDEE model is interactively used to calculate river discharges, there are 192 river mouths. The two approaches are independent, to be actually used by optional choice.

[Reviewer comment]
P7 lines 211-213: how realistic is the assumption that water from the Black Sea is fresh? And does the Q+P-E budget over the Black Sea derive from the AGCM orARCM?

[Reply]
It is a commonly-used treatment when the Mediterranean model doesn't include the Black Sea. The fresh water assumption is entirely justified although the actual water flow from the Black Sea can be salty, since what we evaluated in terms of E, P and Runoff is indeed the fresh water budget. What is important in the model is not the water mass itself, but the salt content. We made some revisions in the new manuscript for this regard.

[Reviewer comment]
P7 line 215 / fig 1: to fit the figure with all your simulations, can you include that boundary conditions can also derive from reanalysis?

[Reply]
It is theoretically possible to include boundary conditions deduced from re-analysis. But our main goal in the platform is to use global coupled simulations as a departure to conduct the whole chain.

[Reviewer comment]
P7 line 229: maybe put the table that shows an overview of experiments in the main text.

[Reply]
We prefer to let that table describing simulation parameters in the Supplementary materials, in order to put the modelling chain and the general concept into a more prominent position.

[Reviewer comment]
P7 line 239: the cited paper is not in the reference list (as are many other citations)

[Reply]
We apologize for this issue. We now double-checked the revised manuscript.

[Reviewer comment]
P8 line 246: "for one period" rather than "for a period"

P8 Fig 1: usually u is zonal wind, v is meridional wind.
P8 line 266: write out WOA

[Reply]
We corrected the manuscript accordingly.

[Reviewer comment]
P9 Fig 2: the legend mentions “HIST-OBS”, I guess you mean experiment “HIST”? Also, why do you use ERA20C here whereas experiment “HIST” is forced with ERA-Interim?

[Reply]
Yes, we corrected the legend and the caption of the graphic. We did not use ERA-interim, since it starts from 1979 only. ERA20C starts from 1970 and is more suitable for our purpose. During the revision, we re-drew the graphic, and improved the description on how different curves were calculated. We also added the global T2m from the ocean-atmosphere coupled model IPSL-CM5A, considered as a baseline, in order to appreciate the improvement that we have in our system.

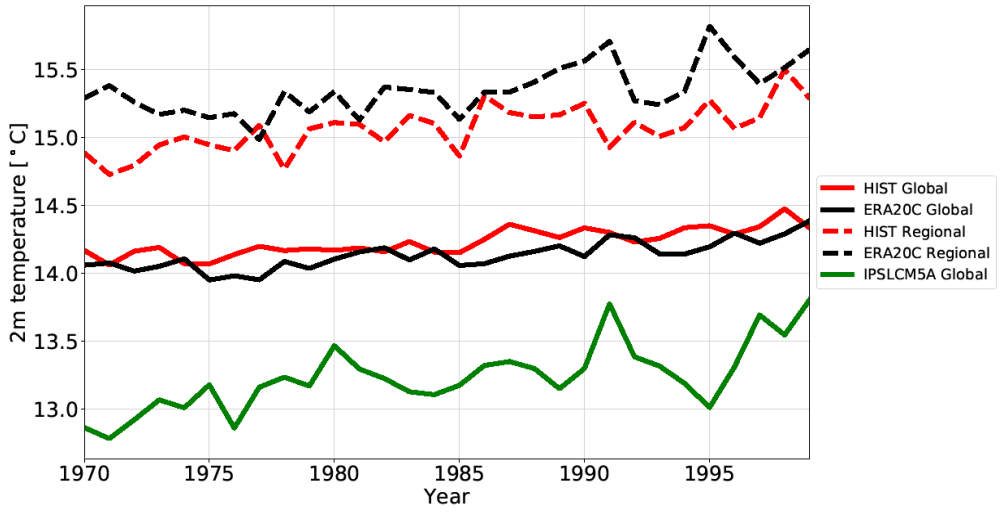

New Figure 2: Time series of annual mean surface air temperatures at 2 m in HIST (red) and ERA20C (black, ref: Stickler et al., 2014) and IPSLCM5A (green) for global average (solid lines) and Mediterranean-region (ocean and continent) average (dashed lines).

[Reviewer comment]
P10 line 291: Table 2, not 3

[Reply]
Yes, we corrected that. In the revised manuscript, it becomes Table 1 summarizing all components of the fresh water budget.

[Reviewer comment]

P10 Fig 3: again a different dataset is used (CRU), whereas Fig. 2 compares to ERA20C, and "HIST" is forced with ERA-Interim. Why would you use such a range of datasets? And why not use a reanalysis that has values over the sea? Also, looking at the color scales, it seems that the overestimation is as large as the modelled precipitation itself over land. So the relative overestimation there is near 100%?

[Reply]
Thank you for your careful reading. We finally decided to change this plot to curves showing zonal and meridional averages. We also modified the relevant text accordingly in section 3.3.

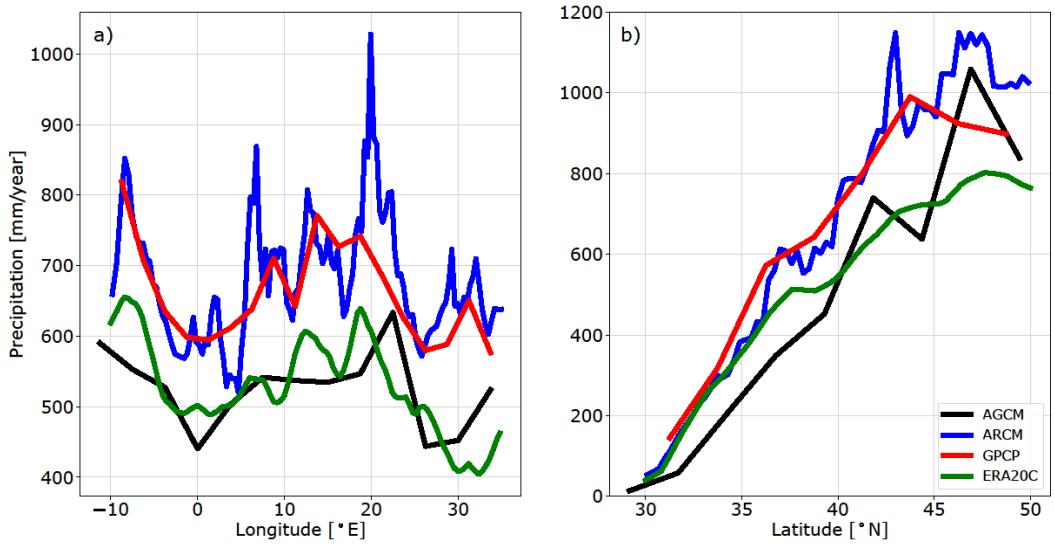

New Figure 3: Annual mean precipitation, a) meridionally averaged (30 to 50°N), b) zonally averaged (-10 to 35°E), in the historical simulations with AGCM (LMDZ-global) and ARCM (LMDZ-regional). Observation comes from GPCP (Global Precipitation Climatology Project, 1979 to 1999, blue line, ref: Adler et al., 2018). and ERA20C (green line, ref: Stickler et al., 2014).

[Reviewer comment]
P11 Fig 5: in the upper panel it seems like there is a contour overlaying the colours, are those from observations?

[Reply]
No, they are not from observations. Contours in the upper panel are the maximum of MLD (mixed-layer depth) throughout the entire simulation.

[Reviewer comment]
P12 Table 1: provide units and define IS.
P12 line 337: refers to 5b, instead of 5a?
P12 line 340: Figure 6a instead of 7a.

[Reply]
Corrected

[Reviewer comment]
P13 lines 350-352: if there is still a lack of modelling capacity to simulate Med-Sea deep circulation, how can you verify that your study is an improvement?

[Reply]
We now removed this phrase which is not very relevant for our manuscript. There are some uncertainties concerning the changes in deep circulation for the Mediterranean Sea. Our simulation is nevertheless in the range of circulation changes provided by different modeling studies. This is encouraging for us to go a step further and to investigate a larger perturbation, such as the early Holocene. In that context, we added some new text in the revised manuscript (l410):
"The simulation of the thermohaline circulation is well captured by the oceanic model and in the range of the state of the art of existing Mediterranean regional models (compared to the simulations of Adloff et al., 2015 and Somot et al., 2006 for instance). This feature inspires confidence in our modelling platform for the investigations of past climate."

[Reviewer comment]
P14 lines 362-364: Figures 2 and 4 show that your simulation results in significantly lower temperatures than observed, yet here you say they are consistent?

[Reply]
Yes, there are cold biases. We changed the corresponding text in the revised manuscript "The atmospheric simulation is acceptable compared with observations for the air temperature at 2m at both global and regional scales "(l405).

[Reviewer comment]
P14 line 365: How can a model overestimate the precipitation over the surrounding land substantially (fig 3) yet have precipitation over the sea close to observation (Table 2) and have lower river runoff than HIST or PICTL (with overestimation of precipitation over land, why is runoff not overestimated too – is this due to bias correction?)

[Reply]
Yes, it is possible for a model to have roughly right precipitation over the Sea, but too much precipitation over the surrounding land. Our model did show such a feature for its basic climatology, and for changes from PICTRL to EHOL. We now calculated all components of the fresh water budget, and discussed their variation among the three simulations (HIST, PICTRL and EHOL, section 3.3 and 4.4). Rivers discharges increase significantly from PICTL to EHOL, making the fresh water deficit to decrease.

[Reviewer comment]
P15 section 3.2: is there any additional ice sheet remaining in the early Holocene in the model?

[Reply]
No, no more remaining ice sheets for the early Holocene, in our model at least. We used a simulation in equilibrium for 9ka using the orbital forcing appropriate for this period with no more Fennoscandian and Laurentide ice sheet (FIC, LIS). Therefore, the sea level also remains unchanged (as to present day)

[Reviewer comment]
P16 line 398-399: “increased Early Holocene summer insolation” or “increased Early Holocene insolation seasonality”.
P16 line 400-404: refer to figures 7c, 7d.
P17 Figure 7: in the caption the “a” after “b) summer temperatures” should be removed

[Reply]
Corrected

[Reviewer comment]
P20 line 494-497: how does the increased Nile runoff in PICTRL (do you mean compared to observations?) compare to the overall lower runoff reported in table 2?

[Reply]
As for HIST, the river runoff for PICTRL is not calculated with the precipitation of the model. PICTRL river runoff is the same as HIST (so prescribed) but with Pre-damming Nile value.

[Reviewer comment]
P21 Fig 11: Especially in late winter and summer, runoff from the Black Sea is decreased by roughly the same order of magnitude as the increase in Nile runoff. Can you reflect on the possible role that the Black Sea runoff alone could have in sapropel formation?

[Reply]
For summer the runoff decrease of the Black Sea is quite “marginal” compared to the Nile increase (-6000/+45000 m3/s). Actually the role of the Black Sea during the Early Holocene is overall quite marginal but some studies pointed out that a freshwater release was likely throughout the deglaciation (as Chepalyga, 2007, Soulet et al., 2011, 2013) , due to the Fennoscandian Ice sheet melting, and thus affect the Aegean Sea and maybe the Eastern Basin during this period.

[Reviewer comment]
P22, lines 522-525: what do you mean by the reference for correction is the preindustrial state? How is river runoff corrected based on pre-industrial climate?

[Reply]
We choose to “correct” the Mediterranean river runoff during the Early Holocene based on the precipitation difference (EHOL – PICTRL) coming from both the ARCM and AGCM and apply it to the PICTRL river runoff (which was prescribed). The procedure of river runoff is detailed in the supplementary material (**Text S2: Bias correction**)

[Reviewer comment]
P22 lines 543-545: I would not say that your simulations show similar changes as Adloff or Bosmans. For instance Adloff (their fig 9) shows strong salinity increases around Greece, and Bosmans (their fig 11) do not show a decreased mixed layer depth in the Ionian sea.

[Reply]

The reviewer is right, we modify the text l598: “Our oceanic simulation depicts these behaviours well and is overall similar”

[Reviewer comment]
P24 Fig 13: add to caption that this can be compared to Fig 6 (PICTRL).

[Reply]
Done

[Reviewer comment]
P24 line 562: “for the first time” – this you could mention more clearly in the introduction.

[Reply]
Thanks. We added a new phrase for this regard: “To tackle this issue, a sequential architecture of a global-regional modelling platform has been developed for the first time and is described in detail in this paper” (l22).

[Reviewer comment]
P25 lines 571-579: this is not a section that should be in the Conclusions. It is more fitting for a discussion section. It also makes me wonder if there is anything known of the effect of keeping the Bosphorus exchange as it is today.

[Reply]
It is not easy to conclude on the role of the Bosphorus during the S1 period. According to the review and the synthetic work of Rohling et al., 2015, it is quite established that the Black Sea, through the Bosphorus, was not a major freshwater source during S1, so that is why we remain that parameter as it was set in HIST and PICTRL. As the reviewer suggested we moved this paragraph at the end of the 4.5 section

[Reviewer comment]
P26 References: make sure all cited literature is in the reference list.

[Reply]
We apologize for this issue concerning the cited references. We double-checked it during the revision.

Main changes

Article:

Figure 2: new curves (t2m IPSLCM5A).

Section 3.3: new descriptions of the new figure 3.

Figure 3: Annual mean precipitation, a) meridionally averaged (30 to 50°N), b) zonally averaged (-10 to 35°E), in the historical simulations.

Table 1: (former table 2) new column with the Black Sea values and the budget.

Figure 7: fix the contour/shading issues.

Figure 9: remove the difference (EHOL vs PICTRL)

Section 4.4: new description of the new figure 11

Figure 11: move the monthly Nile climatology to the supplements

Section 4.5: move the first paragraph of the conclusion to 4.5

SOM:

Addition of figure 1: climatological runoff of the Nile River

Figure S2: addition of IPSLCM5 SST (raw and corrected)

Figure S8: Interannual evolution of the sea surface salinity (EHOL and PICTRL)

Table S1: (former figure S1)

Development of a sequential tool, LMDZ-NEMO-med-V1, to conduct global to regional past climate simulation for the Mediterranean basin: An Early Holocene case study

Tristan Vadsaria[1,3], Laurent Li[2], Gilles Ramstein[1] and Jean-Claude Dutay[1]

[1]Laboratoire des Sciences du Climat~~s~~ et de l'Environnement, CEA-CNRS- Université Paris Saclay, Gif-sur-Yvette, 91191, France
[2]Laboratoire de Météorologie Dynamique, CNRS-ENS-Ecole Polytechnique- Sorbonne Université, Paris, 75005, ~~France~~France
[3]Atmosphere and Ocean Research Institute, University of Tokyo, Kashiwanoha, Chiba, Japan

Correspondence to: Tristan Vadsaria (tristan.vadsaria@lsce.ipsl.fr)

Abstract

Recently, major progress has been made in the simulation of the ocean dynamics of the Mediterranean using atmospheric and oceanic models with high spatial resolution. High resolution is essential to accurately capture the synoptic variability required to initiate intermediate and deep-water formation, the engine of the MTC (Mediterranean Thermohaline Circulation). In paleoclimate studies, one major problem with the simulation of regional climate changes is that boundary conditions are not available from observations or data reconstruction to drive high-resolution regional models. One consistent way to advance paleoclimate modelling is to use a comprehensive global to regional approach. However, this approach needs long-term integration to reach equilibrium (hundreds of years), implying enormous computational resources. To tackle this issue, a sequential architecture of a global-regional modelling platform has been developed for the first time and is described in detail in this paper. First of all, the platform is validated for the historical period. It is then used to investigate the climate and in particular, the oceanic circulation, during the Early Holocene. This period was characterised by a large reorganisation of the MTC that strongly affected oxygen supply to the intermediate and deep waters, which ultimately led to an anoxic crisis (called sapropel). Beyond the case study shown here, this platform may be applied to a large number of paleoclimate contexts from the Quaternary to the Pliocene, as long as regional tectonics remain mostly unchanged. For example, the climate responses of the Mediterranean basin during the last interglacial (LIG), the last glacial maximum (LGM) and the Late Pliocene, all present interesting scientific challenges which may be addressed using this numerical platform.

1 Framework of the study

1.1. Introduction

The Mediterranean basin is a key region for the global climate system. It ~~and~~ is considered to be a climate "hotspot" (~~(~~Giorgi, 2006)~~Giorgi, 2006)~~, due to its high sensitivity to global warming. In the past,

it has been the seat of important human civilisations, and it continues to play a very important role in international geopolitics with a dense population along its coasts. There is great diversity in the Mediterranean ecosystems, both marine and terrestrial. The Mediterranean region is also rich in paleoclimate records with a variety of proxies. Indeed, this area experienced major changes during the glacial-interglacial cycles (~~(~~Jost et al., 2005~~)~~; Ludwig et al., 2018; Ramstein et al., 2007). Another long-term cycle of changes due to high-frequency precession which drastically modified the hydrological patterns of this area (monsoon, sapropels) is also superimposed.

Due to the peculiarities of both the atmospheric and oceanic circulation in the region, high-quality climate modelling of the Mediterranean region needs to have high spatial resolution (~~(~~Li et al., 2006~~)~~). Indeed, the presence of strong gusts of wind in winter are essential to trigger oceanic convection and these can only be correctly represented in high-resolution models. Limited area models (LAM), or regional climate models (RCM), present some advantages in this regard, since they generally demand less computing resources, allowing them to be run at high spatial resolution for a given region. However, their usefulness for paleoclimate purposes is limited because of the lack of adequate lateral boundary conditions to drive the RCMs. The main reason why few comprehensive modelling exercises to explain paleoclimate changes around the Mediterranean have been performed is that the level of computing resources required for high resolution and long simulations is inaccessible. This is especially true in the case of the Mediterranean Thermohaline Circulation (MTC), which has significantly changed in the past, at both centennial and millennial scales.

~~In this paper,~~ Here we describe ~~we developed~~ a modelling suite to define high-resolution atmospheric conditions over the Mediterranean basin from global ESM (Earth System Model) paleoclimate simulations. ~~In a second step, we used t~~This atmospheric forcing can then be used to run a highly resolved ocean model (NEMOMED8 1/8°) to accurately simulate ocean dynamics. This tool allows us to achieve a high spatial resolution and equilibrated simulations with a run time of 100 years. The objective of this study is to develop a modelling platform sufficiently comprehensive to conduct paleoclimate studies of the Mediterranean basin. The potential of this platform is illustrated by investigating climate situations from the present period and from the Early Holocene that is supposed to generate~~d~~ sapropel events.

The sapropel events provide excellent case studies on the impact of global changes on the Mediterranean basin. These periodic events are related to a long period of anoxia of the deep and bottom waters triggered by an enhancement of the African monsoon caused by periodicities of the orbital precession. However, the localisation of the forcing source caused by orbital variability is still a subject of debate. This is especially true for the last sapropel, denoted S1, which occurred during the early Holocene (between 10500 and 6800 ka BP) (~~(~~De Lange et al., 2008~~)~~). Reproducing past climate variations over

the Mediterranean basin, including the sapropel events, is therefore a challenge for the modelling community.

The paper is organised as follows: In the first ~~part~~section, we briefly review the different approaches used to simulate the Mediterranean climate and sea conditions, and we also present the concept of the sequential procedure that we propose. Section 2~~In a second part, we~~ presents in detail the model architecture we developed. Finally, we present applications with simulations of the historical period (1970-1999) in Section 3 and the Early Holocene (around 9.5 ka) in Section 4.

1.2. Overview of current Mediterranean Sea modelling

The Mediterranean Sea, due to its limited size and its semi-enclosed configuration, has a faster equilibrium response (10^2~~100~~ years) than the global ocean (10^3~~1000~~ years). Because of this semi-enclosed configuration, there are a few requirements that modelling of the Mediterranean Sea needs to satisfy so that its evolution can be properly represented. High resolution in both the atmospheric forcing and the oceanic configuration is necessary to correctly simulate the convection areas and the associated thermohaline circulation ~~(~~(Lebeaupin Brossier et al., 2011; Li et al., 2006)~~Li et al. 2006; Lebeaupin Brossier, et al., 2011)~~. Depending on the mechanism studied, the resolution of the ocean model used by the research community ranges from ¼° (e.g. for paleo-climatic simulation), to 1/75° (for hourly description of the mixed layer, tide-based investigation). The results for oceanic convection are highly dependent on the flux of heat~~, and~~ flux of water~~water,~~ and the wind stress at the air-sea interface~~,~~ especially the seasonal variability and intensity. There are many modelling configurations in the scientific literature making it impossible to provide an exhaustive review of all of them. We can summarise them by presenting the different approaches used to drive the Mediterranean oceanic model, along with their advantages and drawbacks. We underline our new, coherent method, which captures the changes in ocean dynamics in the Mediterranean basin derived from global paleoclimate simulations.

Observations and reanalysis

The most common way to simulate the general circulation of the Mediterranean Sea is to run a regional oceanic general circulation model forced by surface fluxes and wind stresses derived from observations and reanalyses. In this way, an oceanic model can be driven by realistic fluxes. In most cases, ~~it~~ this implies an observation-based reconstruction ~~from observed~~of relevant variables ~~(temperature and win for instance) combined~~ with~~-~~ a spatial atmospheric resolution of less than 50 km and a daily temporal resolution, at a minimum, in order to simulate the formation of dense water ~~(~~(Artale, 2002)~~Artale, 2002)~~. This approach is adapted to simulate the present-day Mediterranean Sea and to explore the complexity of its sub-basin circulation and water mass formation ~~(~~(Millot and Taupier-Letage, 2005)~~)~~. However,

~~this method~~it is not well adapted to the study of past and future climate, partly due to the excessive computing resources needed.

Atmospheric model

A second method consists of forcing a regional oceanic model with simulations from an atmospheric model, AGCM (Atmospheric Global Climate Model) or ARCM (Atmospheric Regional Climate Model). Since the AGCM resolution (typically 100 to 300 km horizontally) is coarse, statistical and/or dynamical downscaling is usually needed, especially for wind-stress so that the ORCM (Ocean Regional Circulation Model) can be correctly forced (Béranger et al., 2010)~~(Béranger et al., 2010)~~. Currently, dynamical downscaling with ARCM is the preferred option because it generally improves simulations of the climate in the Mediterranean region and especially of the hydrological cycle (Li et al., 2012)~~(Li et al., 2012)~~.

This configuration is broadly used to assess anthropogenic climate changes (Adloff et al., 2015; Macias et al., 2015; Somot et al., 2006)~~(Adloff et al., 2015; Macias et al., 2015; Somot et al., 2006)~~. In these studies, the Mediterranean Sea simulations are generally driven by the outputs of an ARCM, which is, in turn, driven by the GCM or observation-based reanalysis. It should be noted that biases in oceanic variables can be reduced through constant flux correction (Somot et al., 2006)~~(Somot et al., 2006)~~. This configuration is suitable for high-resolution simulation of the past Mediterranean Sea (~~(~~Mikolajewicz, 2011~~)~~ for the LGM; ~~(~~Adloff et al., 2011~~)~~ ~~Adloff et al., 2011~~ for the Early Holocene among others).

Regional coupled model

Although the majority of the Mediterranean Sea models are ocean-alone models, some of them use a coupled configuration between the Mediterranean Sea and the atmosphere. Such a coupled configuration generally improves the simulation of the air-sea fluxes, including their annual cycle ~~(~~(de Zolt et al., 2003), but may show climate drifts in key parameters such as the SST. Regional coupled models are now emerging as a tool in Mediterranean climate modelling (Artale et al., 2010; Dell'Aquila et al., 2012; ~~(~~Drobinski et al., 2012; ~~(~~Sevault et al., 2014; Somot et al., 2008). However, this full-coupling configuration is currently not possible for high-resolution paleoclimate issues requiring long simulation for ~~a~~ hundreds or ~~a~~ thousands of years.

Importance of boundary conditions

The boundary conditions applied to the Mediterranean Sea domain, in particular, the exchanges of water, salt and heat with the Atlantic Ocean through the Strait of Gibraltar modulate significantly the Mediterranean circulation (Adloff et al., 2015)~~(Adloff et al., 2015)~~. This is especially true at the millennial scale where deglaciation episodes and fluctuations of the AMOC (Atlantic Meridional Overturning Circulation) and the Mediterranean Sea affect each other (~~(~~Swingedouw et al., 2019). The

level of discharge from the main rivers is also crucial as is illustrated by the sapropel episodes, where an increase in freshwater input drastically slowed down the MTC. Most of current models impose prescribed (observed when possible) conditions in the near Atlantic zone, including temperature and salinity. The same methodology can be used to prescribe river discharges. However, it must be acknowledged that determining inputs from rivers into the Mediterranean Sea, either of water or other materials, still presents serious challenges for modelling.

1.3. Concepts for a sequential procedure to perform global-to-regional modelling

In this paper, ~~we propose~~ a new architecture for high-resolution modelling of the climate of the Mediterranean basin for past, present and future ~~climates~~conditions is proposed. This architecture is based on a method as much consistency ~~between~~ among the models as possible and high congruency with data.

Step 1: Global climate

Our goal is to simulate different climate conditions for the Mediterranean basin. The first step of any relevant procedure should be to simulate the global climate conditions from which ~~we drive~~ the simulation of the regional climate is driven. These may be already available in simulations from previous PMIP exercises for various periods (e.g. mid-Holocene, Last Glacial Maximum, Last Interglacial and mid-Pliocene) as well as for different sapropel events and interglacials (e.g. MIS11, MIS13 and MIS19). However, this is not always possible due to the large volume of high-frequency 3-D atmospheric circulation variables involved. An alternative approach, used in some regional climate simulations (~~(~~Chen et al., 2011; ~~(~~Goubanova and Li, 2007; ~~(~~Krinner et al., 2014), consists of using an AGCM (either an independent one or the same one used for the global climate simulation) run with appropriate values for global Sea Surface Temperature (SST) and Sea Ice cover (SIC), derived from PMIP global simulations. SST is crucial to determine atmospheric features and responses, while SIC plays a key role in determining the global albedo. Monthly SST and SIC are necessary and sufficient to drive an AGCM. They can be acquired from global climate simulations or through a bias-correction procedure.

Step 2: Regional climate

After running an AGCM, regional climate can be now reproduced with an ARCM nested into the high-frequency outputs from the AGCM. Of course, the ARCM can be run in parallel to the AGCM, or with a small time delay. Thus, we avoid a large accumulation of intermediate information between the AGCM and the ARCM. In our study, we assume that there would be no feedback from the regional scale to the global scale, so only a “one-way” transfer of information (from global to regional) is considered. In our case, the ARCM is a strongly zoomed-in version of the AGCM and is also driven by monthly SST and SIC values, as used for AGCM. The higher resolution of the ARCM allows the synoptic variability and

seasonality of the Mediterranean region to be depicted so that a realistic wind pattern and hydrological cycle may be reproduced. This approach provides a general framework for use in many different paleoclimate periods from the Pliocene to the Pleistocene, as long as the basin tectonics remain unchanged.

Step 3: Mediterranean Sea Circulation

Daily air-sea fluxes and wind stress provided by the ARCM are used as surface boundary conditions to drive the ORCM to investigate the oceanic dynamics of the Mediterranean. It is reasonable to assume that the boundary conditions of these air-sea fluxes represent the long-term trends of the oceanic dynamics. Rivers may be considered interactive or not depending on the investigative objectives: runoff can be prescribed from climatology or obtained from the hydrological component of the surface model. Again, we highlight that our architecture does not include any feedback, between either the regional ocean and the regional atmosphere, or the regional ocean and the global ocean. This configuration means that we can avoid dealing with certain issues, for example, the influence of the Mediterranean Outflow Water on the North Atlantic Ocean but is well adapted to provide consistent river runoff associated with changes in continental precipitation.

2 Model architecture

~~We used~~ A~~a~~n ensemble of modelling tools that includes two atmospheric models and a regional oceanic model is used. Figure 1 summarises the configuration and shows the experimental flowchart.

2.1. The atmospheric models (AGCM and ARCM)

LMDZ4 (~~(~~Hourdin et al., 2006~~)~~; ~~(~~Li, 1999)~~)~~ is the atmospheric general circulation model developed and maintained by IPSL (Institut Pierre Simon Laplace). It has been widely used in previous phases of CMIP and PMIP projects. The resolution of the model is variable. Its global version used here (referred to as LMDZ4-global) is ~~1~~3.~~8~~75° in longitude and ~~1~~2.~~2~~5° in latitude with 19 layers in the vertical. It provides the boundary conditions to drive LMDZ4-regional. LMDZ4-regional ~~(~~(Li et al., 2012)~~)~~ is a regionally-oriented version of LMDZ4 with the same physics and same vertical discretisation, dedicated to the Mediterranean region. The zoomed-in model covers an effective domain of 13°W to 43°E and 24°N to 56°N with a horizontal resolution of about 30 km inside the zoom. The rest of the globe outside this domain is considered to be the buffer-zone for LMDZ4-regional where a relaxation operation is performed to nudge the model with variables from the AGCM, at a ~~3~~2-hour frequency. The resolution of LMDZ4-regional decreases rapidly outside its effective domain. In both LMDZ4-global and LMDZ4-regional, land-surface processes, including the hydrological cycle, are taken into account through a full coupling with the surface model, ORCHIDEE (Krinner et al., 2005).

2.2 The regional oceanic model (ORCM)

NEMOMED8 (~~(~~Beuvier et al., 2010~~)~~; ~~(~~Herrmann et al., 2010) is the regional Mediterranean configuration of the NEMO oceanic modelling platform (Madec, 2008)~~(Madec, 2008)~~. The horizontal domain includes the Mediterranean Sea and the nearby Atlantic Ocean which serves as a buffer zone (from 11°W to 7.5°W). The horizontal resolution is 1/8° in longitude and 1/8°cosφ in latitude, i.e. 9km to 12km from the north to the south. The model has 43 layers of inhomogeneous thickness (from 7 m at the surface to 200 m in the depths) in the vertical. River discharges are accounted for as freshwater fluxes in the grids corresponding to the river mouths. A ~~first~~ dataset of climatological river discharges is proposed by default to cover the entire Mediterranean draining basin with~~represents~~ 33 river mouths. It is of course switched off when rivers are interactive in the platform. ~~throughout the Mediterranean region. It contains monthly mean climatological values of runoff.~~ The ~~I~~interactive calculation~~s~~ of freshwater discharges from rivers by the land-surface model, ORCHIDEE, include~~s~~ 192 river mouths ~~for~~ to cover the Mediterranean draining basin. The Black Sea, not included in NEMOMED8, counts as a river dumping freshwater into the Aegean. The deposit rate is calculated based on total runoff into the Black Sea, plus the net budget of precipitation (P) minus evaporation (E) over the Black Sea.

When the oceanic model NEMO is used alone, with prescribed surface fluxes, it is indispensable to implement a restoring term with a constant coefficient of 40 W~~/~~/m^{-2}~~.2/~~K^{-1}. This is a standard procedure for NEMO to prevent eventual run-away cases. In our modelling chain, the target temperature for the restoration is the surface air temperature from the regional atmospheric model LMDZ4-regional.

2.3 Modelling Sequence

As shown in Fig. 1, the first step in our modelling chain is to obtain SST and SIC values from an Earth System Model simulation able to reproduce global climate (for the past, present or future). We can reasonably hypothesise that major global climate information can transit from global SST and SIC. This hypothesis was deemed legitimate for climate downscaling purposes for Antarctic and Africa, in Krinner et al. (2014) and ~~(~~Hernández-Díaz et al. (2017) respectively. In the present work we use IPSL-CM5A (Dufresne et al., 2013)~~(Dufresne et al., 2013)~~ to extract relevant SST and SIC values to drive the AGCM (LMDZ4-global) and the ARCM (LMDZ4-regional). The next step is to run the two atmospheric models, LMDZ4-global and LMDZ4-regional, in the usual way as proposed by the AMIP community. This is the most expensive step, as atmospheric models are the most demanding in terms of computing resources. Fortunately, it is not necessary to run them for a long time as the atmosphere reaches equilibrium quickly. We ~~applied 30~~applied 30 years of simulation to both models. We consider this duration to be long enough to depict climate variability for the simulation of past events. The AGCM nudges the ARCM in the conventional way of one-way nesting for temperature, humidity, meridional and zonal wind every two hours. The nudging is done using an exponential relaxation procedure with a

timescale of half an hour outside the zoom and 10 days inside the zoom. Table S21 in the SOM summarises the forcings used, especially the orbital forcing and atmospheric CO_2.

The necessary variables (surface air temperature, wind stress, P-E over the sea, heat fluxes) are provided by ARCM to NEMOMED8 (ORCM) at daily frequency. The salinity and temperature conditions are provided in three dimensions in the Atlantic buffer zone, near the Gibraltar Strait, and updated every month. River runoff, updated every month, depends on the configuration used (prescribed climatological rivers, or interactive rivers). Table S32 in SOM details these boundary conditions.

It is worthy to mention the work of Mikolajewicz (2011) who used a similar modelling chain (from a coarse-resolution earth system model to a high-resolution regional oceanic model) to simulate the Mediterranean Sea climate during the last glacial maximum. However, Mikolajewicz (2011) used only an AGCM (ECHAM5) as the intermediate step. In our case, we found that the use of ARCM was indispensable to produce high-quality forcing to ~~well~~correctly simulate the oceanic convection in NEMOMED8.

2.4 Bias correction

The sequential modelling chain, despite the lack of interactivity and feedback at interfaces, allows for error removal and bias correction at each step of the methodology. This adjustment is sometimes crucial, especially when model outputs need to be of very high quality to be incorporated into impact studies. This concept was further described in (~~K~~Krinner et al.~~,~~ (2019), as illustrated in Fig. 16 of their paper. Therefore, to enhance our confidence in the realism of the simulation results, bias-correction may be introduced when necessary. The correction method used in the present work generally follows the conventional procedure, which is based on the difference between the model outputs for present day simulations and actual observations. Biases corrected in this way, theoretically only valid for the historical simulation (named HIST hereafter), are assumed to remain unchanged for past and future simulation scenarios. However, the transferability between past and future periods is questionable. There is no guarantee that the model error for ~~a~~ one period is the same for other periods, even though the model physics may be the same. In addition, paleodata are often rare and incomplete, and so, are unsuitable for evaluation and correction of model errors. The most reliable basis is that established for the present day. The reader can find a full description of the bias corrections and their eventual use in our applications in the supplementary online material, “Text S2: Bias correction”.

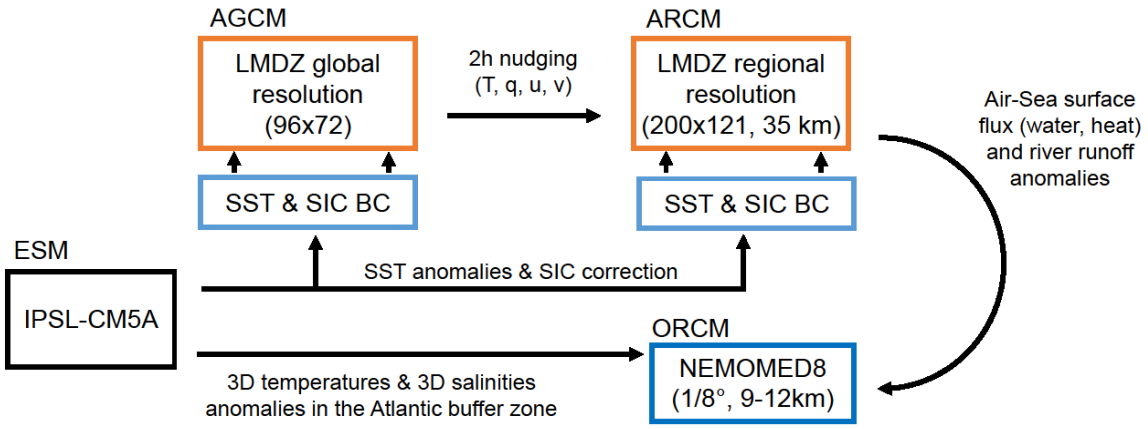

Figure 1: Flowchart of the modelling chain including the four main components~~:~~ generally represented by ESM, AGCM, ARCM and ORCM, respectively, and actually implemented in our platform by IPSL-CM5A, LMDZ-global, LMDZ-regional and NEMOMED8. BC: boundary condition, u: ~~meridional~~ zonal wind, v: ~~zonal~~ meridional wind, q: specific humidity, T: temperature, S: salinity, SST: sea surface temperature, ~~SSS~~SIC: sea ~~surface salinities~~ ice concentration.

3 Validation of the modelling chain for present-day climate 1970-1999

In this section, ~~we evaluate~~ the capacity of the model to reproduce the climate of the recent past is evaluated, in particular, its ability to simulate sea surface characteristics as well as the Mixed Layer Depth (MLD) and oceanic convection patterns as these are key elements to reproduce the evolution of the Mediterranean Sea in past climate conditions.

3. 1 Experimental design

For the HIST experiment, ~~we used~~ SST and SIC observations (~~source:~~ ERA-Interim,~~(~~ Dee et al., 2011~~)~~) are used to force the AGCM. River runoff is from the climatology of Ludwig et al., (2009). Monthly mean climatological sea temperatures and salinities (~~from WOA~~World Ocean Atlas database from ~~(~~Locarnini et al., 2013~~), (~~Zweng et al., 2013~~)~~) are used for the Atlantic boundary zone. HIST atmospheric simulations for both global and regional simulations have a duration of 30 years. The length of the HIST oceanic simulation is also 30 years, but obtained after a 150-year spin-up. The forcings for each experiment are detailed in "Tables S2~~1~~" and ~~Table~~ S3~~2~~" in the supplementary online material. Spin-up phases for each simulation are also shown from "Figure S4~~4~~" to "Figure S8~~7~~" for the overturning stream function and the index of stratification.

3.2 Evolution of temperatures

Figure 2 depicts the temporal evolution, between 1970 and 1999, of annual mean surface air temperatures at two metres in the atmospheric simulations (global and regional) compared to observations for the whole globe and over the Mediterranean region. The two models reproduce a range of temperatures similar to the observations, with the Mediterranean temperatures warmer than the global temperatures. The global simulation, after SST bias correction, ranged with the observation, compared to IPSLCM5A (Figure 2). The regional model reproduces the warming trend and aspects of the interannual variability which are quite close to observations.

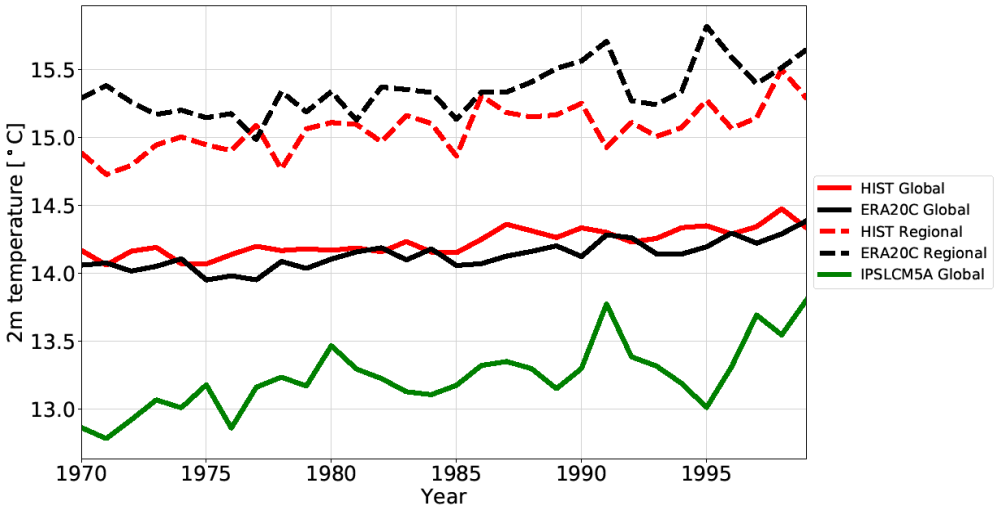

Figure 2: Time series of annual mean surface air temperatures at 2 m in HIST (red) and ERA20C (black, ref: (Stickler et al., 2014)) and IPSLCM5A (green) for global average (solid lines) and Mediterranean-only region (ocean and continent) average (dashed lines).

3.3 Precipitation and freshwater budget

Figure 3 a and b shows the average annual precipitation for 1970-1999 in HIST over the Mediterranean region and the differences with observations. The main features of the distribution of precipitation over the Mediterranean region are simulated, in particular the distinct contrast between the very low precipitation in the southern region and higher precipitation in the north. The ARCM tends to generates higher precipitation than the AGCM due to the resolution refinement. Compared to observation, AGCM results range withis closer to ERA20C (Stickler et al., 2014) precipitation data, whereas ARCM range withis closer to GPCP data (Adler et al., 2018). However, the regional model still overestimates the amount of precipitation, especially at 42°N, from 45° to 50° N, at 8°E and 20°E. It corresponds to most of Europe, especially over the Alps, the Pyrenees, the Balkans and other mountainous regions. However,

~~the regional model tends to overestimate precipitation over most of Europe, especially over the Alps, the Pyrenees, the Balkans and other mountainous regions.~~ The freshwater budget over the Mediterranean Sea from observations ~~(from~~ a synthesis ~~study by~~from Sanchez-Gomez et al., 2011 and from other sources) and in the various simulations conducted in this study are summed up in ~~t~~Table ~~3~~1. ~~(from a synthesis study by Sanchez-Gomez et al., 2011).~~ The simulated continental precipitation is overestimated, but both the precipitation and evaporation over the Mediterranean Sea in HIST is very close to the observations. Two other simulations, PICTRL and EHOL, are those designed in Section 4 to investigate the Early Holocene climate.

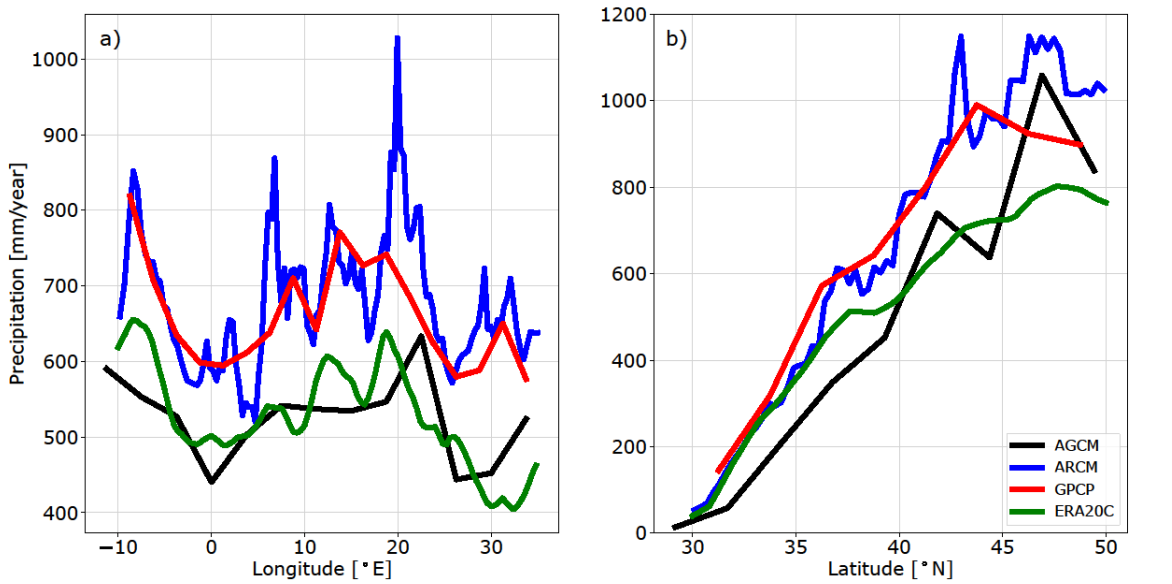

Figure 3: ~~**Annual mean precipitation (mm/day) in HIST (panel a). Deviation of HIST simulation from observation-based CRU data (HIST-CRU, panel b, over land only, averaged over the entire simulation).**~~ **Annual mean precipitation, a) meridionally averaged (30 to 50°N), b) zonally averaged (-10 to 35°E), in the historical simulations with ~~(~~AGCM (LMDZ-global)~~,~~ and ARCM (LMDZ-regional). Observation comes from GPCP (Global Precipitation Climatology Project, 1979 to 1999, blue line, ref: ~~(~~Adler et al., 2018). and ERA20C (green line, ref: Stickler et al., 2014).**

Dataset or experiment	E	P	R	B	E – P – R - B
OBS	1096-1136	256-595	102-142	73-121	238-705
HIST	1106	443	74	104	485
PICTRL	1031	451	98	104	378

EHOL	1094	460	225	104	305

Table 1: The Mediterranean Sea freshwater budget, expressed as mm.year^{-1} for the whole water area (about 2.5 million of km^2). E, evaporation, P, precipitation, R, river runoff, B, Black Sea discharge into the Mediterranean Sea. OBS is a summary from Sanchez-Gomez et al., (2011) for P, E and P-E, from Ludwig et al., (2009) for R, from Lacombe and Tchernia, (1972), Stanev et al., (2000) and Kourafalou and Barbopoulos, (2003) for B. River discharges in HIST are from the climatology of Ludwig et al., (2009). PICTRL uses the Nile of its pre-industrial (pre-damming) value, 2930 m^3.s^{-1}, annually (Rivdis database, Vorosmarty et al., 1998). River discharges in EHOL are deduced from the difference between EHOL and PICTRL.

3.4 Mediterranean Sea surface characteristics

Figure 4 displays the temperatures and salinities of the Mediterranean Sea simulated in HIST and the deviations from observations. The model is able to capture the main characteristics of the pronounced west-east gradient of SSS in the Mediterranean Sea (Figure 4 a). Values are within the range of observations (mean bias = -0.32 PSU, error = 0.37 PSU, table 42). In the simulation, the Aegean Sea is not salty enough (about -1.5 PSU) and the Adriatic/Ionian Sea is too salty (+1 PSU).

The model reproduced the northwest to southeast temperature gradient, as shown in Figure 4b. However, the model shows a general cold bias (from -0.5 to -1.5 °C) over the entire Mediterranean (Figure 4e), due to the cold bias already observed for the air temperature at 2m in the regional atmospheric forcing (cf Figure 2).

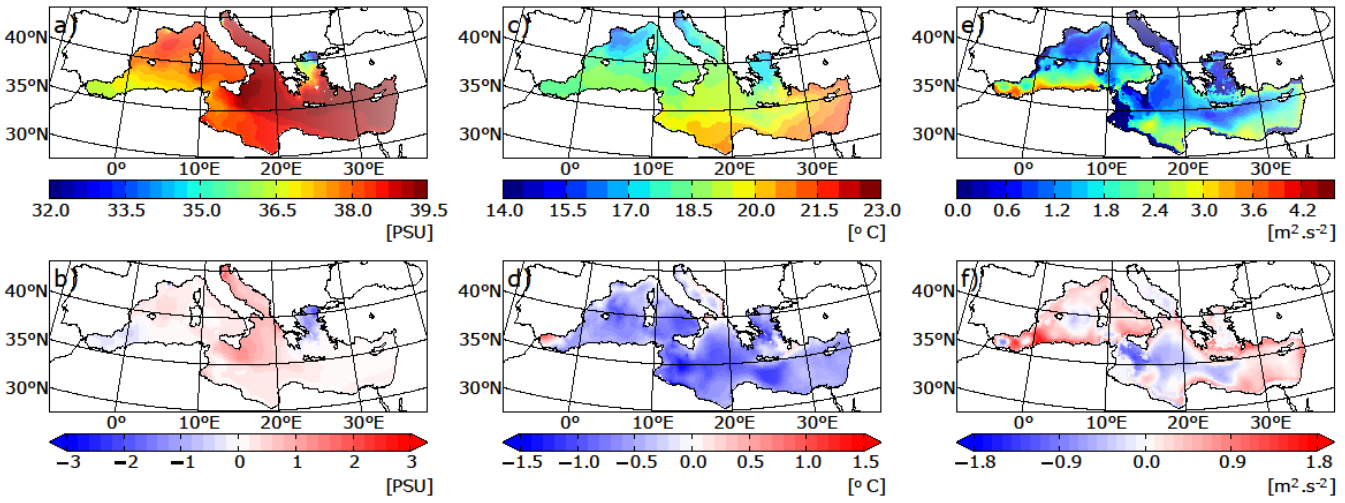

Figure 4: Annual mean sea-surface salinity (left panels, SSS in PSU), sea-surface temperature (middle panels, SST in °C) and index of water column stratification (right panels, winter IS in

$m^2.s^{-2}$ ~~m^2/s^2~~) simulated in HIST (top panels) and the HIST deviation (model – obs) from the observation-based MEDATLAS data (averaged over the entire simulation).

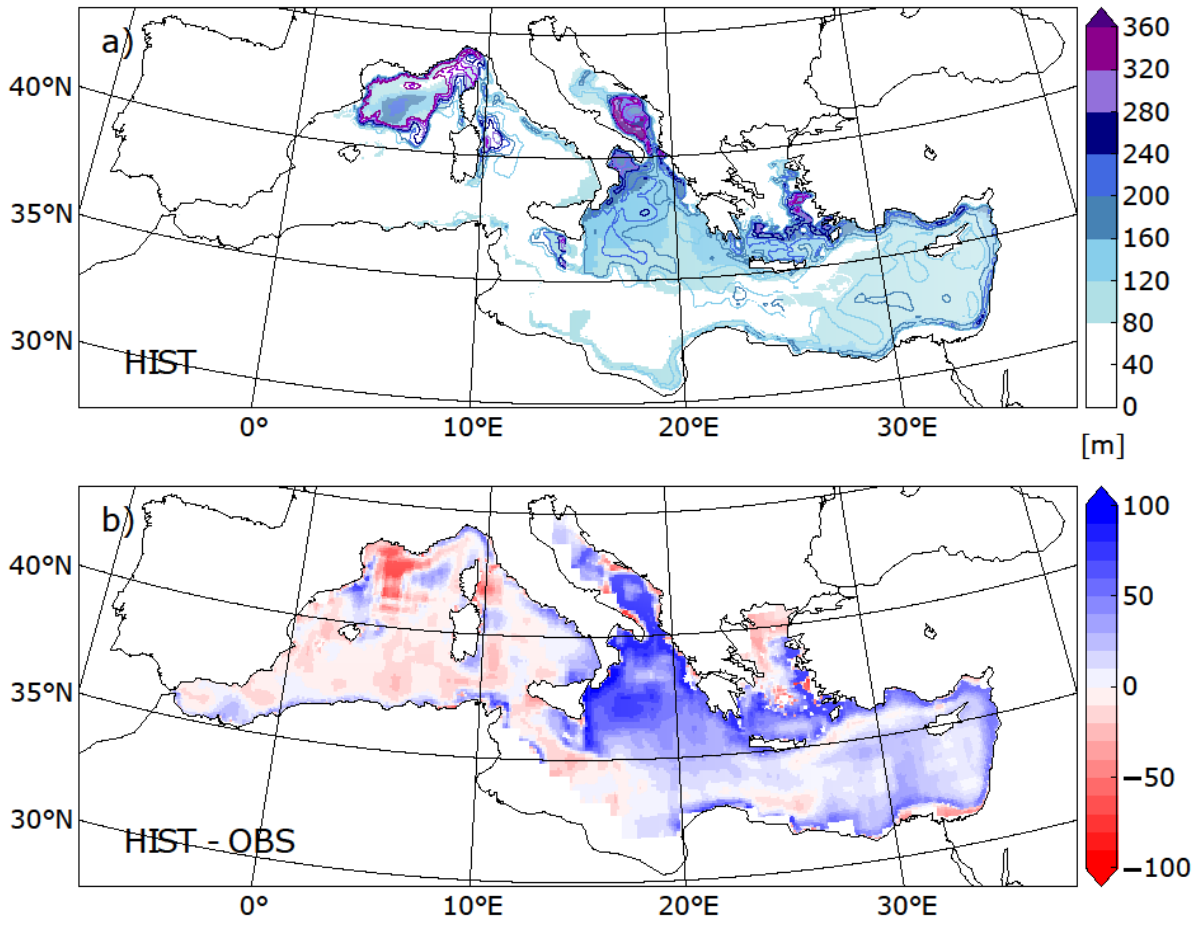

Figure 5: a) Mixed layer depth simulated in HIST (panel a, in m) and as deviation (b) of HIST from observations of Houpert et al., (2015) averaged over the entire simulation for JFM (January February March). Contour lines in the upper panel a) represents the maximum of MLD throughout the HIST simulation.

	SST (°C)	SSS (PSU)	IS ($m^2.s^{-2}$)
Mean bias (model – obs)	-0.64	-0.32	-0.91
RMS error	0.45	0.37	0.29

Table ~~1~~2: Mean biases of sea surface temperature (SST), sea surface salinity (SSS) and index of stratification (IS) in the HIST simulation, expressed as the deviation from observations (MEDATLAS-II), and associated root mean square errors.

3.4 Mediterranean Thermohaline circulation

Here, ~~we evaluate~~ the general characteristics of the simulated thermohaline circulation is evaluated in regions where deep and intermediate water formation occurs. Figure 4c displays the stratification index (IS[1]) for HIST. IS is a vertical integration of the Brunt-Vaisala frequency. A lower IS implies that convection is more likely. The range of IS biases (Figure 4f), is from -1 to 1 $m^2.s^{-2}$ (mean bias = ~~-~~0.91 $m^2.s^{-2}$, error = 0.29 $m^2.s^{-2}$). The model satisfactorily reproduces the convection in known intermediate and deep-water formation areas, namely the Gulf of Lions, the Adriatic Sea, the Ionian Sea, the Aegean Sea and the North Levantine.

Comparison with observations of the mixed-layer depth (Houpert et al., 2015)~~(Houpert et al., 2015)~~ confirms that the model reproduces realistic intermediate and deep-water formation patterns ~~(figure 5a)~~, with a thicker MLD in the eastern basin, due to salty condition (Figure 4a and e), and a shallower MLD in the Gulf of Lions (figure 5b~~a~~).

~~We then analyse t~~The simulated Mediterranean overturning circulation is analysed (figure 6). The Zonal Overturning stream Function (ZOF[2]) in f~~f~~igure 6~~7~~a depicts the surface and intermediate circulation and the intermediate/deep circulation. The surface current from the Strait of Gibraltar flows up to 30°E and back to the Atlantic Ocean in the intermediate layers, through the Levantine Intermediate Water (LIW) outflow. Figure 6 c, e, and g represents the Meridional Overturning stream Function (MOF[3]) in the Gulf of Lions, the Adriatic Sea and the Aegean Sea, respectively. The surface cell in the longitude-depth plan is comparable to previous studies done with the same regional oceanic model, but with different forcings (Adloff et al., 2015; Somot et al., 2006): the mean strength of the surface cell ranges from 0.8 to 1.0 Sv, and the longitudinal extension is from 5°W to 30°E. The simulated intermediate and deep cells are recognized in existing studies as having different characteristics. Our simulated pattern is very close to a similar historical run in Adloff et al., (2015), but is weaker than a historical run in Somot et al., (2006), and a second historical configuration (with refined air-sea flux) in Adloff et al., (2015). The ZOF

[1] $IS(x,y,h) = \int_0^h N^2(x,y)zdz$. N^2 is the Brunt-Väisälä frequency. IS is calculated at each model grid (x,y) for a given depth h (set as the bottom of the sea, or as 1000 m when the depth is greater than 1000 m).

[2] $ZOF(x,z) = \int_h^z \int_{ys}^{yn} u(x,y,z)dydz$. u is the zonal currents, h is the depth of the bottom, yn and ys are the north and south coordinates respectively.

[3] $MOF(y,z) = \int_h^z \int_{xe}^{xw} v(x,y,z)dxdz$. v is the meridional currents, h is the depth of the bottom, xw and xe are the west and east coordinates respectively.

depicteds in HIST simulation is consistent with the reanalyses (1987-2013) of (Pinardi et al., (2019)) over the Western basin, but shows a weaker Eastern deep cell compared to the reconstruction. A large spread between the models for this pattern indicates that there is still a lack of modelling capacity to simulate the deep circulation of the Mediterranean Sea.

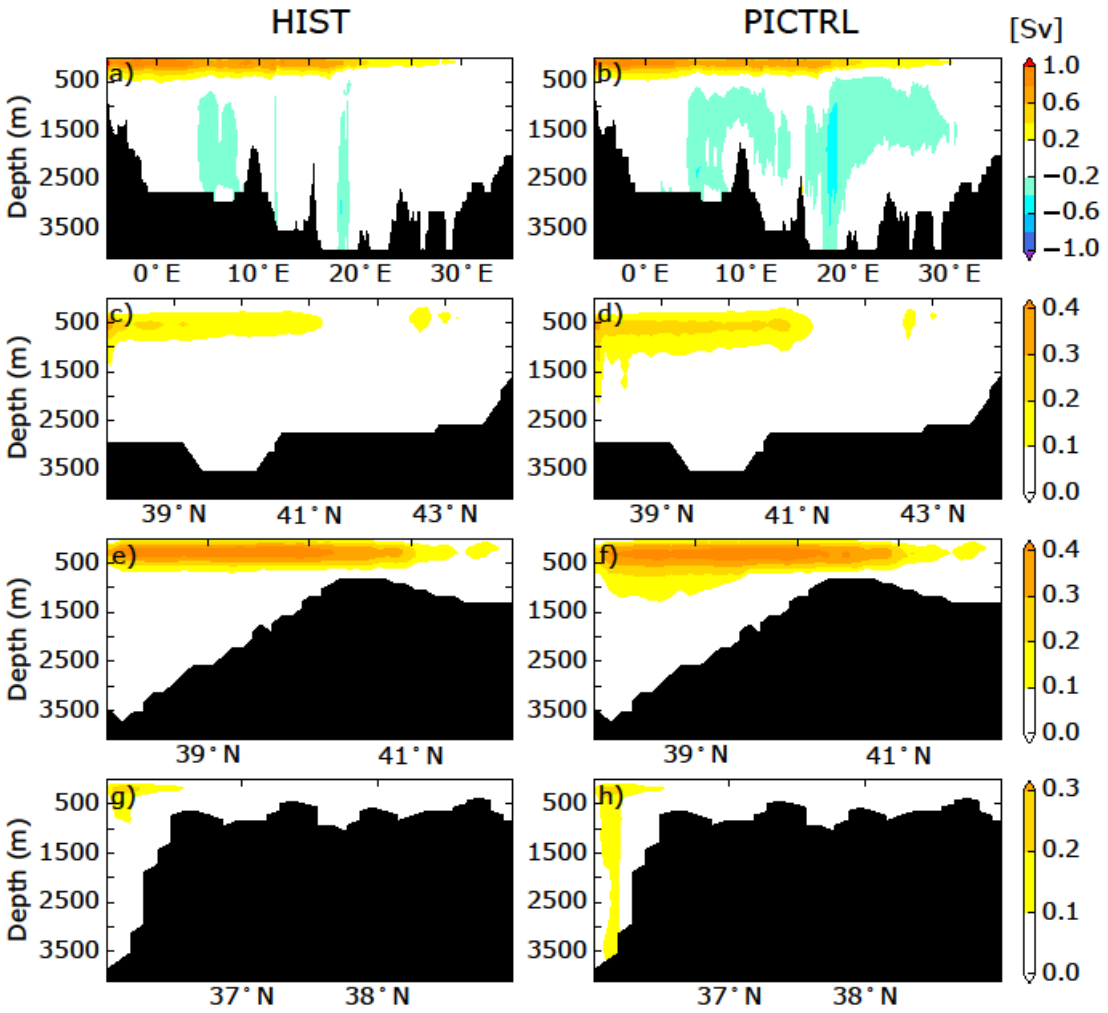

Figure 6: Zonal Overturning stream-Function (ZOF, first ~~column~~ row ~~from left~~, panels a, and b) integrated from north to south and shown as a longitude-depth section for the whole Mediterranean Sea, for HIST, and PICTRL simulations (from top to bottom), respectively. Other panels show Meridional Overturning stream-Function (MOF) shown as a latitude-depth section, integrated west/east for the Gulf of Lion (second ~~column from left~~row, longitudinal extent: 4.5° to 8°E), the Adriatic/Ionian Sea (third ~~column from left~~row, 12° to 21°E), and the Aegean Sea (fourth

row, 24° to 28°E) averaged over the entire simulation for HIST and over the last 30 years of simulation for PICTRL~~)~~.

3.5 Summary of Validation

Validation of our platform was based on the historical period, 1970 to 1999. The atmospheric simulation is ~~consistent~~ ~~acceptable~~~~reasonable~~acceptable compared with observations for the air temperature at 2m at both global and regional scales. The simulated precipitation from the atmospheric models produces a signal that ranges with the observation, but t~~T~~here is significant overestimation of precipitation over the mountainous area and over the land surrounding the Mediterranean Sea. However, the freshwater budget over the sea is close to observations for both evaporation and precipitation. ~~When freshwater river discharges into the Mediterranean Sea are bias-corrected against the observed climatology,~~ T~~t~~he areas of intermediate and deep convection produced by the model are realistic, and~~.~~ t~~T~~he simulation of the thermohaline circulation is well captured by the oceanic model and in the range of the state-of-the-art existing Mediterranean regional models (compared to the simulations of Adloff et al., 2015 and Somot et al., 2006 for instance) and reanalysis as well (Pinardi et al., 2019)~~.~~~~,~~ ~~which~~ These features inspire~~s~~ confidence in our modelling platform for the investigations of past climate.

4 Application of the modelling chain to the Early Holocene

In this section, ~~we present~~ results obtained when our sequential modelling chain is applied in a paleoclimate context are presented, which was our initial motivation for developing this modelling tool. We chose to test the performance of our tool on the Early Holocene, a period marked by significant changes in climate and ocean dynamics over the Mediterranean basin, when the last sapropel event, S1, occurred in the Mediterranean Sea. Our experimental design relies on the comparison of two simulations: the Early Holocene (EHOL) with PICTRL based on pre-industrial conditions, the latter acting as a reference.

4.1 Experimental design

As indicated in the general flowchart of our modelling platform, global SST and SIC are required to initiate our sequential modelling. The basic assumption is that the climate change signal can be reconstructed from global SST and SIC, an accepted practice within the climate modelling community. In this study, ~~we use~~ two existing long-term coupled simulations from IPSL-CM5A is used, one covering the pre-industrial period and the other covering the Early Holocene (around 9.5 ka)~~-~~. Taking the last 100 years of each simulation, ~~we construct~~ a climatological SST and SIC is constructed. After conducting bias-correction, these outputs from IPSL-CM5A are then used to drive the AGCM (LMDZ-global) and

the ARCM (LMDZ-regional) in a further step. The duration of the PICTRL and EHOL atmospheric simulations is 30 years (both global and regional models).

Oceanic temperature and salinity in the Atlantic buffer-zone, as well as freshwater discharges from Mediterranean rivers, are all bias-corrected for NEMOMED8, as described in the general methodology. However, it needs to be pointed out that the reference point for the Nile river discharge is not modern observations but is set at pre-industrial values (2930 $m^3./s^{-1}$ for annual mean, (Vorosmarty et al., 1998)) corresponding to a period before construction of the Aswan dam. The oceanic simulation is 90 years for EHOL and 30 years for PICTRL, performed after a 200-year spin-up of PICTRL.

4.2 Climate features depicted in LMDZ-global (AGCM)

Because Early Holocene simulations are mainly driven by insolation forcing, an important feature is the model response to seasonal temperatures. Figure 7 shows the difference between EHOL and PICTRL, as reproduced in the AGCM, LMDZ-global, for the summer/winter temperature, JJAS precipitation and JAS surface runoff. The atmospheric model imprints a stronger seasonality due to the increased Early Holocene summer insolation. Warmer summer temperatures over Europe and North Africa (+ 6 °C, figure 7b) and lower winter temperatures over Africa (-2 °C, figure 7a) reflect this feature. Variations of the precession also trigger an enhancement of the African Monsoon (+ 10 $mm./day^{-1}$ over the Ethiopian region, figure 7c). The main consequence of this increase in precipitation is an enhanced surface runoff over the Ethiopian region. This hydrological state is similar to the African Humid Period caused by the enhanced African Monsoon and the resultant increase in surface runoff, as shown in (Rossignol-Strick et al., (1982). Rossignol-Strick et al. (1982).

Our results are similar to those of previous modelling exercises for the Early- and Mid-Holocene (e.g. Adloff et al., 2011; (Bosmans et al., 2012); (Braconnot et al., 2007); (Marzin and Braconnot, 2009)). They are also consistent with various reconstructions of mMid-Holocene precipitation (Harrison et al., 2014). A detailed comparison can be made with the Early Holocene simulation reported in Marzin and Braconnot (2009) which used for their experiment the same orbital parameters and the same atmospheric model as we didEHOL. However, their model was coupled to an oceanic model, while we used an atmospheric model and and prescribed SST and SIC as boundary conditions are used in this study. Generally speaking, our results for both surface air temperature and precipitation are very similar to those of Marzin and Braconnot (2009), attesting to the validity of our approach using a simple atmospheric model constrained by boundary conditions. In the ensemble of PMIP simulations, available for the Early Holocene and mid-Holocene, there are some robust outputs for the climate response to orbital forcing but there are also some weaknesses common to most of the models (Braconnot et al., 2007; (Kageyama et al., 2013)). One of these weaknesses is the underestimation of the spread of the

African monsoon towards North Africa. However, the increased discharge from the Nile river, induced by the enhanced monsoon is well supported by data (Adamson et al., 1980; Revel et al., 2014; Williams, 2000).

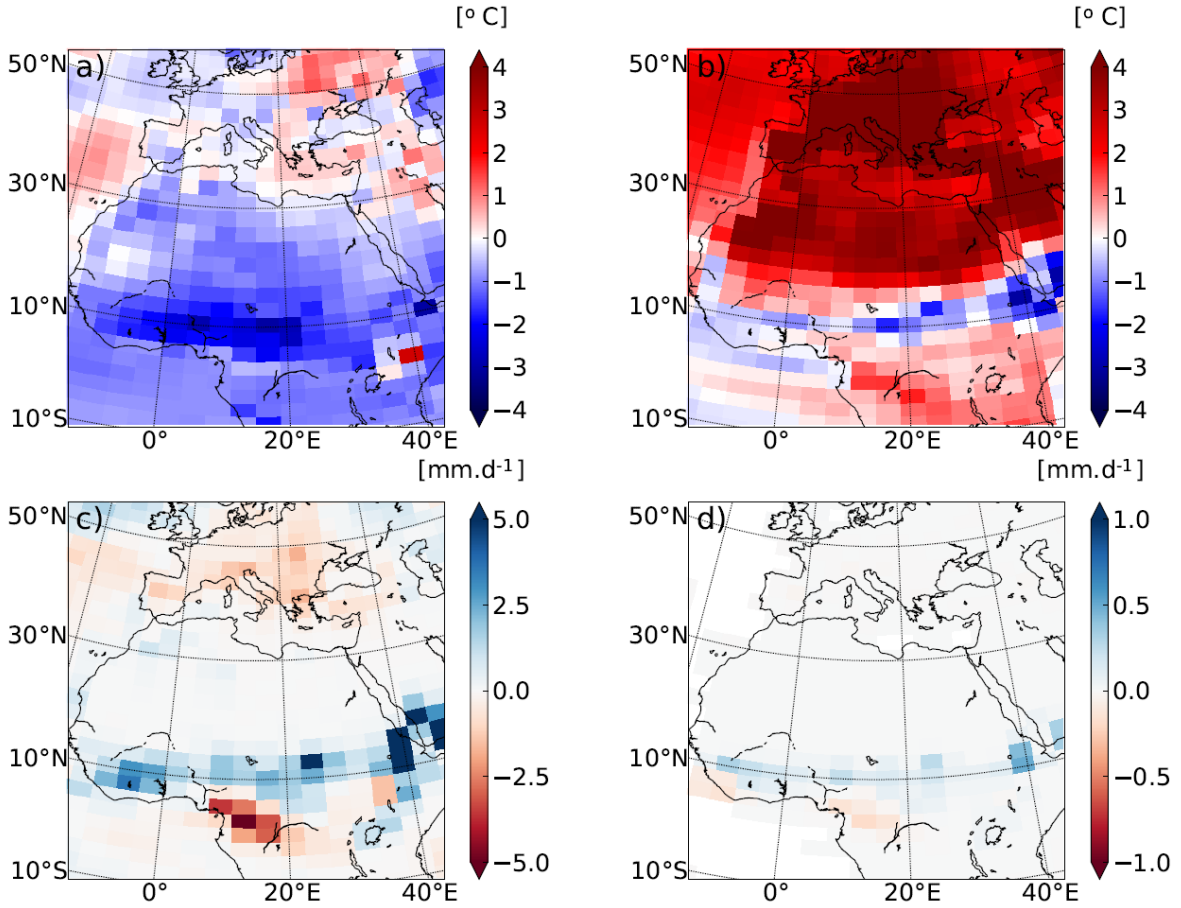

Figure 7: Temperature and precipitation ~~D~~deviations ~~between~~ of EHOL ~~and~~ from PICTRL in LMDZ-global, the AGCM~~GLOBAL~~ for a) winter surface air temperatures at 2 m, b) summer surface air temperatures at 2 m, c) June to ~~September~~ August precipitation, and d) July to September surface runoff (averaged over the entire simulation).

4.3 Mediterranean climate features with dynamical downscaling refinement

Figures 8, 9 and 10 show the results from the regional atmospheric model (LMDZ-regional), compared to those from LMDZ-global~~)~~ for PICTRL and EHOL over the Mediterranean region. In both the global and regional simulations, an increased seasonality is depicted, with warmer summer~~s~~ (+2 to +6 °C) and colder winter~~s~~, especially over land (-3 to -1 °C, Figure 8)~~, is depicted~~. Downscaling with LMDZ-regional slightly reduces the amplitude of the summer warming and shows a more homogenous signal in winter over land. The general circulation of the surface wind in PICTRL is west to east (Figure 9b), in line with the dominant winter regime of westerlies in the region. This important feature is almost

missed in the global model (Figure 9a) which reproduces a lower intensity than the ~~ARCM~~regional model. ~~In the regional model, the EHOL-PICTRL difference (figure 9d) shows a northward shift in position, with maximum changes occurring in the Levantine basin. The global model depicts a different response, with a dipole of change in wind intensity (figure 9c).~~ The winter precipitation in EHOL, for ARCM (LMDZ-regional), increases over land in the Balkans and Italy and over the Adriatic, Ionian and Aegean Seas (~~f~~Figure 10b). These changes are also present in the AGCM (LMDZ-global) that, furthermore, shows an increase in Spain and Portugal (~~f~~Figure 10a). It is in summer that the two models show the largest differences. In ARCM (LMDZ-regional), the Mediterranean basin experiences drier conditions, except in Italy and the North of the Balkans. Over the sea, precipitations slightly increase in EHOL (~~f~~Figure 10). However, the AGCM (LMDZ-global) shows drier conditions in the northern two thirds of the Mediterranean domain, with more humid conditions in the southern third (~~f~~Figure 10c). Changes in precipitation lead to unavoidable modifications in the runoff and river discharge into the Mediterranean Sea.

Although it is not straightforward to compare our "snapshot" simulations against environmental records (often used to reconstruct a timeline), our results compare well with the available data for this area (see supplementary online material, "Text S3: Comparison of model simulation outputs and reconstructed data for the Mediterranean basin"). Numerous proxies provide information on lake levels, paleo fires, pollen, isotopic signals recovered from speleothems which together describe the Mediterranean climate in the past. All of these proxies need to be brought together to provide a clear impression of the Mediterranean climate for this period (Magny et al., 2013; Peyron et al., 2011). ~~(~~Magny et al.~~,~~ (2007), based on records from Lake Acessa (Italy), suggested that aridification took place around 9200–7700 cal BP. ~~(~~Zanchetta et al.~~,~~ (2007), based on data recovered from speleothems in Italy, conclude that the Western Mediterranean basin experienced enhanced rainfall during the S1 (10000-7000 cal BP). ~~(~~Jalut et al.~~,~~ (2009), using pollen data, suggest that the summers were short and dry and that there was abundant rainfall in winter (autumn and spring as well) and remarked that these wetter conditions favoured broad-leaf tree vegetation. Different proxies seem to provide contradictory information and therefore, seasonality must be introduced to reconcile them. Peyron et al., (2011) mentioned wet winters and dry summers during the 'Holocene optimum'. Magny et al., (2013) support the hypothesis of seasonal contrast based on the analysis of multi-proxies.

Our EHOL simulation successfully depicts this temperature contrast between winter and summer. Precipitation is enhanced in winter. In summer, the Mediterranean region is globally drier, except over Northern Italy and the northern Balkans. As explained above, there is no precipitation signal over Northern Africa, although evidence of paleo-lakes has been found in Algeria (Callot and Fontugne, 1992; Petit-Maire et al., 1991), Tunisia (Fontes and Gasse, 1991) and Libya (Gaven et al., 1981; Lézine and Casanova, 1991) during the E~~e~~early Holocene indicating increased rainfall in this area. In the

supplementary material, ~~we provide~~ a comparison between simulated continental precipitation outputs and pollen reconstruction data is provided. This comparison shows that the winter precipitation anomalies are consistent in both cases but that there is a distinct difference in summer values due to the more contrasted summer in the EHOL simulation ~~(supplementary material 1)~~.

~~simulated precipitation changes over the Mediterranean region for Mid and Late Holocene using an atmospheric regional model. Their simulations and those presented in this study are quite difficult to compare because of the period simulated (mid and late Holocene/ Early Holocene) and the reference period used to compare them (Present-day/Pre-industrial).~~

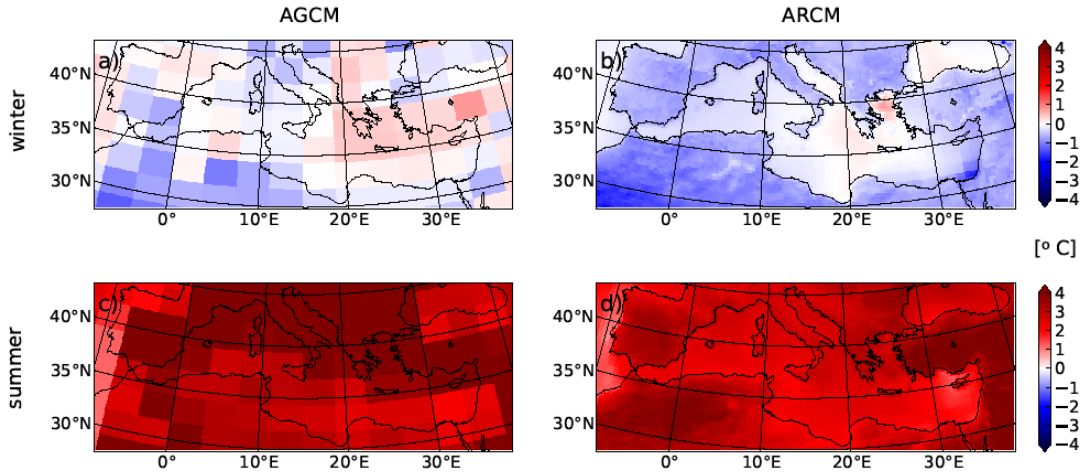

Figure 8: Deviations ~~between (~~EHOL ~~and~~ PICTRL, averaged over the entire simulation) of surface air temperature ~~(°C)~~ at 2 m for winter ~~temperatures at 2m (first row~~upper panels) and ~~in~~ summer ~~temperature at 2m (second row~~lower panels), respectively.~~for the~~ AGCM (~~first column~~LMDZ-global) is displayed on the left and ~~the~~ ARCM (~~second column~~LMDZ-regional) on the right~~, averaged over the entire simulation~~.

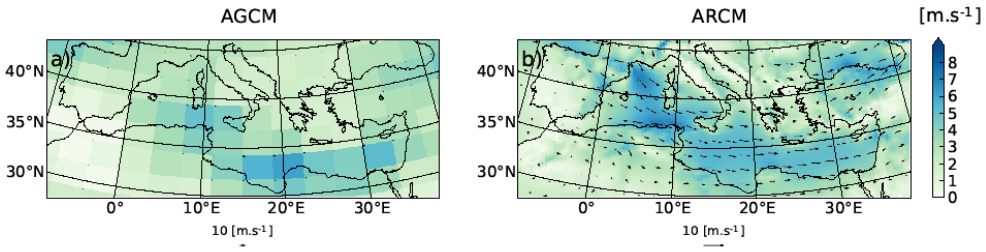

Figure 9: Winter wind-speed in PICTRL ~~(first row)~~ for a) the AGCM and b) the ARCM. ~~Deviations (EHOL-PICTRL, second row) for c) the AGCM and d) the ARCM, averaged over the entire simulation.~~

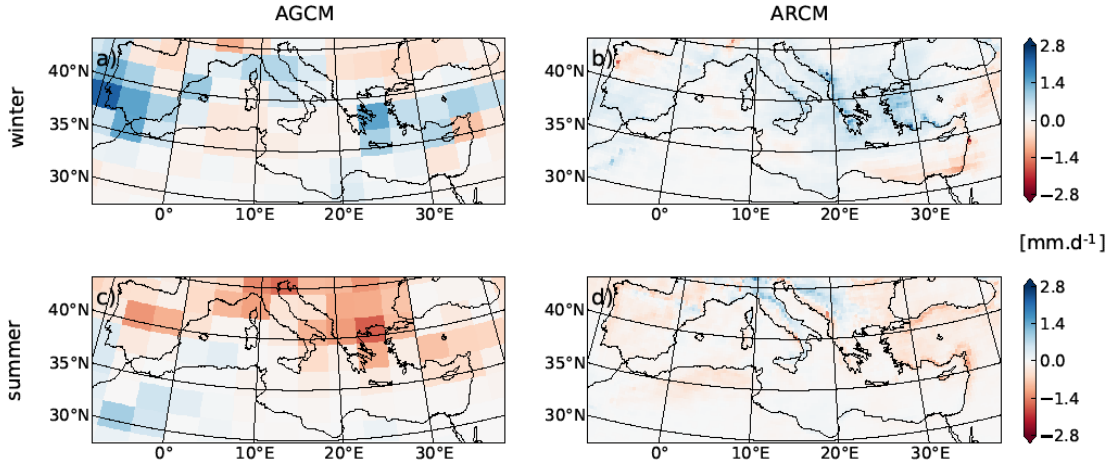

Figure 10: Same as in Figure 8, but for precipitation rate (mm/day). ~~Deviations between EHOL and PICTRL for winter precipitation (first row) and in summer precipitation (second row), for AGCM (first column) and ARCM (second column), averaged over the entire simulation.~~

4.4 Hydrological changes

~~Figure 11 shows the runoff simulated by the atmospheric model. The Nile River is shown in Figure 11a. Figures 11b and 11c plot the anomalies in river discharge between EHOL and PICTRL. The signal for the simulated Nile runoff in PICTRL shows an increase due to an overestimation of precipitation compared to pre-damming values. Both observations and simulations reach their maxima in summ~~

Figure 11 ~~b and c~~ shows ~~box plots for that~~ the anomalies~~y~~ (EHTHOL – PICTRL) of river ~~in~~ freshwater supplies~~y~~ into the ~~Eastern~~ Mediterranean basin as simulated by the ARCM (LMDZ-regional). Bars~~ox plots~~ are displayed for each calendar month to show the strong seasonal variation, and for the western and eastern basins separately. Due to their particular role and their specific treatment in our current modelling practice, the Nile and the Black Sea are also shown for the eastern basin, but not accounted in the sum. The North African rivers are not displayed since they don't show much changes for their catchment area. The Nile River shows important seasonal variation, with increase ~~I~~in summer and autumn and decrease in winter and spring. ~~the freshwater is mainly due to the Nile River in the Eastern basin (figure 11a). However, in winter, t~~The Albanian rivers (Drini, Mat, Dures, Shkumbin and Vjosa) as well as the Vardar and the Buyukmenderes, produce positive anomalies in EHOL in winter, due to enhanced winter ~~continental~~ land precipitation in this simulation (~~f~~Figure 10 b and ~~d~~e). The Black Sea net freshwater supply also changes in EHOL with important decreases in January, February, March and July, but increase in April. In EHOL, the supplementary winter freshwater input is less pronounced for the western basin than for the eastern basin (~~f~~Figure 11b), but major rivers, such as Rhone and Ebro, do show a strong seasonal cycle. As a whole the western basin sees an increase of river discharges from March to June. ~~However~~Moreover, ~~the North African rivers have not been represented because precipitation has not changed much in their catchment area (figure 10 b and d and figure S2 ke).~~

In terms of areal means for the entire Mediterranean draining basin, the different components of the freshwater budget are shown in Table 1 (bottom) for both PICTRL and EHOL, to be compared to the observation-based estimation OBS and the historical simulation HIST. ~~We can see that,~~ F~~f~~rom PICTRL to EHOL, the annual precipitation over the Mediterranean Sea itself does not change much, but the annual evaporation amount shows a slight increase (from 1031 ~~mm~~ to 1094 mm.year^{-1}). However, the most remarkable feature is the increase of river discharges: 98 mm.year^{-1} ~~mm~~ in PICTRL to 225 mm.year^{-1} ~~mm~~ in EHOL. The total water deficit finally decreases from 378 to 305 mm.year^{-1}~~mm~~.

~~Knowing the hydrological changes we can then bias correct the river runoff in order to simulate the characteristics of the Mediterranean Ocean during the early Holocene, following the procedure~~

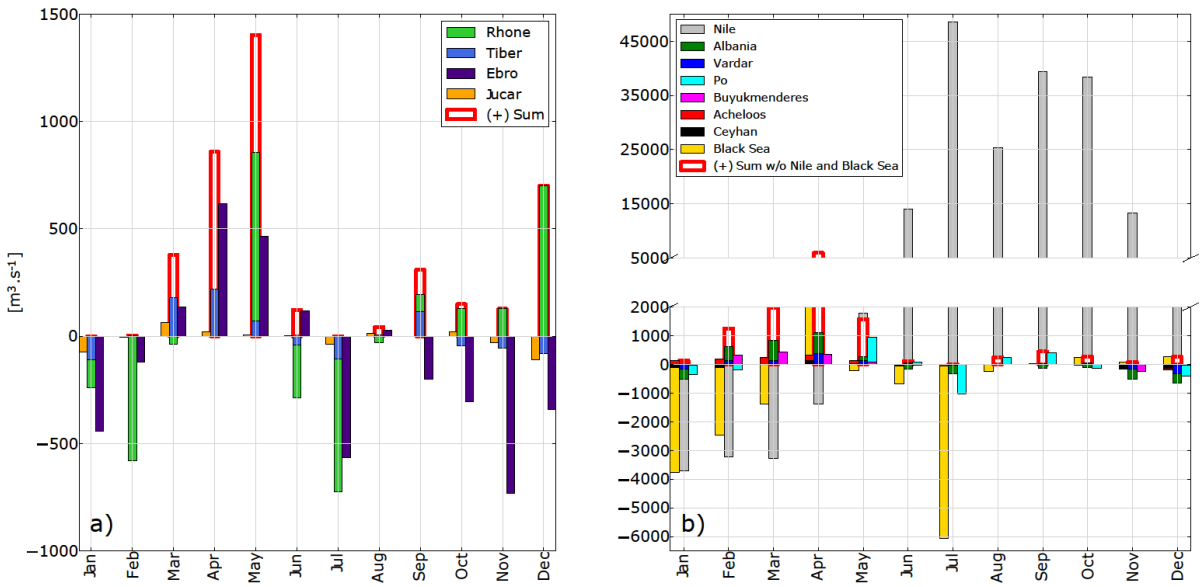

Figure 11: ~~a) climatological runoff of the Nile River: observed pre-damming values (red), PICTRL (blue), EHOL (green), EHOL – PICTRL anomalies applied to observations. Absolute monthly anomalies between EHOL and PICTRL in the simulated river runoff as simulated by the ARCM for~~ b) a), ~~rivers flowing into the eastern basin~~ and b), ~~rivers flowing into the western basin. c) rivers flowing into the western basin including the Nile River (the scale is different between the upper and lower b) and c) sub-figures).~~ Monthly anomalies (EHOL – PICTRL, with seasonal variation) of fresh water discharges (m^3/s^{-1}) for major rivers flowing into the western basin (left panel) and the eastern basin (right panel). The sum of all rivers for each basin is also plotted. The Nile and the Black Sea are also shown as rivers of the eastern basin, but not accounted into the basin-scale sum.

~~Experiments or /variables (mm/yr)~~	~~Evaporation~~	~~Precipitation~~	~~River runoff~~		
~~OBS~~	~~1129~~	~~426~~	~~102-142~~		
~~HIST~~	~~1106~~	~~443~~	~~74~~		
~~PICTRL~~	~~1031~~	~~451~~	~~98~~		
~~EHOL~~	~~1094~~	~~460~~	~~225~~		

~~Table 21: The Mediterranean Sea freshwater budget, expressed as mm/year for the whole water area (about 2.5 million of km2). OBS is a summary of from Sanchez-Gomez et al, 2011 (for the period 1958-~~

~~2008). River discharges in HIST are taken from the climatology of Ludwig et al., 2009. The same applies to PICTRL uses with the Nile set at of its pre-industrial (pre-damming) value, 2930 m3/s, annually (Rivdis). River discharges in EHOL are deduced from the difference based on changes in continental runoff between EHOL and PICTRL.~~

4.5 Changes in water properties of the Mediterranean Sea

At the end of our modelling chain, ~~we can examine~~ changes in the properties of the Mediterranean seawater produced by NEMOMED8 for PICTRL and EHOL are examined. It is important to mention at this stage, that for the correction of the river runoff the reference is the pre-industrial state, and not the historical simulation (as is the case for SST and SIC). Our aim was to keep river runoff anomalies free of anthropogenic influence. In addition, the fact that the "pre-industrial" Nile river runoff (in other words before damming) is well known influenced this choice. Figure 12 shows changes (EHOL minus PICTRL) for sea surface salinities, ~~stratification index~~index of stratification and MLD for the last 30 years of simulation. The EHOL simulation reasonably reaches the steady state in terms of ~~for the~~ IS, ~~the~~ ZOF and ~~the~~ SSS, as ~~displayed~~shown in ~~the f~~Figures S6 to S8 of the supplementary material. The freshwater inputs from the Nile and the north-eastern margin imply a lower salinity in the eastern basin. This decrease in salinity enhances stratification throughout the Mediterranean Sea (with the exception of the Sicily Sea) and affects the convection areas by decreasing the MLD, especially in the Gulf of Lions, in the Adriatic and Ionian Seas and in the Aegean. Such a situation is expected and consistent with the basic climatology of MLD, shown in Figure 5. This global stratification in EHOL is followed by a general reduction in the thermohaline circulation compared to PICTRL (ZOF and MOF, ~~f~~Figure 13 ~~a, b, c, d~~).

Numerous studies have documented the sapropel event~~,~~ S1 and the state of the Mediterranean Sea that caused it. ~~(~~Emeis et al.~~,~~ (2000)~~Emeis et al., (2000),~~ mentioned a decreased SSS during this period in both the eastern and western basins (~~A~~as did ~~(~~Kallel et al., 1997~~)~~ in the Tyrrhenian basin). In the subsection "*Sea Surface Temperatures*" and "*Sea Surface Salinity*" of the section "Text S3"in the supplementary online material, ~~we compared the~~ simulated SST and SSS to reconstructions are compared. Although simulated SST is in good agreement with the reconstructed data, there is a gap between the simulated SSS and reconstructions. This discrepancy is not surprising. Indeed, there are many explanations for the underestimation in our model of the salinity. One of them is a common weakness in Early to Mid-Holocene simulations, namely, the underestimation of the northward spread of the African monsoon and therefore, the underestimation of the freshwater flow from North Africa. Adloff (2011), already pointed to a shortfall in freshwater input to reconcile the simulated and observed SSS during the Early Holocene. Our oceanic simulation depicts these behaviours well and is overall

similar to previous modelling studies with lower resolution (Adloff et al., 2011; Bosmans et al., 2015; Myers et al., 1998).

Two other issues need to be discussed for the Early Holocene. The first one is sea level, which was 20 metres lower than the present day (Peltier et al., 2015). For the sake of simplicity, this difference of sea level is not taken into account in the EHOL simulation. The second issue is the timing of the (re)connection between the Black Sea and the Aegean Sea. This topic is still being debated. Sperling et al. (2003) suggested this reconnection occurred around 8.4 ka BP, while by the calculations of Soulet et al. (2011) it happened around 9 ka BP. Other studies found that an overflow from the Black Sea likely occurred before this reconnection due to Fennoscandian ice-sheet melting during the deglaciation (Chepalyga, 2007; Major et al., 2002; Soulet et al., 2011). For the purposes of this work, the Bosphorus is maintened open in EHOL simulation, with the water exchange set at its modern value. ~~Moreover we decided to set the Early Holocene pCO2 to pre-industrial level instead to its recorded value (260ppm).~~

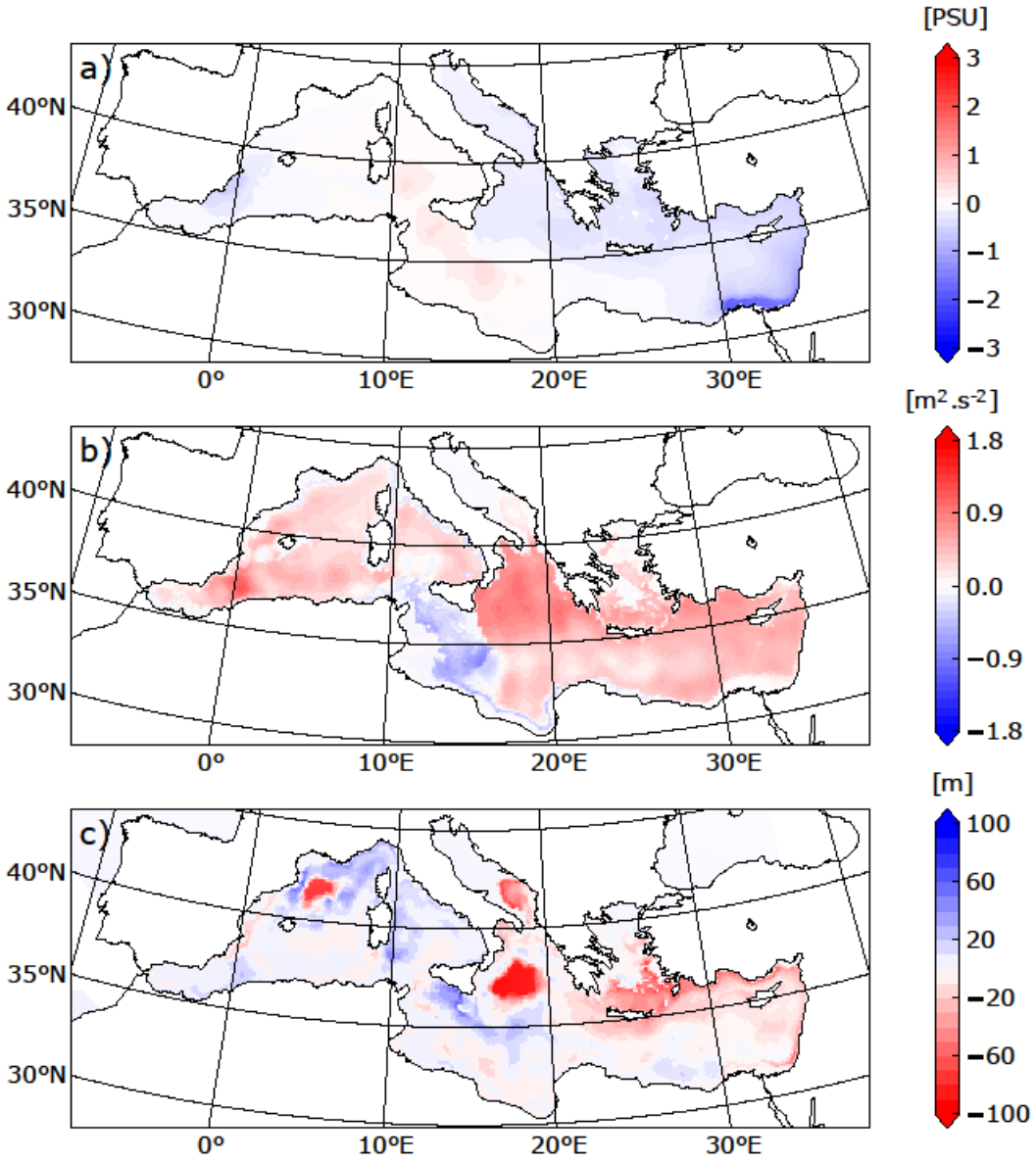

Figure 12: Deviations between EHOL and PICTRL in a) sea surface salinity, b) ~~stratification index~~index of stratification, c) mixed-layer depth, averaged over the last 30 years of simulation

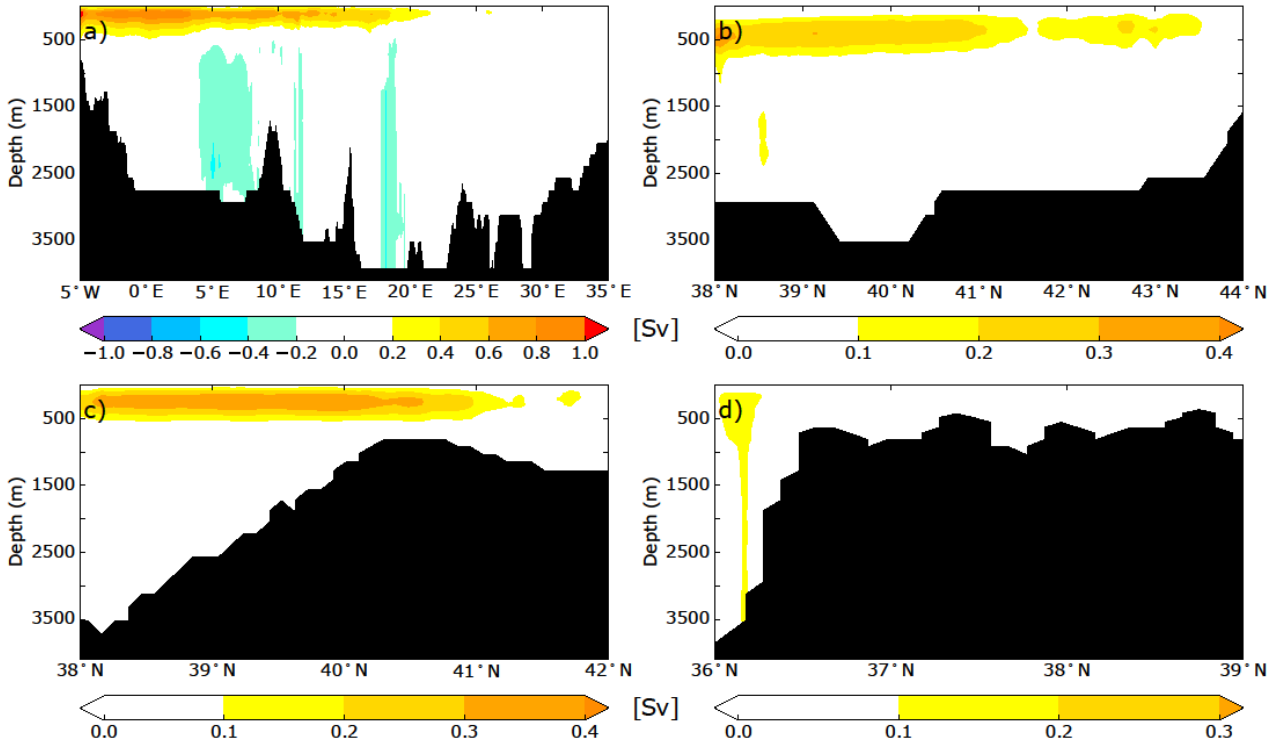

Figure 13: ZOF (a) and MOF (b, Gulf of Lion, c, Adriatic/Ionian Sea, d, ~~Ionian~~ Aegean Sea) for EHOL experiment, averaged over the last 30 years of simulation. These overturning stream-functions were calculated in the same way as in Fig. 6, providing a strict comparison with the experiments HIST and PICTRL.

5 Conclusion and perspectives for the modelling platform

This study aimed to develop a modelling platform to simulate different climatic conditions of the Mediterranean basin. We developed a useful regional climate investigation platform with high spatial resolution over the Mediterranean region. This is particularly relevant for the study of impacts on the circulation of the Mediterranean Sea. The model chain has been evaluated for the historical period. We have presented Early Holocene simulations as an example of the potential of this platform to simulate past climate. For the Early Holocene, our model reproduced satisfactorily the global and regional climate features, compared to the observed data. Our platform allowed, for the first time, the generation of a high-resolution freshwater budget for this period, with a particular focus on continental precipitation, a key factor for the Mediterranean Sea in the assessment of its impact on circulation during the onset of the sapropel event, S1. An important limitation of our sequential approach is the fact that it does not take account of feedback of ocean changes on atmospheric circulation. However, this architecture allows eventual bias correction, conducted at different levels of the platform if needed. One way to overcome

this problem of interactive ocean would be to consider an "asynchronous mode", namely, to take account of feedback from the ocean component to the atmosphere at a yearly or decadal frequency.

~~Two other issues need to be discussed for the Early Holocene. The first one is sea level, which was 20 metres lower than the present day . For the sake of simplicity, we did not take into account this difference of sea level in the EHOL simulation. The second issue is the timing of the (re)connection between the Black Sea and the Aegean Sea. This topic is still being debated. suggested this reconnection occurred around 8.4 ka BP, while by the calculations of it happened around 9 ka BP. Other studies found that an overflow from the Black Sea likely occurred before this reconnection due to Fennoscandian ice-sheet melting during the deglaciation . For the purposes of this work, we decided to maintain the Bosphorus open in our simulation, with the water exchange set at its modern value.~~

The modelling sequence, moving from global simulation at low resolution to high-resolution regional ocean modelling, avoids the problem of boundary conditions, and provides a fully consistent platform that may be used for many paleoclimate studies. We focused here on the Early Holocene period but this architecture could be used to study other periods investigated in MIPs, such as the Last Glacial Maximum or the deposition of older sapropels, from the Pliocene to the Quaternary, as long as the tectonics remain mainly unchanged (PMIP, PlioMIP).

Code and data availability. The current version of LMDZ and NEMO are available from the project website: -https://forge.ipsl.jussieu.fr/igcmg_doc/wiki/DocImodelBlmdz -and http://forge.ipsl.jussieu.fr/nemo/wiki/Users under the terms of the CeCill license for LMDZ and NEMO both. The exact version of the model used to produce the results used in this paper is archived on Zenodo ~~(~~(Vadsaria et al., 2019)~~)~~, as are input data and scripts to run the model and produce the plots for all the simulations presented in this paper.

Author's contribution. This study was co-designed and approved by all co-authors. The simulation protocol was constructed by TV and LL from a modelling architecture provided by LL. TV conducted the numerical simulations and drafted the first version of the manuscript. All co-authors are largely involved in the writing and revision of the manuscript.

Acknowledgments. We thank Mary Minnock for her professional English revision. This work was supported by the French National program LEFE "HoMoSapIENS". This work was granted access to the HPC resources of TGCC under the allocation 2017-A0010102212, 2018-A0030102212 and 2018-A004-01-00239 made by GENCI.

References

Adamson, D. A., Gasse, F., Street, F. A. and Williams, M. A. J.: Late Quaternary history of the Nile, Nature, 288(5786), 50–55, doi:10.1038/288050a0, 1980.

Adler, R., Sapiano, M., Huffman, G., Wang, J.-J., Gu, G., Bolvin, D., Chiu, L., Schneider, U., Becker, A., Nelkin, E., Xie, P., Ferraro, R. and Shin, D.-B.: The Global Precipitation Climatology Project (GPCP) Monthly Analysis (New Version 2.3) and a Review of 2017 Global Precipitation, Atmosphere (Basel)., 9(4), 138, doi:10.3390/atmos9040138, 2018.

Adloff, F., Mikolajewicz, U., Kučera, M., Grimm, R., Maier-Reimer, E., Schmiedl, G. and Emeis, K.-C.: Upper ocean climate of the Eastern Mediterranean Sea during the Holocene Insolation Maximum – a model study" published in Clim. Past, 7, 1103–1122, 2011, Clim. Past, 7(4), 1149–1168, doi:10.5194/cp-7-1149-2011, 2011.

Adloff, F., Somot, S., Sevault, F., Jordà, G., Aznar, R., Déqué, M., Herrmann, M., Marcos, M., Dubois, C., Padorno, E., Alvarez-Fanjul, E. and Gomis, D.: Mediterranean Sea response to climate change in an ensemble of twenty first century scenarios, Clim. Dyn., 45(9–10), 2775–2802, doi:10.1007/s00382-015-2507-3, 2015.

Artale, V.: Role of surface fluxes in ocean general circulation models using satellite sea surface temperature: Validation of and sensitivity to the forcing frequency of the Mediterranean thermohaline circulation, J. Geophys. Res., 107(C8), 3120, doi:10.1029/2000JC000452, 2002.

Artale, V., Calmanti, S., Carillo, A., Dell'Aquila, A., Herrmann, M., Pisacane, G., Ruti, P. M., Sannino, G., Struglia, M. V., Giorgi, F., Bi, X., Pal, J. S. and Rauscher, S.: An atmosphere–ocean regional climate model for the Mediterranean area: assessment of a present climate simulation, Clim. Dyn., 35(5), 721–740, doi:10.1007/s00382-009-0691-8, 2010.

Béranger, K., Drillet, Y., Houssais, M.-N., Testor, P., Bourdallé-Badie, R., Alhammoud, B., Bozec, A., Mortier, L., Bouruet-Aubertot, P. and Crépon, M.: Impact of the spatial distribution of the atmospheric forcing on water mass formation in the Mediterranean Sea, J. Geophys. Res., 115(C12), C12041, doi:10.1029/2009JC005648, 2010.

Beuvier, J., Sevault, F., Herrmann, M., Kontoyiannis, H., Ludwig, W., Rixen, M., Stanev, E., Béranger, K. and Somot, S.: Modeling the Mediterranean Sea interannual variability during 1961–2000: Focus on the Eastern Mediterranean Transient, J. Geophys. Res., 115(C8), C08017, doi:10.1029/2009JC005950, 2010.

Bosmans, J. H. C., Drijfhout, S. S., Tuenter, E., Lourens, L. J., Hilgen, F. J. and Weber, S. L.: Monsoonal response to mid-holocene orbital forcing in a high resolution GCM, Clim. Past, 8(2), 723–740, doi:10.5194/cp-8-723-2012, 2012.

Bosmans, J. H. C., Drijfhout, S. S., Tuenter, E., Hilgen, F. J., Lourens, L. J. and Rohling, E. J.: Precession and obliquity forcing of the freshwater budget over the Mediterranean, Quat. Sci. Rev., 123, 16–30, doi:10.1016/j.quascirev.2015.06.008, 2015.

Braconnot, P., Otto-Bliesner, B., Harrison, S., Joussaume, S., Peterchmitt, J., Abe-Ouchi, A., Crucifix, M., Driesschaert, E., Fichefet, T., Hewitt, C. D., Kageyama, M., Kitoh, A., Laîné, A., Loutre, M., Marti, O., Merkel, U., Ramstein, G., Valdes, P., Weber, S. L., Yu, Y. and Zhao, Y.: Results of PMIP2 coupled simulations of the Mid-Holocene and Last Glacial Maximum – Part 1: experiments and large-scale features, Clim. Past, 3(2), 261–277, doi:10.5194/cp-3-261-2007, 2007.

Callot, Y. and Fontugne, M.: Les étagements de nappes dans les paléolacs holocènes du nord-est du Grand Erg Occidental (Algérie)., 1992.

Chen, J., Brissette, F. P. and Leconte, R.: Uncertainty of downscaling method in quantifying the impact of climate change on hydrology, J. Hydrol., 401(3–4), 190–202, doi:10.1016/j.jhydrol.2011.02.020, 2011.

Chepalyga, A. L.: The late glacial great flood in the Ponto-Caspian basin, in The Black Sea Flood Question: Changes in Coastline, Climate, and Human Settlement, pp. 119–148, Springer Netherlands., 2007.

Dee, D. P., Uppala, S. M., Simmons, A. J., Berrisford, P., Poli, P., Kobayashi, S., Andrae, U., Balmaseda, M. A., Balsamo, G., Bauer, P., Bechtold, P., Beljaars, A. C. M., van de Berg, L., Bidlot, J., Bormann, N., Delsol, C., Dragani, R., Fuentes, M., Geer, A. J., Haimberger, L., Healy, S. B., Hersbach, H., Hólm, E. V., Isaksen, L., Kållberg, P., Köhler, M., Matricardi, M., McNally, A. P., Monge-Sanz, B. M., Morcrette, J.-J., Park, B.-K., Peubey, C., de Rosnay, P., Tavolato, C., Thépaut, J.-N. and Vitart, F.: The ERA-Interim reanalysis: configuration and performance of the data assimilation system, Q. J. R. Meteorol. Soc., 137(656), 553–597, doi:10.1002/qj.828, 2011.

Dell'Aquila, A., Calmanti, S., Ruti, P., Struglia, M., Pisacane, G., Carillo, A. and Sannino, G.: Effects of seasonal cycle fluctuations in an A1B scenario over the Euro-Mediterranean region, Clim. Res., 52(1), 135–157, doi:10.3354/cr01037, 2012.

Drobinski, P., Anav, A., Lebeaupin Brossier, C., Samson, G., Stéfanon, M., Bastin, S., Baklouti, M., Béranger, K., Beuvier, J., Bourdallé-Badie, R., Coquart, L., D'Andrea, F., de Noblet-Ducoudré, N., Diaz, F., Dutay, J.-C., Ethe, C., Foujols, M.-A., Khvorostyanov, D., Madec, G., Mancip, M., Masson, S., Menut, L., Palmieri, J., Polcher, J., Turquety, S., Valcke, S. and Viovy, N.: Model of the Regional Coupled Earth system (MORCE): Application to process and climate studies in vulnerable regions, Environ. Model. Softw., 35, 1–18, doi:10.1016/j.envsoft.2012.01.017, 2012.

Dufresne, J.-L., Foujols, M.-A., Denvil, S., Caubel, A., Marti, O., Aumont, O., Balkanski, Y., Bekki, S., Bellenger, H., Benshila, R., Bony, S., Bopp, L., Braconnot, P., Brockmann, P., Cadule, P., Cheruy, F., Codron, F., Cozic, A., Cugnet, D., de Noblet, N., Duvel, J.-P., Ethé, C., Fairhead, L., Fichefet, T., Flavoni, S., Friedlingstein, P., Grandpeix, J.-Y., Guez, L., Guilyardi, E., Hauglustaine, D., Hourdin, F., Idelkadi, A., Ghattas, J., Joussaume, S., Kageyama, M., Krinner, G., Labetoulle, S., Lahellec, A., Lefebvre, M.-P., Lefevre, F., Levy, C., Li, Z. X., Lloyd, J., Lott, F., Madec, G., Mancip, M., Marchand, M., Masson, S., Meurdesoif, Y., Mignot, J., Musat, I., Parouty, S., Polcher, J., Rio, C., Schulz, M., Swingedouw, D., Szopa, S., Talandier, C., Terray, P., Viovy, N. and Vuichard, N.: Climate change projections using the IPSL-CM5 Earth System Model: from CMIP3 to CMIP5, Clim. Dyn., 40(9–10), 2123–2165, doi:10.1007/s00382-012-1636-1, 2013.

Emeis, K.-C., Struck, U., Schulz, H.-M., Rosenberg, R., Bernasconi, S., Erlenkeuser, H., Sakamoto, T. and Martinez-Ruiz, F.: Temperature and salinity variations of Mediterranean Sea surface waters over the last 16,000 years from records of planktonic stable oxygen isotopes and alkenone unsaturation ratios, Palaeogeogr. Palaeoclimatol. Palaeoecol., 158(3–4), 259–280, doi:10.1016/S0031-0182(00)00053-5, 2000.

Fontes, J. C. and Gasse, F.: PALHYDAF (Palaeohydrology in Africa) program: objectives, methods, major results, Palaeogeogr. Palaeoclimatol. Palaeoecol., 84(1–4), 191–215, doi:10.1016/0031-0182(91)90044-R, 1991.

Gaven, C., Hillaire-Marcel, C. and Petit-Maire, N.: A Pleistocene lacustrine episode in southeastern Libya, Nature, 290(5802), 131–133, doi:10.1038/290131a0, 1981.

Giorgi, F.: Climate change hot-spots, Geophys. Res. Lett., 33(8), L08707, doi:10.1029/2006GL025734, 2006.

Goubanova, K. and Li, L.: Extremes in temperature and precipitation around the Mediterranean basin in an ensemble of future climate scenario simulations, Glob. Planet. Change, 57(1–2), 27–42, doi:10.1016/j.gloplacha.2006.11.012, 2007.

Harrison, S. P., Bartlein, P. J., Brewer, S., Prentice, I. C., Boyd, M., Hessler, I., Holmgren, K., Izumi, K. and Willis, K.: Climate model benchmarking with glacial and mid-Holocene climates, Clim. Dyn., 43(3–4), 671–688, doi:10.1007/s00382-013-1922-6, 2014.

Hernández-Díaz, L., Laprise, R., Nikiéma, O. and Winger, K.: 3-Step dynamical downscaling with empirical correction of sea-surface conditions: application to a CORDEX Africa simulation, Clim. Dyn., 48(7–8), 2215–2233, doi:10.1007/s00382-016-3201-9, 2017.

Herrmann, M., Sevault, F., Beuvier, J. and Somot, S.: What induced the exceptional 2005 convection event in the northwestern Mediterranean basin? Answers from a modeling study, J. Geophys. Res., 115(C12), C12051, doi:10.1029/2010JC006162, 2010.

Houpert, L., Testor, P., Durrieu de Madron, X., Somot, S., D'Ortenzio, F., Estournel, C. and Lavigne, H.: Seasonal cycle of the mixed layer, the seasonal thermocline and the upper-ocean heat storage rate in the Mediterranean Sea derived from observations, Prog. Oceanogr., 132, 333–352, doi:10.1016/j.pocean.2014.11.004, 2015.

Hourdin, F., Musat, I., Bony, S., Braconnot, P., Codron, F., Dufresne, J.-L., Fairhead, L., Filiberti, M.-A., Friedlingstein, P., Grandpeix, J.-Y., Krinner, G., LeVan, P., Li, Z.-X. and Lott, F.: The LMDZ4 general circulation model: climate performance and sensitivity to parametrized physics with emphasis on tropical convection, Clim. Dyn., 27(7–8), 787–813, doi:10.1007/s00382-006-0158-0, 2006.

Jalut, G., Dedoubat, J. J., Fontugne, M. and Otto, T.: Holocene circum-Mediterranean vegetation changes: Climate forcing and human impact, Quat. Int., 200(1–2), 4–18, doi:10.1016/j.quaint.2008.03.012, 2009.

Jost, A., Lunt, D., Kageyama, M., Abe-Ouchi, A., Peyron, O., Valdes, P. J. and Ramstein, G.: High-resolution simulations of the last glacial maximum climate over Europe: a solution to discrepancies with continental palaeoclimatic reconstructions?, Clim. Dyn., 24(6), 577–590, doi:10.1007/s00382-005-0009-4, 2005.

Kageyama, M., Braconnot, P., Bopp, L., Caubel, A., Foujols, M.-A., Guilyardi, E., Khodri, M., Lloyd,

J., Lombard, F., Mariotti, V., Marti, O., Roy, T. and Woillez, M.-N.: Mid-Holocene and Last Glacial Maximum climate simulations with the IPSL model—part I: comparing IPSL_CM5A to IPSL_CM4, Clim. Dyn., 40(9–10), 2447–2468, doi:10.1007/s00382-012-1488-8, 2013.

Kallel, N., Paterne, M., Labeyrie, L., Duplessy, J.-C. and Arnold, M.: Temperature and salinity records of the Tyrrhenian Sea during the last 18,000 years, Palaeogeogr. Palaeoclimatol. Palaeoecol., 135(1–4), 97–108, doi:10.1016/S0031-0182(97)00021-7, 1997.

Kourafalou, V. H. and Barbopoulos, K.: High resolution simulations on the North Aegean Sea seasonal circulation, Ann. Geophys., 21(1), 251–265, doi:10.5194/angeo-21-251-2003, 2003.

Krinner, G., Viovy, N., de Noblet-Ducoudré, N., Ogée, J., Polcher, J., Friedlingstein, P., Ciais, P., Sitch, S. and Prentice, I. C.: A dynamic global vegetation model for studies of the coupled atmosphere-biosphere system, Global Biogeochem. Cycles, 19(1), 1–33, doi:10.1029/2003GB002199, 2005.

Krinner, G., Largeron, C., Ménégoz, M., Agosta, C. and Brutel-Vuilmet, C.: Oceanic Forcing of Antarctic Climate Change: A Study Using a Stretched-Grid Atmospheric General Circulation Model, J. Clim., 27(15), 5786–5800, doi:10.1175/JCLI-D-13-00367.1, 2014.

Krinner, G., Beaumet, J., Favier, V., Déqué, M. and Brutel-Vuilmet, C.: Empirical Run-Time Bias Correction for Antarctic Regional Climate Projections With a Stretched-Grid AGCM, J. Adv. Model. Earth Syst., 11(1), 64–82, doi:10.1029/2018MS001438, 2019.

Lacombe, H. and Tchernia, P.: Caractères hydrologiques et circulation des eaux enMéditerranée., in The Mediterranean Sea: A natural sedimentation laboratory, edited by D. . Stanley, pp. 25–36, Dowden, Hutchinson & Ross, Stroudsburg., 1972.

De Lange, G. J., Thomson, J., Reitz, A., Slomp, C. P., Speranza Principato, M., Erba, E. and Corselli, C.: Synchronous basin-wide formation and redox-controlled preservation of a Mediterranean sapropel, Nat. Geosci., 1(9), 606–610, doi:10.1038/ngeo283, 2008.

Lebeaupin Brossier, C., Béranger, K., Deltel, C. and Drobinski, P.: The Mediterranean response to different space–time resolution atmospheric forcings using perpetual mode sensitivity simulations, Ocean Model., 36(1–2), 1–25, doi:10.1016/j.ocemod.2010.10.008, 2011.

Lézine, A.-M. and Casanova, J.: Correlated oceanic and continental records demonstrate past climate and hydrology of North Africa (0-140 ka), Geology, 19(4), 307–310, doi:10.1130/0091-

7613(1991)019<0307:COACRD>2.3.CO;2, 1991.

Li, L., Bozec, A., Somot, S., Bouruet-Aubertot, P. and Crepon, M.: Regional atmospheric, marine processes and climate modelling, in Mediterranean climate variability and predictability, edited by P. Lionello, P. Malanotte-Rizzoli, and R. Boscolo, Elsevier., 2006.

Li, L., Casado, A., Congedi, L., Dell'Aquila, A., Dubois, C., Elizalde, A., L'Hévéder, B., Lionello, P., Sevault, F., Somot, S., Ruti, P. and Zampieri, M.: Modeling of the mediterranean climate system, in The Climate of the Mediterranean Region, pp. 419–448, Elsevier Inc., 2012.

Li, Z.-X.: Ensemble Atmospheric GCM Simulation of Climate Interannual Variability from 1979 to 1994, J. Clim., 12(4), 986–1001, doi:10.1175/1520-0442(1999)012<0986:EAGSOC>2.0.CO;2, 1999.

Locarnini, R. A., Mishonov, A. V., Antonov, J. I., Boyer, T. P., Garcia, H. E., Baranova, O. K., Zweng, M. M., Paver, C. R., Reagan, J. R., Johnson, D. R., Hamilton, M. and Seidov, D.: World Ocean Atlas 2013. Vol. 1: Temperature., S. Levitus, Ed.; A. Mishonov, Tech. Ed.; NOAA Atlas NESDIS, 73(September), 40, doi:10.1182/blood-2011-06-357442, 2013.

Ludwig, P., Shao, Y., Kehl, M. and Weniger, G.-C.: The Last Glacial Maximum and Heinrich event I on the Iberian Peninsula: A regional climate modelling study for understanding human settlement patterns, Glob. Planet. Change, 170, 34–47, doi:10.1016/j.gloplacha.2018.08.006, 2018.

Ludwig, W., Dumont, E., Meybeck, M. and Heussner, S.: River discharges of water and nutrients to the Mediterranean and Black Sea: Major drivers for ecosystem changes during past and future decades?, Prog. Oceanogr., 80(3–4), 199–217, doi:10.1016/j.pocean.2009.02.001, 2009.

Macias, D. M., Garcia-Gorriz, E. and Stips, A.: Productivity changes in the Mediterranean Sea for the twenty-first century in response to changes in the regional atmospheric forcing, Front. Mar. Sci., 2, doi:10.3389/fmars.2015.00079, 2015.

Madec, G.: NEMO ocean engine-version 3.0-Laboratoire d'Océanographie et du Climat: Expérimentation et Approches Numériques, 2008.

Magny, M., de Beaulieu, J.-L., Drescher-Schneider, R., Vannière, B., Walter-Simonnet, A.-V., Miras, Y., Millet, L., Bossuet, G., Peyron, O., Brugiapaglia, E. and Leroux, A.: Holocene climate changes in the central Mediterranean as recorded by lake-level fluctuations at Lake Accesa (Tuscany, Italy), Quat. Sci. Rev., 26(13–14), 1736–1758, doi:10.1016/j.quascirev.2007.04.014, 2007.

947 Magny, M., Combourieu-Nebout, N., de Beaulieu, J. L., Bout-Roumazeilles, V., Colombaroli, D.,
948 Desprat, S., Francke, A., Joannin, S., Ortu, E., Peyron, O., Revel, M., Sadori, L., Siani, G., Sicre, M. A.,
949 Samartin, S., Simonneau, A., Tinner, W., Vannière, B., Wagner, B., Zanchetta, G., Anselmetti, F.,
950 Brugiapaglia, E., Chapron, E., Debret, M., Desmet, M., Didier, J., Essallami, L., Galop, D., Gilli, A.,
951 Haas, J. N., Kallel, N., Millet, L., Stock, A., Turon, J. L. and Wirth, S.: North–south
952 palaeohydrological contrasts in the central Mediterranean during the Holocene: tentative synthesis and
953 working hypotheses, Clim. Past, 9(5), 2043–2071, doi:10.5194/cp-9-2043-2013, 2013.
954
955 Major, C., Ryan, W., Lericolais, G. and Hajdas, I.: Constraints on Black Sea outflow to the Sea of
956 Marmara during the last glacial–interglacial transition, Mar. Geol., 190(1–2), 19–34,
957 doi:10.1016/S0025-3227(02)00340-7, 2002.
958
959 Marzin, C. and Braconnot, P.: Variations of Indian and African monsoons induced by insolation changes
960 at 6 and 9.5 kyr BP, Clim. Dyn., 33(2–3), 215–231, doi:10.1007/s00382-009-0538-3, 2009.
961
962 Mikolajewicz, U.: Modeling Mediterranean Ocean climate of the Last Glacial Maximum, Clim. Past,
963 7(1), 161–180, doi:10.5194/cp-7-161-2011, 2011.
964
965 Millot, C. and Taupier-Letage, I.: Circulation in the Mediterranean Sea, pp. 29–66., 2005.
966
967 Myers, P. G., Haines, K. and Rohling, E. J.: Modeling the paleocirculation of the Mediterranean: The
968 Last Glacial Maximum and the Holocene with emphasis on the formation of sapropel S 1,
969 Paleoceanography, 13(6), 586–606, doi:10.1029/98PA02736, 1998.
970
971 Peltier, W. R., Argus, D. F. and Drummond, R.: Space geodesy constrains ice age terminal deglaciation:
972 The global ICE-6G_C (VM5a) model, J. Geophys. Res. Solid Earth, 120(1), 450–487,
973 doi:10.1002/2014JB011176, 2015.
974
975 Petit-Maire, N., Fontugne, M. and Rouland, C.: Atmospheric methane ratio and environmental change
976 in the Sahara an Sahel during the last 130 kyrs, Palaeogeogr. Palaeoclimatol. Palaeoecol., 86(1–2), 197–
977 206, doi:10.1016/0031-0182(91)90009-G, 1991.
978
979 Peyron, O., Goring, S., Dormoy, I., Kotthoff, U., Pross, J., de Beaulieu, J.-L., Drescher-Schneider, R.,
980 Vannière, B. and Magny, M.: Holocene seasonality changes in the central Mediterranean region
981 reconstructed from the pollen sequences of Lake Accesa (Italy) and Tenaghi Philippon (Greece), The
982 Holocene, 21(1), 131–146, doi:10.1177/0959683610384162, 2011.
983

Pinardi, N., Cessi, P., Borile, F. and Wolfe, C. L. P.: The Mediterranean sea overturning circulation, J. Phys. Oceanogr., 49(7), 1699–1721, doi:10.1175/JPO-D-18-0254.1, 2019.

Ramstein, G., Kageyama, M., Guiot, J., Wu, H., Hély, C., Krinner, G. and Brewer, S.: How cold was Europe at the Last Glacial Maximum? A synthesis of the progress achieved since the first PMIP model-data comparison, Clim. Past, 3(2), 331–339, doi:10.5194/cp-3-331-2007, 2007.

Revel, M., Colin, C., Bernasconi, S., Combourieu-Nebout, N., Ducassou, E., Grousset, F. E., Rolland, Y., Migeon, S., Bosch, D., Brunet, P., Zhao, Y. and Mascle, J.: 21,000 Years of Ethiopian African monsoon variability recorded in sediments of the western Nile deep-sea fan, Reg. Environ. Chang., 14(5), 1685–1696, doi:10.1007/s10113-014-0588-x, 2014.

Rossignol-Strick, M., Nesteroff, W., Olive, P. and Vergnaud-Grazzini, C.: After the deluge: Mediterranean stagnation and sapropel formation, Nature, 295(5845), 105–110, doi:10.1038/295105a0, 1982.

Sanchez-Gomez, E., Somot, S., Josey, S. A., Dubois, C., Elguindi, N. and Déqué, M.: Evaluation of Mediterranean Sea water and heat budgets simulated by an ensemble of high resolution regional climate models, Clim. Dyn., 37(9–10), 2067–2086, doi:10.1007/s00382-011-1012-6, 2011.

Sevault, F., Somot, S., Alias, A., Dubois, C., Lebeaupin-Brossier, C., Nabat, P., Adloff, F., Déqué, M. and Decharme, B.: A fully coupled Mediterranean regional climate system model: design and evaluation of the ocean component for the 1980–2012 period, Tellus A Dyn. Meteorol. Oceanogr., 66(1), 23967, doi:10.3402/tellusa.v66.23967, 2014.

Somot, S., Sevault, F. and Déqué, M.: Transient climate change scenario simulation of the Mediterranean Sea for the twenty-first century using a high-resolution ocean circulation model, Clim. Dyn., 27(7–8), 851–879, doi:10.1007/s00382-006-0167-z, 2006.

Somot, S., Sevault, F., Déqué, M. and Crépon, M.: 21st century climate change scenario for the Mediterranean using a coupled atmosphere–ocean regional climate model, Glob. Planet. Change, 63(2–3), 112–126, doi:10.1016/j.gloplacha.2007.10.003, 2008.

Soulet, G., Ménot, G., Garreta, V., Rostek, F., Zaragosi, S., Lericolais, G. and Bard, E.: Black Sea "Lake" reservoir age evolution since the Last Glacial — Hydrologic and climatic implications, Earth Planet. Sci. Lett., 308(1–2), 245–258, doi:10.1016/j.epsl.2011.06.002, 2011.

Sperling, M., Schmiedl, G., Hemleben, C., Emeis, K. ., Erlenkeuser, H. and Grootes, P. .: Black Sea impact on the formation of eastern Mediterranean sapropel S1? Evidence from the Marmara Sea, Palaeogeogr. Palaeoclimatol. Palaeoecol., 190, 9–21, doi:10.1016/S0031-0182(02)00596-5, 2003.

Stanev, E. V., Le Traon, P.-Y. and Peneva, E. L.: Sea level variations and their dependency on meteorological and hydrological forcing: Analysis of altimeter and surface data for the Black Sea, J. Geophys. Res. Ocean., 105(C7), 17203–17216, doi:10.1029/1999JC900318, 2000.

Stickler, A., Brönnimann, S., Valente, M. A., Bethke, J., Sterin, A., Jourdain, S., Roucaute, E., Vasquez, M. V., Reyes, D. A., Allan, R. and Dee, D.: ERA-CLIM: Historical Surface and Upper-Air Data for Future Reanalyses, Bull. Am. Meteorol. Soc., 95(9), 1419–1430, doi:10.1175/BAMS-D-13-00147.1, 2014.

Swingedouw, D., Colin, C., Eynaud, F., Ayache, M. and Zaragosi, S.: Impact of freshwater release in the Mediterranean Sea on the North Atlantic climate, Clim. Dyn., 53(7–8), 3893–3915, doi:10.1007/s00382-019-04758-5, 2019.

Vadsaria, T., Li, L., Ramstein, G. and Dutay, J.-C.: Model and output for Vadsaria et al, "Development of a sequential tool LMDZ-NEMO-med-V1 for global to regional past climate simulation over the Mediterranean basin: an early Holocene case study", GMD publication, , doi:10.5281/ZENODO.3258410, 2019.

Vorosmarty, C. J., Feteke, B. M. and Tucker, B. A.: Global River Discharge, 1807-1991, V. 1.1 (RivDIS), , doi:https://doi.org/10.3334/ORNLDAAC/199, 1998.

Williams, M.: Late Quaternary environments in the White Nile region, Sudan, Glob. Planet. Change, 26(1–3), 305–316, doi:10.1016/S0921-8181(00)00047-3, 2000.

Zanchetta, G., Drysdale, R. N., Hellstrom, J. C., Fallick, A. E., Isola, I., Gagan, M. K. and Pareschi, M. T.: Enhanced rainfall in the Western Mediterranean during deposition of sapropel S1: stalagmite evidence from Corchia cave (Central Italy), Quat. Sci. Rev., 26(3–4), 279–286, doi:10.1016/j.quascirev.2006.12.003, 2007.

de Zolt, S., Lionello, P. and Malguzzi, P.: Implementation of an aorcm in the mediterranean sea, 2003.

Zweng, M. M., Reagan, J. R., Antonov, J. I., Mishonov, A. V., Boyer, T. P., Garcia, H. E., Baranova, O. K., Johnson, D. R., Seidov, D. and Bidlle, M. M.: World Ocean Atlas 2013, Volume 2: Salinity, NOAA Atlas NESDIS, 2(1), 39, doi:10.1182/blood-2011-06-357442, 2013.

1058

1059

Supplementary Online Material for

Development of a sequential tool, LMDZ-NEMO-med-V1, to conduct global to regional past climate simulation for the Mediterranean basin: an Early Holocene case study

Tristan Vadsaria[1], Laurent Li[2], Gilles Ramstein[1] and Jean-Claude Dutay[1]

[1]Laboratoire des Sciences du Climat~~s~~ et de l'Environnement, CEA-CNRS- Université Paris Saclay, Gif-sur-Yvette, 91191, France
[2]Laboratoire de Météorologie Dynamique, CNRS-ENS-Ecole polytechnique- Sorbonne Université, Paris, 75005, France

Correspondence to: Tristan Vadsaria (tristan.vadsaria@lsce.ipsl.fr)

The supplementary material includes:

- **Supplementary text**

Text S1: LMDZ-NEMO-med**,** user manual

Text S2: Bias correction

Text S2: Comparison of model simulation outputs with reconstructed data for the whole Mediterranean basin

- **Supplementary figures**

Fig. S1. Runoff of the Nile River

~~**Fig. S21.** Model/reconstruction data C~~~~comparison of model with data for continental precipitation~~

Fig. S2~~3~~2. Model/reconstruction data comparison ~~Comparison of model with data~~ for SST

Fig. S3~~4~~3. Model/reconstruction data comparison ~~Comparison of model with data~~ for SSS

Fig. S4~~5~~4. ~~Interannual evolution of the~~Time series of IS over the Mediterranean Sea in ~~the~~ HIST ~~simulation~~

Fig. S5~~6~~5. Time series of maximum~~Interannual evolution of the~~ ZOF in the eastern Mediterranean Sea in ~~the~~ HIST ~~simulation~~

Fig. S6~~7~~6. ~~Interannual evolution~~Time series of ~~the~~ IS over the Mediterranean Sea in ~~the~~ PICTRL and EHOL ~~simulations~~

Fig. S8~~7~~7. Time series ~~Interannual evolution~~ of ~~the~~ maximum ZOF in the eastern Mediterranean Sea in ~~the~~ PICTRL and EHOL ~~simulations~~

Fig. S8~~9~~9. Time series of SSS for the Mediterranean Sea in PICTRL and EHOL

- **Supplementary tables**

Tab. S1. Model-data comparison for continental precipitation ~~Forcings and parameters used in both AGCM and ARCM~~

Tab. S2. Forcings and parameters used in both AGCM and ARCM

Tab. S3~~2~~. Forcings used in the ORCM

Text S1: LMDZ-NEMO-med, user manual

This section is intended as a user manual to ~~provide an explanation on~~explain how to compile and run LMDZ-NEMO-med on a Linux system. It is not, however, a detailed description of the source code. Files relevant to the running of the pre-industrial control simulation presented in the article have been archived and made publicly available for downloading: https://zenodo.org/record/3258410 (Vadsaria et al., 2019).

1 Atmospheric global model

LMDz4, used here in both the global and regional versions, is version 4 of the LMDZ model. It has the same major code structure and practical organi~~z~~sation as ~~the last version,~~what is consultable on the web page: https://forge.ipsl.jussieu.fr/igcmg_doc/wiki/DocImodelBlmdz

1.1 Compiling the model

The compiling environment is MODIPSL, a convention for code compilation when the code is distributed into different directories. The following directory should be consulted:

"cd vadsaria_et_al_model/LMDZ_and_NEMOMED8_models/modipsl/util"

Edit the "**AA_make.gdef**": the user~~s~~ should create a new entry to fit its computational architecture. Compiler options have been set up in this file and will be propagated to "Makefile" at different places.

It is recommended that all previous configurations be cleared by typing "**./clr_make**". A new configuration to match the right computer platform can then be created:

"**./ins_make -t NAME_OF_YOUR_ARCHITECTURE_SYSTEM"**

Before code compilation, the library netcdf and a Fortran compiler need to be installed. FCM (Flexible Configuration Management: https://metomi.github.io/fcm/doc/), a tool developed by the UK Met Office to manage the dependence ~~between~~ among different subroutines of a complex code is also required. Compiling options for FCM are stored under "machine/arch.path" and "machine/arch.fcm". They need to be coherent with what stored under "**AA_make.gdef**" and "Makefile".

To compile the code, the following directory needs to be consulted:

"cd vadsaria_et_al_model/LMDZ_and_NEMOMED8_models/modipsl/config/LMDZ"

Then, with the help of "Makefile", the following can be compiled:

“gmake lmdz96x71global”

where “**lmdz96x71global**” is a keyword ~~found~~ defined in the “**AA_make**” script allowing a configuration to be chosen.

If the compilation is successful, then the executable codes “create_etat0_limit.e”, “make_relax_times.e” and “gcm.e” are stocked at the following directory:

“cd vadsaria_et_al_model/LMDZ_and_NEMOMED8_models/modipsl/modipsl/bin”

1.2 Running the model

The first step is the creation of boundary conditions for the global atmospheric model. The supporting files needed for this step can be found ~~here~~in the following directory:

“cd vadsaria_et_al_model/files_and_boundary_conditions_for_LMDZ_global/start_limit”

A boundary condition file is already provided in this directory: “**limit_picontrol_debiais.nc**”. It is based on a bias-corrected file for SST and SIC data (following the procedure described in the main article) derived from the IPSLCM5 ~~simulation~~ model for the pre-industrial simulation. The procedure to generate this boundary condition file is the following:

- Prepare a netcdf file with SST and SIC bias-corrected data, interpolated on a 1°x1° grid: “**CM5-piControl-pseudo_amip_1x1_tos_sic.3600-3699_climato.after_correction.nc**” (in the sub-directory “/interpol”, a code to generate a 1°x1° “AMIP” grid is provided : “interpol_ipslcm5_amip_tos_sic.F90”)

- Create symbolic links:

“ln –s CM5-piControl-pseudo_amip_1x1_tos_sic.3600-3699_climato.after_correction.nc amipbc_sic_1x1.nc”

“ln –s CM5-piControl-pseudo_amip_1x1_tos_sic.3600-3699_climato.after_correction.nc amipbc_sst_1x1.nc”

- Move the file obtained from the previous compilation of the model to the current directory and execute:

“./create_etat0_limit.e”

This execution is based on a few “.nc” files containing information on topography, surface albedo, etc. It also takes relevant information from definition files of the model (gcm.def, physic.def and orchidee.def). ~~More information can be found by following the link mentioned at the head of the section).~~ It should create a “**limit.nc**” file.

After creating the initial states and boundary conditions, we are now ready to run the model with an example from the following directory

“cd vadsaria_et_al_model/files_and_boundary_conditions_for_LMDZ_global”

The bash script “**launch_picontrol_run_global_type**” is an example of how to run the atmospheric global model. The script firstly organizes files for boundary conditions and initial state (all presented in the current directory), and then executes the model “**gcm.e**” to generate outputs. This script was initially created for use in the supercomputing centre, TGCC. It contains some TGCC-specific instructions for the management of environmental variables, including the necessary pathways for the model’s preferences and allocation of computing resources, are available. The script is executed with a time step of one month.

To start the execution of the model:

./**launch_picontrol_run_global_make 1**

“**1**” being the first month. It will create the **launch_picontrol_run_global_launcher** bash file. The user should then execute this file according to its the actual operating system. If the script works, it will automatically generate the next iteration (the next month) until the maximum iteration is reached, denoted as the “**stop**” variable in the “**launch_picontrol_run_global_type**” file, set here at 360 months (30 years).

2 Atmospheric regional model

2.1 Compiling the model

The code of this model is identical to that of the global version, but in “Makefile”, the key word should be changed from “lmdz96x71global” to “lmdz200120_oneway”

Go to the following directory:

“cd vadsaria_et_al_model/LMDZ_and_NEMOMED8_models/modipsl/config/LMDZ”

Then compile the code through Makefile:

gmake lmdz200120_oneway

where “**lmdz200120_oneway**” is a keyword ~~found~~ defined in the “**AA_make**” script allowing a configuration to be chosen.

If the compilation is successful, executable files ~~found~~ are stored in the following directory ~~can be applied~~:

“cd vadsaria_et_al_model/LMDZ_and_NEMOMED8_models/modipsl/modipsl/bin”

2.2 Running the model

The first step is to create the boundary conditions for the regional atmospheric model. A boundary condition file, “**limit_picontrol_debiais.nc**”, is already provided in the following directory:

“**/vadsaria_et_al_model/files_and_boundary_conditions_for_LMDZ_regional/start_limit**”

It is of course different from that of the global model, but it is also obtained from ~~a~~ the same bias-corrected ~~file of~~ SST and SIC data, derived from the IPSLCM5 global coupled model for the pre-industrial simulation. The procedure to generate this boundary condition file is the same as described for the global version.

To run the model, an example is given in the following directory

“cd vadsaria_et_al_model/files_and_boundary_conditions_for_LMDZ_regional”

The example bash script “**launch_picontrol_run_regional_type**” shows how to run the atmospheric regional model. Unlike the global model, additional files are needed to nudge the regional model with the global output. “**biline_poids_s.nc’’**, “**biline_poids_u.nc**” and “**biline_poids_v.nc**” (presented in the current directory) are interpolation files allowing efficient transformation of global variables for the regional model grid. Nudged forcing, with a ~~3~~2-hour time step, from the global model is stored in “**sortie_histfrq.nc**.

Since the global and regional models share a common structure, their launch is also very similar, although with different configuration files.

3 Mediterranean oceanic model

NEMOMED8 is the Mediterranean regional version of the NEMO ocean modelling platform. Documentation ~~on the latest version~~ of the model can be found ~~here~~at: http://forge.ipsl.jussieu.fr/nemo/wiki/Users

3.1 Compiling the model

The compilation of NEMOMED8 is managed entirely through MODIPSL, so the generation of Makefile is the same as described earlier for LMDZ. The keyword to be used in the argument of "gmake" is "nemomed8". The compilation procedure is simply the following:

"cd vadsaria_et_al_model/LMDZ_and_NEMOMED8_models/modipsl/config/NEMOMED8"

"gmake nemomed8"

"cd vadsaria_et_al_model/LMDZ_and_NEMOMED8_models/modipsl/modipsl/bin"

If the compilation is successful, then it creates the executable file, "**opa**". In our study, NEMOMED8 is compiled to run with 121 cores in parallel mode.

3.2 Running the model

Before running the model, the 3D boundary conditions for salinity and potential temperature over the buffer zone in the Atlantic close to the Gibraltar need to be generated. This operation is conducted in the following directory:

"cd vadsaria_et_al_model/files_and_boundary_conditions_for_NEMOMED8"

These boundary conditions are found in the files "**data_1m_potential_temperature_nomask_picontrol_debiais_climato.nc**" and "**data_1m_salinity_nomask_picontrol_debiais_climato.nc**", bias-corrected from the IPSLCM5 pre-industrial simulation. The grid of the NEMOMED8 model ("**meshmask_med8.nc**") is provided allowing the user to interpolate their own boundary conditions from this grid.

The second step is to generate the surface fluxes from the atmospheric regional model. ~~For this purpose, a bilinear interpolation is used to convert the LMDz4 air-sea fluxes into the NEMOMED8 grid.~~ For this purpose, an interpolation is used to convert the LMDZ~~z~~4 air-sea fluxes into the

NEMOMED8 grid (bilinear for wind stress and conservative remapping for other fluxes). For NEMOMED8, the water, radiative, latent, sensible fluxes and wind stress are required. In the sub-directory "/lmdz_to_nemo", a code is provided to generate the bilinear interpolation scheme: "interpol_between_lmdz_et_nemo.F90". During the execution of the executable file, a weight file is required ("opalmdmo", also provided in the sub-directory).

"**sst_picontrol_debiais.nc.000101**",

"**flx_picontrol_debiais.nc.000101**",

"**taux_picontrol_debiais.nc.000101**" and

"**tauy_picontrol_debiais.nc.000101**".

Finally, the bash script "**launch_picontrol_run_mediterranean_ocean_type**" is an example of the instructions necessary to run the oceanic regional model. The procedure is similar to the global and regional atmospheric model.

Text S2: Bias correction

The bias correction for our experiments driven by IPSL simulations is illustrated. IPSL-CM5A is a fully coupled climate system model. It operates autonomously for either present-day climate, future climate scenarios, or paleo climate reconstructions, depending on the external forcings or boundary conditions imposed on it. For its historical simulation of modern climate (from 1850 to 2005), we point out a few general biases that need to be corrected before running our regional system for paleo periods (Early Holocene). ~~Below~~In the following, the bias-correction method for the oceanic 3-D structures~~:~~, SST and SIC,~~;~~ as well as~~,~~ the freshwater discharges from rivers, is described.

SST and SIC global fields

The global fields of SST and SIC are the most important variables in our methodology since they contain the main climate change information to be transferred from ~~the~~ global scale to ~~the~~ regional scale. They are used to force both the AGCM and the ARCM. SST derived from IPSL-CM5A has a cold bias globally, which would exert ~~that has a~~ strong impacts on the Mediterranean Sea and the nearby Atlantic region. To remove this bias, we simply applied an offset based on the difference between the IPSL-CM5A historical simulation and the ERA-Interim reanalysis (Dee et al., 2011) for the period 1970-1999.

IPSL-CM5A, on the other hand, tends to overestimate temperatures at the poles, which leads to an underestimation of the SIC. This bias affects the surface albedo and the global energy budget. It also affects the meridional temperature gradient and consequently the mid-latitude atmospheric eddies. The bias correction used for SIC is the analogue method presented in ~~(~~Beaumet et al.~~,~~ (2019). The basic idea

is to adjust the total areas covered by sea ice for each hemisphere and for each month following the geographic and temporal biases. As with the previous corrections for SST, the hemispheric and monthly bias correction for SIC is based on the difference between IPSL simulations and observed SIC (Climatological monthly mean for 1970-1999 from ERA-Interim). Finally, the geographic distribution of SIC is determined by hemisphere and by month following an analogue relationship extracted to match observations from 1970 to 2012.

3D temperatures and salinities in the buffer-zone

The 3-D fields of oceanic temperature and salinity (over the whole water column) in the Atlantic buffer zone has been adjusted in the same way as for SST. We used the World Ocean Atlas (WOA) (Locarnini et al., 2013) as a reference to correct the outputs from the IPSL-CM5A historical simulation.

River runoff to the Mediterranean Sea

Freshwater discharge from rivers around the Mediterranean Sea is an important factor controlling the overturning circulation of the Mediterranean. Due to the high sensitivity of oceanic circulation to this variable, we decided to apply a bias-correction to calibrate the river discharges produced by LMDZ-regional. based on (Ludwig et al., (2009)Ludwig (Climatology 2009) modified using simulated precipitation anomalies between Early Holocene and present day. Since Actually, the atmospheric model (LMDZ4, and especially the regional configuration, LMDZ4 regional), coupled to the land surface model, ORCHIDEE, tends to overestimate the amount of freshwater runoffs in LMDZ4 compared to present-day observations (fFigure S1)., The bias-corrected that we applied a bias-correction withis based on the observed climatological runoff (Ludwig et al. 2009; Vorosmarty et al., 1998) and the differences between the Early Holocene simulation and present-day simulation. When the difference is relatively not significant, the corrected runoff is set to the climatology, mainly to avoid negative values[1]. However, in order to stay consistent with the methodology for SST and SIC bias correction, we chose the absolute difference correction method for the river runoff. This correction is based on the monthly difference between LMDZ4 runoff and climatology (Ludwig et al., 2009; Vorosmarty et al., 1998).

Text S3: Comparison of model simulation outputs and reconstructed data for the Mediterranean basin

Continental precipitation

The reconstructed data used for the comparison with the EHOL simulation is taken from (Dormoy et al., (2009) for the Aegean Sea, from (Peyron et al., (2011) for the Lake Accesa and from Tenaghi Philippon, and (Magny et al., (2013) for Lake Pergusa. In these studies, continental precipitation is

[1] Namely, when the difference does not exceed 25%, of the annually average annual difference for the Nile river runoff (due to the simulated amplitude, cf section 4.4) and 5% for the rest of the rivers.

reconstructed based on pollen sequences to emphasis the changes in precipitation seasonality. Several methods are used to determine these changes. We chose to reconstruct these changes using the Modern Analogue Technique (MAT, ~~(~~Guiot, 1990~~)~~), because, in their study, Magny et al. (2013) compared their data to Peyron et al. (2011)~~'s MAT~~. We extracted data values framing a few hundred years around 9.5 ka cal BP, consistent with~~because~~ the orbital parameters of our atmospheric simulations (both global and regional) ~~were set as they were during this period~~. For the Northern Sahara, data are based on $\delta^{18}O$ from ~~(~~Bar-Matthews et al.~~,~~(2003).

Comparison between model outputs and reconstruction data in terms of annual and seasonality changes can be conducted ~~-~~and anomalies against modern values can be shown. In winter, the model shows positive precipitation anomalies for the four sites (Lake Accesa, model: ~~+~~20-36 mm, data: ~~+~~20-40mm, Tenaghi Philippon, model: ~~+~~30-45 mm, data: ~~+~~10-35 mm, Aegean, model: ~~+~~29-45 mm, data: ~~+~~10-80mm, Lake Pergusa, model: ~~+~~7-26 mm, data: ~~+~~35-60mm, ~~f~~Figure ~~2~~Table S1~~1, a d g i~~). In summer, the model shows a more contrasted response, with negative anomalies in summer temperatures (~~Figure 2~~1, ~~b e, h, j~~Table S1) due to the homogenous drought (~~f~~Fig ~~8~~10d in the main article). However, this comparison cannot reflect the precipitation changes for ~~-~~the entire continent. Indeed, in north of Lake Accesa we see positive summer anomalies (~~f~~Fig ~~8~~10d in the main article). ~~Our model underestimates precipitation over northern Sahara and northern Africa as do most Mid and Early Holocene simulations. As mentioned earlier, the LMDZz model cannot reproduce the northward shift of the last African Humid Period, leading to an underestimatione of precipitation.~~

Sea Surface Temperatures

We conducted a comparison of model output and data for SST as Adloff et al., (2011) did with the reconstruction of Kucera et al., (2011) (unpublished work). This reconstruction is based on census counts of foraminiferal species, and on the artificial neural network for the transfer function. The data used span the Holocene Insolation maximum interval (8.5 - 9.5 ka BP). Winter SST values (January to March, ~~f~~Figure S2~~3~~2, f) are a bit lower than the reconstruction ~~figures~~ especially for the Eastern basin (-1 to -2 °C). The simulated summer SSTs (July to September, ~~f~~Figure S3~~2~~, j) are higher between the Tyrrhenian Sea and the Levantine Sea (+1 to +4 °C). This enhanced contrast between winter and summer values for simulated SST produced an annual signal in good agreement with the reconstructed values (~~f~~Figure S3~~2~~, c). Our results depict the same signal pattern as the simulations of Adloff et al.~~,~~ (2011) do, with some differences in the enhanced seasonal contrast. In ~~f~~Figure S~~2~~3 are also depicted the same climatology for the bias Early Holocene SST and the bias corrected Early Holocene SST boundary conditions used in the model architecture. This figure shows how the SST signal have been improved, from the bias correction to the ORCM simulation, in order to range the reconstruction with the use of the regional models.

Sea Surface Salinities

The comparison of SSS~~s~~ over the Mediterranean Sea provides an appropriate indicator of freshwater perturbation induced by enhanced river fluxes. ~~In order to perform the~~As a reference for comparison, we use~~d~~ a synthesis ~~(Kallel et al., 1997)~~ of SSS ~~values~~ sampled from the S1 deposition, and provided by Kallel et al. (1997). Our EHOL simulation takes the Nile river enhancement into account, that is an annual river discharge of 13000 m^3.~~/~~s^{-1}, against ~~annually (~~2930 $m^3.s^{-1}$ ~~m^3/s,~~ for the pre-industrial value)~~,~~ ~~and t~~ The North-East river~~s margin enhancement~~ (Buyukmenderes, Vardar, Acheloos, Vjosa, Semanit, Shkumbin, Durres, Mat and Drini)~~,~~ have their annual fresh water discharges increasing from 1082 $m^3.s^{-1}$ ~~m^3/s~~ at pre-industrial level to ~~for a total of~~ 1622 $m^3.s^{-1}$ ~~m^3/s~~. The fresh water discharge from February to May increases even more, from 1619 $m^3.s^{-1}$ ~~m^3/s~~ at pre-industrial level to ~~annually and~~ 3228 $m^3.s^{-1}$ ~~m^3/s~~ for EHOL.~~from February to May (1082/1619 m^3/s pre-industrial), inferred from the precipitation anomalies of the regional atmospheric model.~~ Our EHOL simulation, even ~~using the strongest~~with a significant increase of freshwater inputs, still cannot reproduce a sufficient decrease ~~in~~ of SSS ~~sufficient~~ to match the reconstructed values, as shown in ~~f~~Figure S3~~4~~3. ~~This reflects the results of~~ . ~~Indeed, as demonstrated by~~ Rohling (1999, 2000~~),~~) pointed out that this mismatch can be partly attributed to uncertainties in salinity reconstruction. It is not always straightforward to interpret the isotopic composition of oxygen in terms of salinity. Finally, it is likely that an additional non-negligible fresh water source is missing. To explain the substantial SSS decrease, an additional source of freshwater associated with an amplification of the flux of the North African rivers could potentially be superimposed on the Nile. Indeed, changes of this type in the hydrology are clearly indicated by the data but are not reproduced in most of the Early and Mid-Holocene simulations.

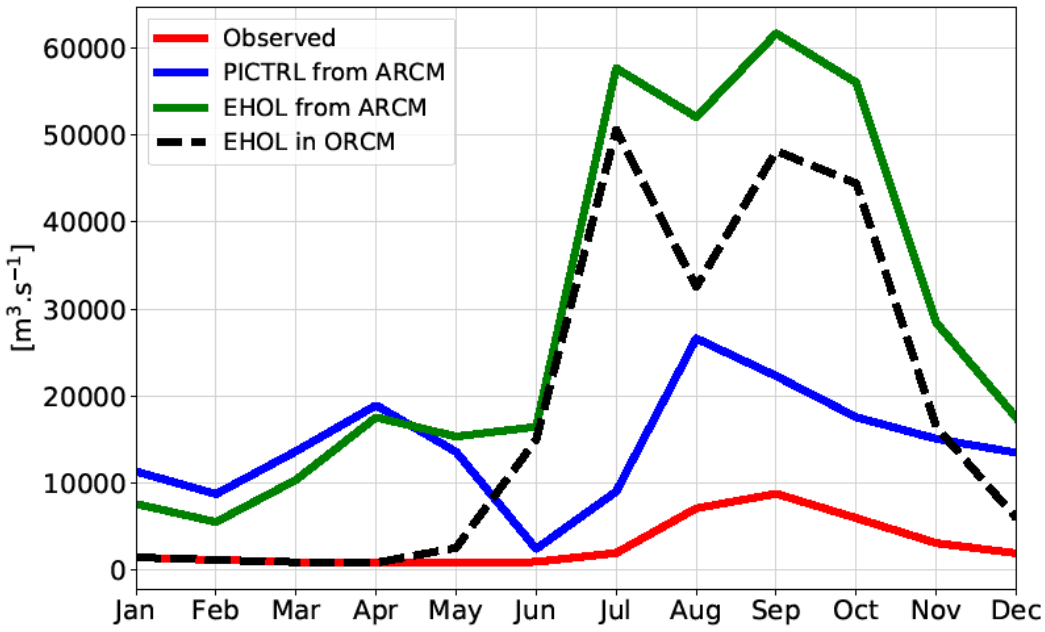

Figure S1: climatological runoff of the Nile River, observed pre-damming values (red), runoff as simulated by the ARCM, PICTRL (blue) and EHOL (green), and corrected runoff used in the ORCM.

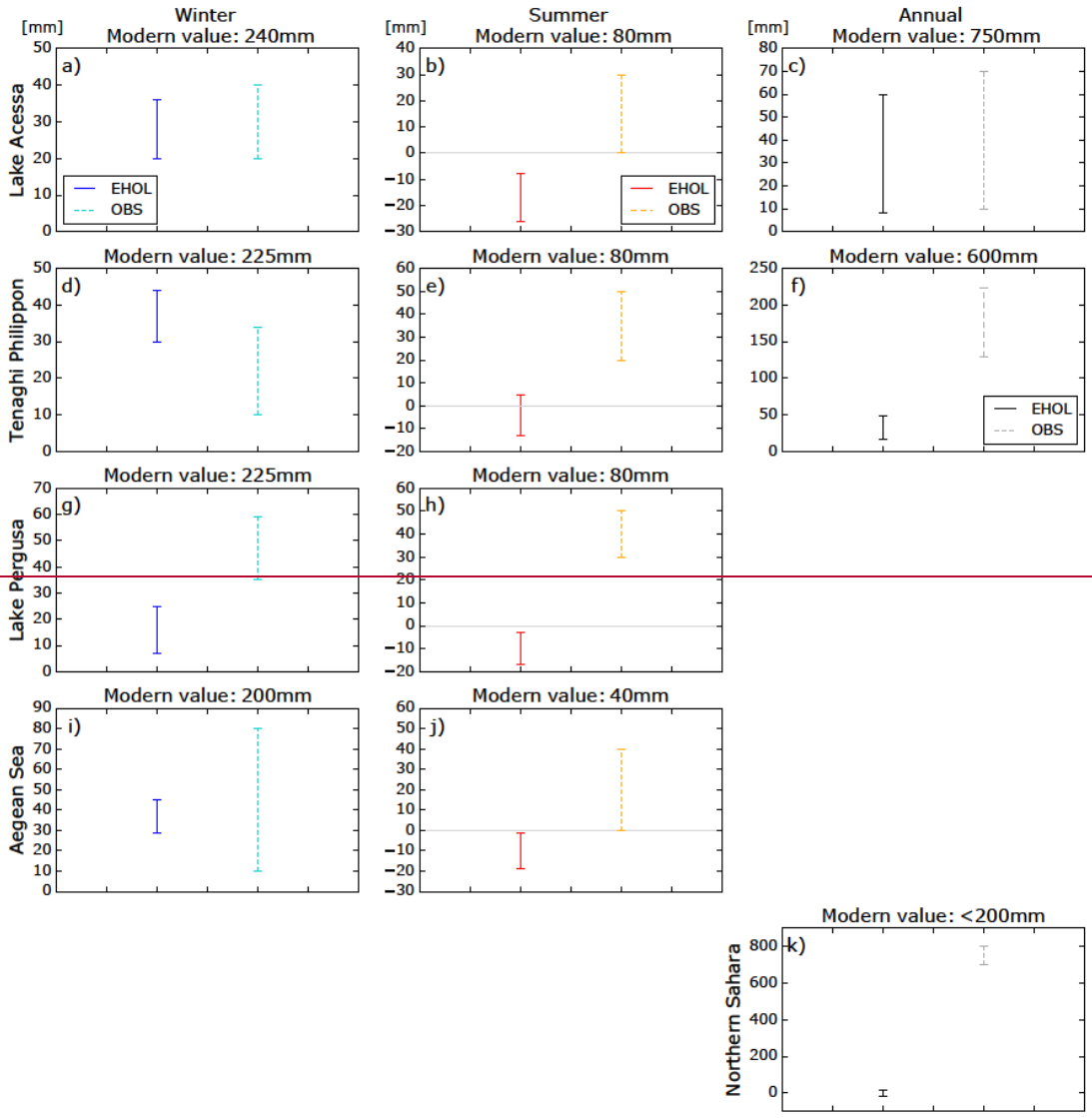

~~**Figure S1: Model-data comparison for continental precipitation (solid lines = EHOL simulation, dashed lines = pollen data reconstruction). First row: Lake Accesa (Northern Italy) (Peyron et al., 2011), Second row: Tenaghi Philippon, (Greece) (Peyron et al., 2011), Third row: Lake Pergusa (Sicily), (Magny et al., 2013), Fourth row: Aegean Sea, (Dormoy et al., 2009), Fifth row: Northern Sahara (Bar-Matthews et al., 2003). First column: winter precipitation, Second column: summer precipitation, Third column: annual precipitation.**~~

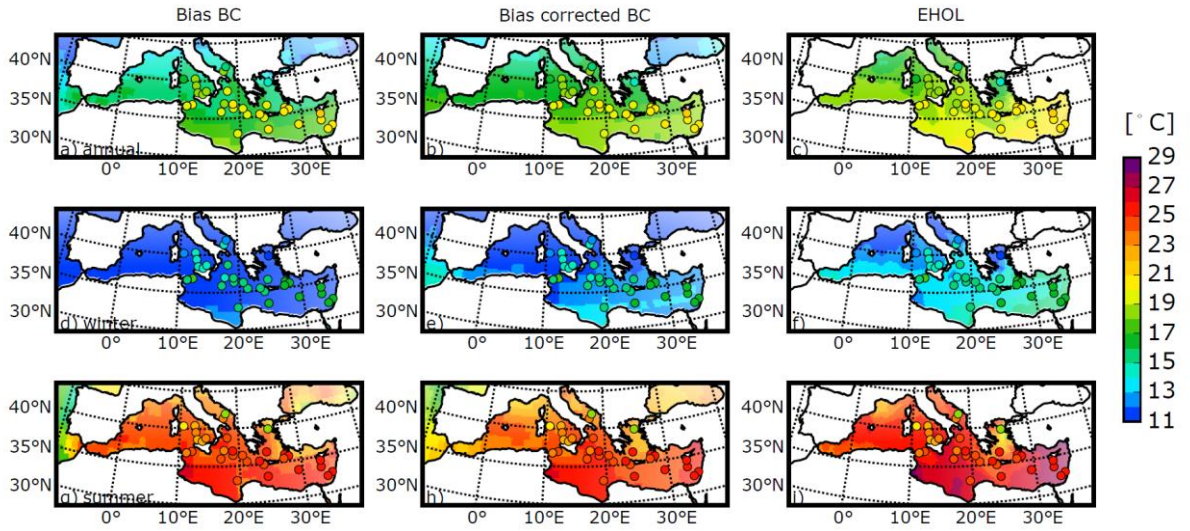

Figure S4~~2~~2: Model-data comparison for SST, adapted from Adloff (2011). Dots represent the unpublished synthesis of Kucera et al. (2011), published in Adloff (2011). The background colour represents~~ , in the first column, the bias SST boundary conditions (BC) derived from the Early Holocene IPSL-CM5 simulation (AMIP resolution), in the second column, the bias corrected SST BC as it has been used to drive the AGCM and the AGCM both (AMIP resolution), and, in the third column, SST in the EHOL ~~simulation~~experiment realized with the ORCM (1/8°, averaged over the last 30 years of simulation). ~~.~~

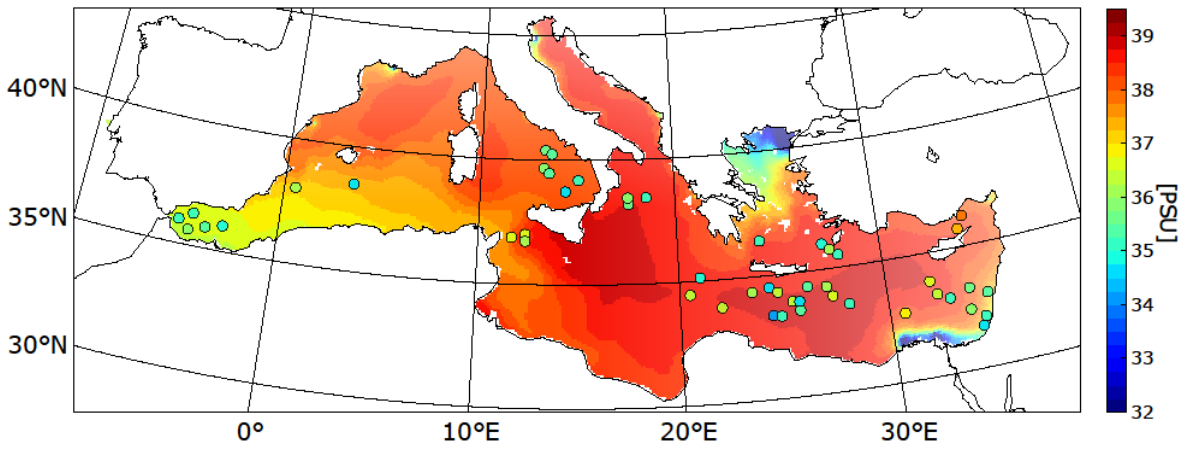

Figure S5~~3~~3: Model-data comparison for SSS. Dots represent the synthesis of Kallel et al. (1997a). The background colour represents the EHOL simulation.

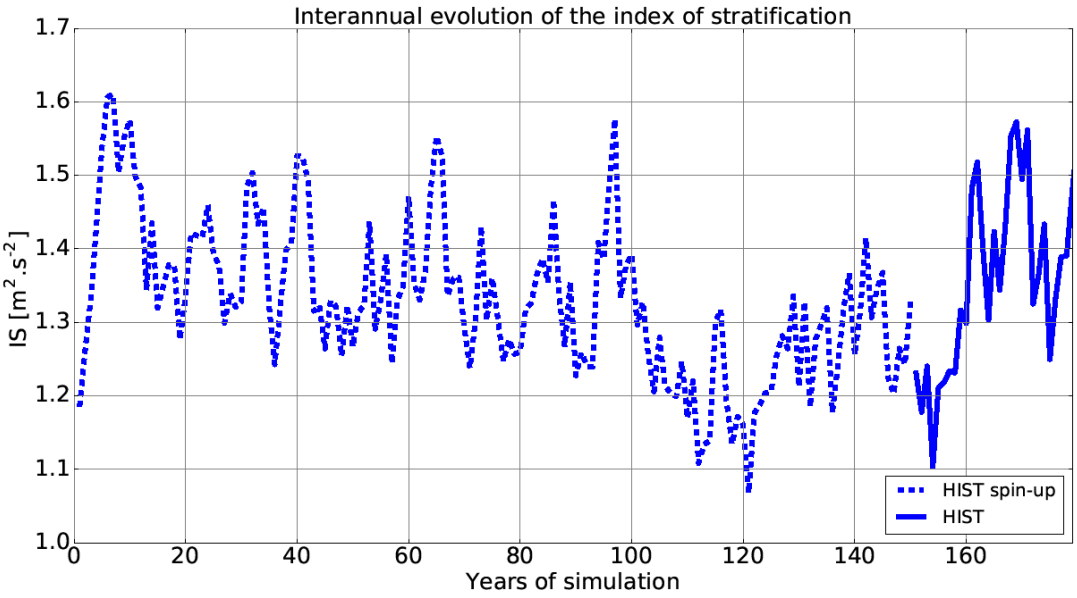

Figure S~~6~~44: Interannual evolution of the index of stratification (IS) for the Mediterranean Sea for the HIST simulation (including the spin-up phase).

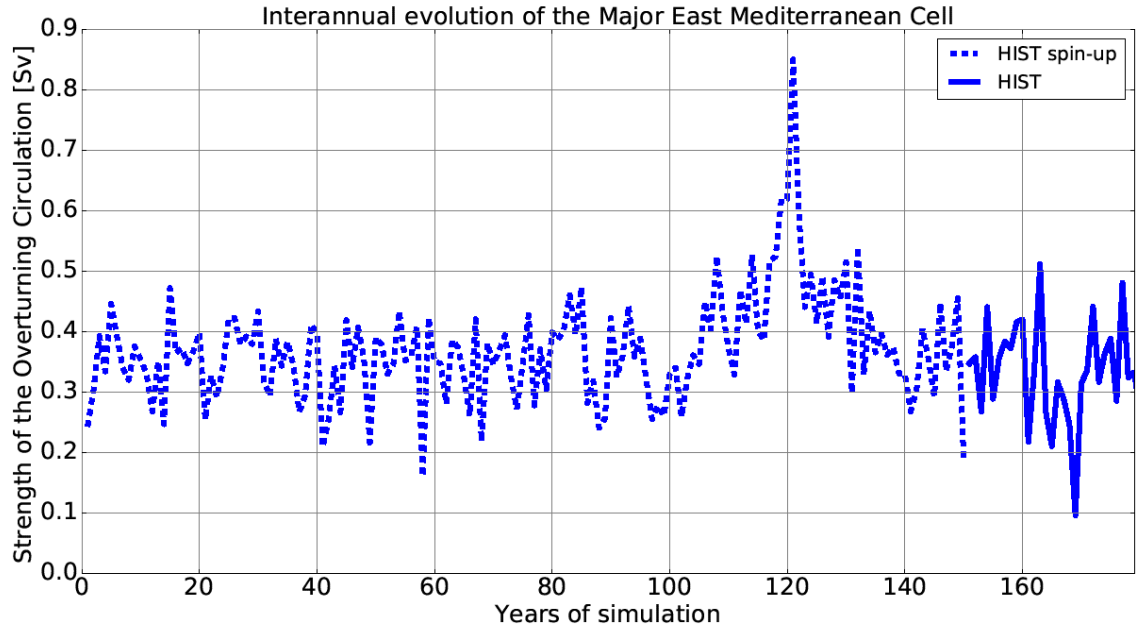

Figure S~~7~~55: Interannual evolution of the Zonal overturning Stream Function (ZOF) in the eastern Mediterranean Sea for the HIST simulation (including the spin-up phase).

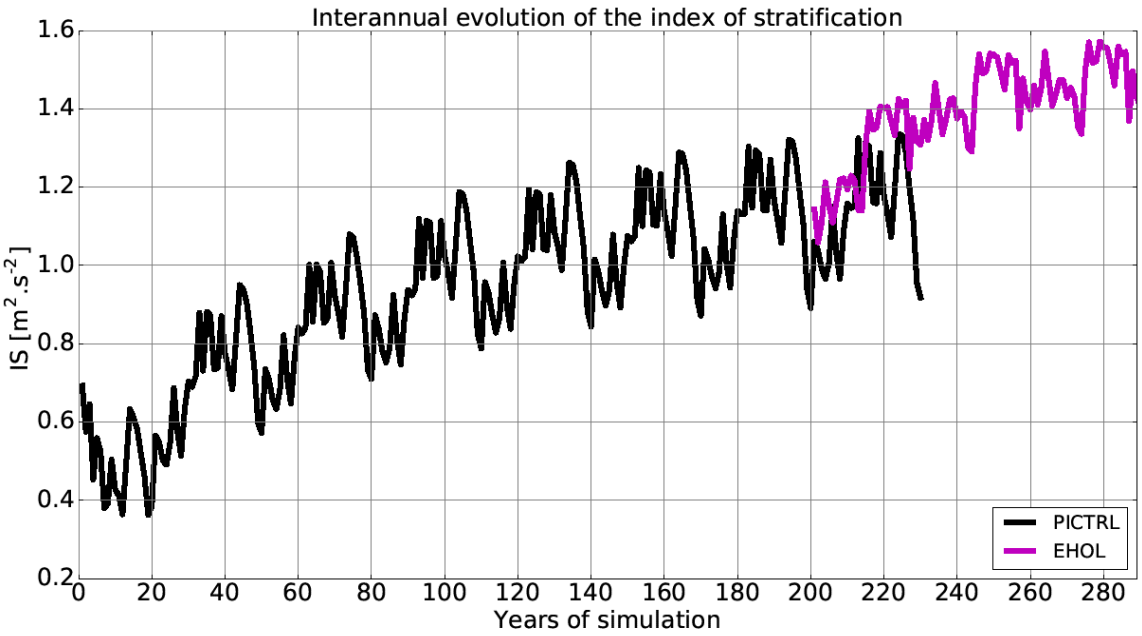

Figure S~~8~~6: Interannual evolution of the index of stratification (IS) for the Mediterranean Sea for the PICTRL and EHOL simulations (including the ~~PTCRL~~ PICTRL spin-up phase).

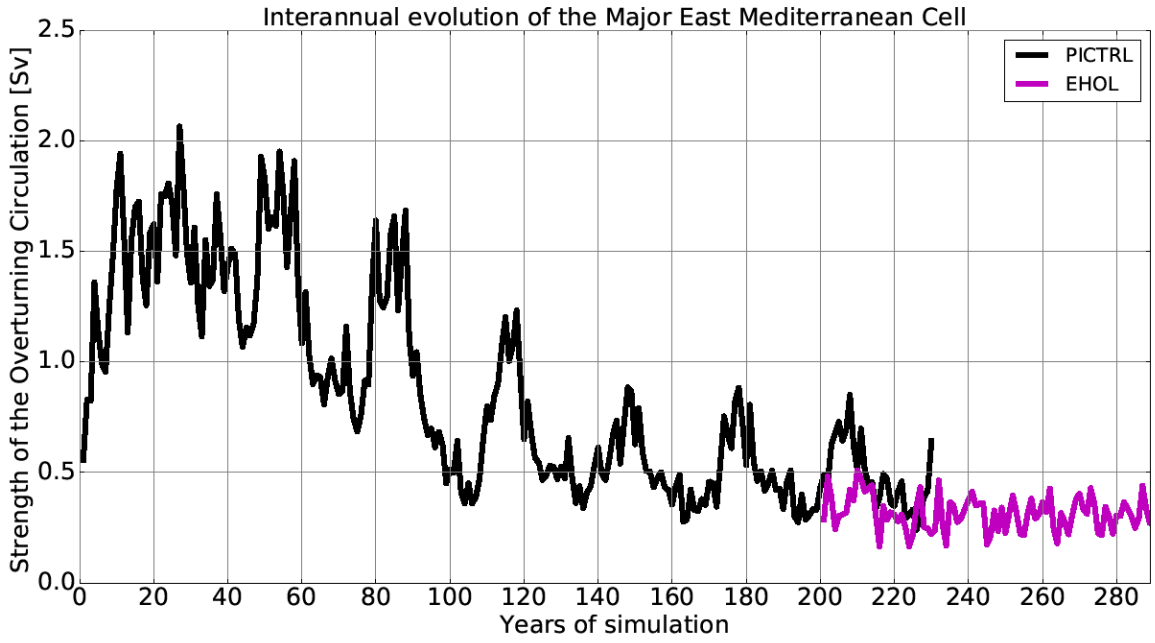

Figure S~~9~~7: Interannual evolution of the Zonal overturning Stream Function (ZOF) in the eastern Mediterranean Sea for the PICTRL and EHOL simulations (including the PICTRL spin-up phase).

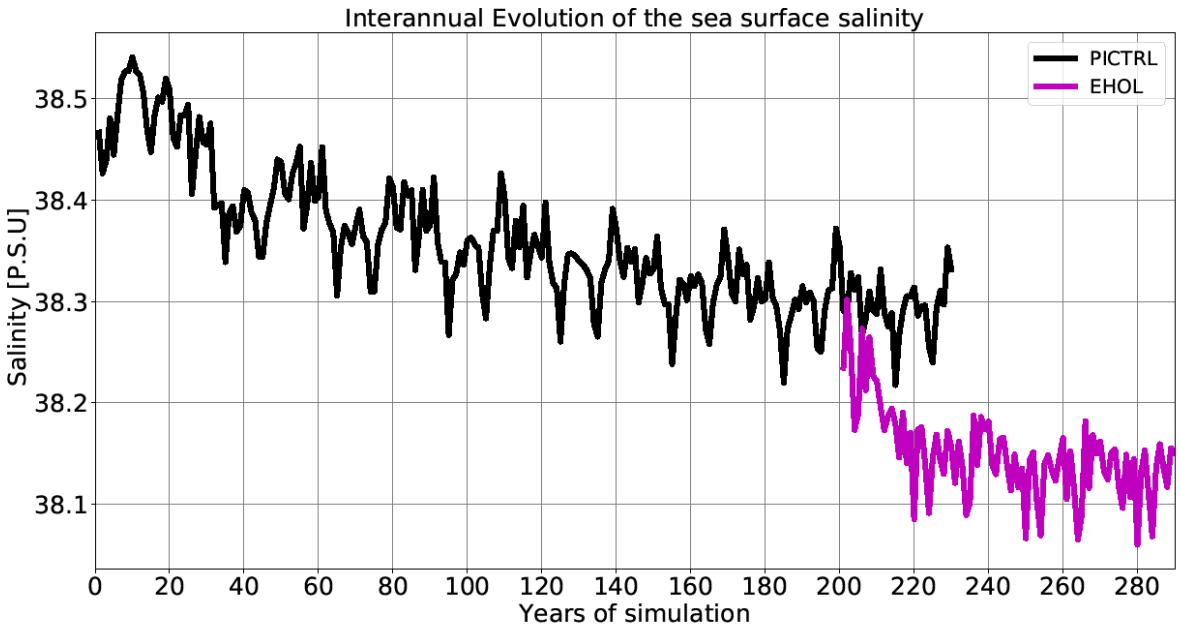

Figure S8~~10~~: Interannual evolution of the sea surface salinity (SSS) for the Mediterranean Sea for the PICTRL and EHOL simulations (including the PICT~~C~~RL spin-up phase).

Precipitation (mm)	Winter			Summer			Annual		
	MODERN	ΔOBS	ΔEHOL	MODERN	ΔOBS	ΔEHOL	MODERN	ΔOBS	ΔEHOL
Lake Acessa	240	20-40	20-36	80	0-30	(-26)-(-8)	750	10-70	8-60
Tenaghi Philippon	225	10-35	30-45	80	20-50	(-13)-5	600	130-225	17-49
Lake Pergusa	225	35-60	7-26	80	30-50	(-17)-(-3)			
Aegean Sea	200	10-80	29-45	40	0-40	(-19)-0			
Northern Sahara							<200	700-800	(-20)-15

Table S1: Model-data comparison for continental. First row: Lake Accesa (Northern Italy) (Peyron et al., 2011), Second row: Tenaghi Philippon, (Greece) (Peyron et al., 2011), Third row: Lake Pergusa (Sicily), (Magny et al., 2013), Fourth row: Aegean Sea, (Dormoy et al., 2009), Fifth row: Northern Sahara (Bar-Matthews et al., 2003). "MODERN" refers to the present values of precipitation, "OBS" to the data (around 9.5 ka cal BP), and "EHOL" for the Early Holocene simulation described in the article.

	HIST	PICTRL	EHOL
Orbital parameters	e = 0.01672 ε = 23.44 ω -180 = 102.7	~~Idem~~Same as in HIST	e = 0.01935 ε = 24.231 ω -180 = 303.3
Atmospheric CO_2	Annual observed global mean (1970-1999)	284~~0~~ ppm	2~~64884~~0 ppm
SST forcing	Era-Interim monthly forcing (1970-1999	IPSL-CM5A picontrol + SST correction	IPSL-CM5A early Holocene + SST correction
SIC forcing	Era-Interim monthly forcing (1970-1999	IPSL-CM5A picontrol + SIC correction	IPSL-CM5A Early Holocene + SIC correction

Table S2~~1~~: Forcings and parameters used in both AGCM and ARCM. ε is the elliptic orbit obliquity, e, the eccentricity and ω, the longitude of the perihelion.- The reader can notice that the

pCO_2 should be 260 ppm as suggested by the PMIP protocol for mid-Holocene. The goal in this paper was mainly to have a sensitivity to orbital parameters.

	HIST	PICTRL	EHOL
Buffer-zone T3D & S3D	WOA monthly forcing (1970-1999 mean)	IPSL-CM5A picontrol + T3D/S3D correction	IPSL-CM5A early Holocene + T3D/S3D correction
River runoff	Ludwig et al 2009, Rivdis database	Ludwig et al 2009, Rivdis database (But Pre-damming Nile)	Anomalies inferred from EHOL – PICTRL atmospheric simulations (NILE + East-North margin)

Table S3~~2~~: Forcings used in the ORCM.

References

Adloff, F., Mikolajewicz, U., Kučera, M., Grimm, R., Maier-Reimer, E., Schmiedl, G. and Emeis, K. C.: Upper ocean climate of the Eastern Mediterranean Sea during the Holocene Insolation Maximum - A model study, Clim. Past, 7(4), 1103–1122, doi:10.5194/cp-7-1103-2011, 2011.

Bar-Matthews, M., Ayalon, A., Gilmour, M., Matthews, A. and Hawkesworth, C. J.: Sea - land oxygen isotopic relationships from planktonic foraminifera and speleothems in the Eastern Mediterranean region and their implication for paleorainfall during interglacial intervals, Geochim. Cosmochim. Acta, 67(17), 3181–3199, doi:10.1016/S0016-7037(02)01031-1, 2003.

Beaumet, J., Krinner, G., Déqué, M., Haarsma, R. and Li, L.: Assessing bias-corrections of oceanic surface conditions for atmospheric models, Geosci. Model Dev. Discuss., (December), 1–29, doi:10.5194/gmd-2017-247, 2017.

Dee, D. P., Uppala, S. M., Simmons, A. J., Berrisford, P., Poli, P., Kobayashi, S., Andrae, U., Balmaseda, M. A., Balsamo, G., Bauer, P., Bechtold, P., Beljaars, A. C. M., van de Berg, L., Bidlot, J., Bormann, N., Delsol, C., Dragani, R., Fuentes, M., Geer, A. J., Haimberger, L., Healy, S. B., Hersbach, H., Hólm, E. V., Isaksen, L., Kållberg, P., Köhler, M., Matricardi, M., Mcnally, A. P., Monge-Sanz, B.

M., Morcrette, J. J., Park, B. K., Peubey, C., de Rosnay, P., Tavolato, C., Thépaut, J. N. and Vitart, F.: The ERA-Interim reanalysis: Configuration and performance of the data assimilation system, Q. J. R. Meteorol. Soc., 137(656), 553–597, doi:10.1002/qj.828, 2011.

Dormoy, I., Peyron, O., Combourieu Nebout, N., Goring, S., Kotthoff, U., Magny, M. and Pross, J.: Terrestrial climate variability and seasonality changes in the\rMediterranean region between 15 000 and 4000 years BP deduced\rfrom marine pollen records, Clim. Past, 5, 615–632, 2009.

Guiot, J.: Methodology of the last climatic cycle reconstruction in France from pollen data, Palaeogeogr. Palaeoclimatol. Palaeoecol., 80(1), 49–69, doi:10.1016/0031-0182(90)90033-4, 1990.

Kallel, N., Paterne, M., Labeyrie, L., Duplessy, J. C. and Arnold, M.: Temperature and salinity records of the Tyrrhenian Sea during the last 18,000 years, Palaeogeogr. Palaeoclimatol. Palaeoecol., 135(1–4), 97–108, doi:10.1016/S0031-0182(97)00021-7, 1997.

Kucera, M., Rohling, E. J., Hayes, A., Hopper, L. G. S., Kallel, N., Buongiorno Nardelli, B., Adloff, F. and Mikolajewicz, U.: Sea surface temperature of the Mediterranean Sea during the early Holocene insolation maximum, Clim. Past, 2011.

Locarnini, R. A., Mishonov, A. V., Antonov, J. I., Boyer, T. P., Garcia, H. E., Baranova, O. K., Zweng, M. M., Paver, C. R., Reagan, J. R., Johnson, D. R., Hamilton, M. and Seidov, D.: World Ocean Atlas 2013, Volume 1: Temperature, NOAA Atlas., edited by S. Levitus and A. Mishonov., 2013.

Ludwig, W., Dumont, E., Meybeck, M. and Heussner, S.: River discharges of water and nutrients to the Mediterranean and Black Sea: Major drivers for ecosystem changes during past and future decades?, Prog. Oceanogr., 80(3–4), 199–217, doi:10.1016/j.pocean.2009.02.001, 2009.

Magny, M., Combourieu-Nebout, N., De Beaulieu, J. L., Bout-Roumazeilles, V., Colombaroli, D., Desprat, S., Francke, A., Joannin, S., Ortu, E., Peyron, O., Revel, M., Sadori, L., Siani, G., Sicre, M. A., Samartin, S., Simonneau, A., Tinner, W., Vannière, B., Wagner, B., Zanchetta, G., Anselmetti, F., Brugiapaglia, E., Chapron, E., Debret, M., Desmet, M., Didier, J., Essallami, L., Galop, D., Gilli, A., Haas, J. N., Kallel, N., Millet, L., Stock, A., Turon, J. L. and Wirth, S.: North-south palaeohydrological contrasts in the central mediterranean during the holocene: Tentative synthesis and working hypotheses, Clim. Past, 9(5), 2043–2071, doi:10.5194/cp-9-2043-2013, 2013.

Peyron, O., Goring, S., Dormoy, I., Kotthoff, U., Pross, J., de Beaulieu, J.-L., Drescher-Schneider, R., Vannière, B. and Magny, M.: Holocene seasonality changes in the central Mediterranean region reconstructed from the pollen sequences of Lake Accesa (Italy) and Tenaghi Philippon (Greece), The Holocene, 21(1), 131–146, doi:10.1177/0959683610384162, 2011.

Rohling, E. J.: Environmental control on Mediterranean salinity and δ 18 O, Paleoceanography, 14(6), 706–715, doi:10.1029/1999PA900042, 1999.

Rohling, E. J.: Paleosalinity: Confidence limits and future applications, Mar, Mar. Geol., 163, 1–11, doi:10.1016/S0025-3227(99)00097-3, 2000.

Vadsaria, T., Li, L., Ramstein, G., & Dutay, J.-C.: Model and output for Vadsaria et al, "Development of a sequential tool LMDZ-NEMO-med-V1 for global to regional past climate simulation over the Mediterranean basin: an early Holocene case study", GMD publication. doi:10.5281/zenodo.3258409, 2019.

Vorosmarty, C. J., Feteke, B. M. and Tucker, B. A.: Global River Discharge, 1807-1991, V. 1.1 (RivDIS), 1998.

Requested minor revisions to gmd-2019-196

Dear Lauren Gregoire,
We are very pleased about your decision about the manuscript.
We also thank you for the new comments you addressed. Please see our reply.

L228: Clarify the procedure for boundary conditions applied when running NEMO ocean only model. This paragraph is currently too vague and It's difficult to make sense of it. Clarify what the flux are, what the restoring term is and what the constant coefficient controls. If there is a paper you can cite that would be great, otherwise please include an equation.

Indeed, that the flux and restoring term comes from Barnier et al., 1995, we inserted the reference in the new version of the manuscript (L226 and L715).

L306: "The global simulation, after SST bias correction, ranged with the observation, compared to IPSLCM5A (Figure 2)." "ranged with the observation" is not clear. Do you mean "has the same range of variability as e.g. the 2m temperature over the Mediterranean region from ERA20C" ?

We apologize that there was a misunderstanding in our results description. Actually, the line you mentioned only describes the global average of 2m temperature and it is not related to the Mediterranean. We suspect that the word "range" was inappropriately used. We made the necessary changes in the new manuscript. By the way, we also make a slight change for the regional aspect over the Mediterranean:

L302

Previous sentence: "The global simulation, after SST bias correction, ranged with the observation, compared to IPSLCM5A (Figure 2)"

New sentence: "The global simulation (continued red curve in Fig. 2), after SST bias correction, is very close to the observation (continued black curve), with a tremendous improvement compared to IPSLCM5A (green curve in Figure 2)." The regional model reproduces the warming trend and aspects of the interannual variability close to observations, **but with a mean cold shift of about -0.6°C.**

L219 "A first dataset of climatological river discharges is proposed by default to cover the entire Mediterranean draining basin with represents 33 river mouths." What do you mean by "is proposed" to whom, for what? How is it used? Please clarify the text.

We apologize again for the confusion. Actually, that dataset of rivers freshwater discharges was constructed by the initial NEMOMED model developers, and was proposed to us (authors of the manuscript) to be used if we don't include the rivers interactively. We changed this paragraph into past tense ("is" to "was", L216), which can help to remove the confusion. "A dataset of climatological river discharges was proposed by default within the NEMOMED8 platform to cover the entire Mediterranean draining basin with 33 river mouths."

"[Reviewer comment]

P7 lines 211-213: how realistic is the assumption that water from the Black Sea is fresh? And does the Q+P-E budget over the Black Sea derive from the AGCM orARCM?
[Reply]
It is a commonly-used treatment when the Mediterranean model doesn't include the Black Sea. The fresh water assumption is entirely justified although the actual water flow from the Black Sea can be salty, since what we evaluated in terms of E, P and Runoff is indeed the fresh water budget. What is important in the model is not the water mass itself, but the salt content. We made some revisions in the new manuscript for this regard."
I can't see how and where you have addressed this point. Please clarify with citation of the text.

For this purpose, we update the text at l221 "The Black Sea fresh water assumption comes from NEMOMED modeling community that consider it as a yearly source of freshwater" and l450 "For this part, the water budget over the Black Sea is calculated from the ARCM output"

"[Reviewer comment]
P14 lines 362-364: Figures 2 and 4 show that your simulation results in significantly lower temperatures than observed, yet here you say they are consistent?
[Reply]
Yes, there are cold biases. We changed the corresponding text in the revised manuscript "The atmospheric simulation is acceptable compared with observations for the air temperature at 2m at both global and regional scales "(l405)."
I am not satisfied with how you have addressed this point. Changing the word "consistent" with "acceptable" just makes a wrong statement into something vague and subjective. Please quantify and describe the cold bias and discuss the implications here.

Indeed, we made the following correction l417: "Validation of our platform was based on the historical period from1970 to 1999. after bias correction of global SST, the 2-m surface air temperature in the HIST global simulation is comparable to the observational counterpart. However, the simulated surface air temperature within the regional model is colder (as shown in Figure2), which implies SST cold biases for the Mediterranean Sea"

"[Reviewer comment]
P22, lines 522-525: what do you mean by the reference for correction is the preindustrial state? How is river runoff corrected based on pre-industrial climate?
[Reply]
We choose to "correct" the Mediterranean river runoff during the Early Holocene based on the precipitation difference (EHOL – PICTRL) coming from both the ARCM and AGCM and apply it to the PICTRL river runoff (which was prescribed). The procedure of river runoff is detailed in the supplementary material (**Text S2: Bias correction**)"
This point hasn't been addressed adequately, please correct the text when you make reference to the "correction" to clarify that you apply a bias correct as described in Text S2.

If we understand well, we just need to clarify the response in the manuscript l593. « The procedure of river runoff is detailed in the supplementary material (Text S2: Bias correction) »

Editorial corrections (suggested changes in bold):

Thanks, we took all of these suggestions into account.

~~L 153: "This architecture is based on a method **that provides** as much **compatibility** as possible among**st** the models used and high **consistency** with data."~~

~~L224L "river mouths **that** cover the …"~~

~~L330 " both the precipitation and evaporation over the Mediterranean Sea in HIST **are** very close to the observations"~~ Quantify how close.

L331"but both the precipitation and evaporation over the Mediterranean Sea in HIST are very close to the observations**, with 10 mm.yr^{-1} of oceanic precipitation difference between HIST and the mean observation value (by taking the upper and the lower value), and 18 mm.yr^{-1} for the oceanic evaporation.**"

~~L331 "**The** two other simulations **included in Table 1**, PICTRL and EHOL, are those designed to investigate**s** the Early Holocene climate **(see Section 4)**."~~

~~L407: "The ZOF **in HIST depicted in Figure 6)"**~~

~~Figure 6: replace row numbers with figure labels (a-h)~~

~~L425 It is not correct to say "ranges with the observation". Do you mean "has the same range of variability as the observations"~~

Please see the new version of the main manuscript, the supplement remains unchanged.

Regards

Tristan Vadsaria on Behalf of all co-authors

Added reference L715:

Barnier, B., Siefridt, L. and Marchesiello, P.: Thermal forcing for a global ocean circulation model using a three-year climatology of ECMWF analyses, J. Mar. Syst., 6(4), 363–380, doi:10.1016/0924-7963(94)00034-9, 1995.

Development of a sequential tool, LMDZ-NEMO-med-V1, to conduct global to regional past climate simulation for the Mediterranean basin: An Early Holocene case study

Tristan Vadsaria[1,3], Laurent Li[2], Gilles Ramstein[1] and Jean-Claude Dutay[1]

[1]Laboratoire des Sciences du Climat et de l'Environnement, CEA-CNRS- Université Paris Saclay, Gif-sur-Yvette, 91191, France
[2]Laboratoire de Météorologie Dynamique, CNRS-ENS-Ecole Polytechnique- Sorbonne Université, Paris, 75005, France
[3]Atmosphere and Ocean Research Institute, University of Tokyo, Kashiwanoha, Chiba, Japan

Correspondence to: Tristan Vadsaria (tristan.vadsaria@lsce.ipsl.fr)

Abstract

Recently, major progress has been made in the simulation of the ocean dynamics of the Mediterranean using atmospheric and oceanic models with high spatial resolution. High resolution is essential to accurately capture the synoptic variability required to initiate intermediate and deep-water formation, the engine of the MTC (Mediterranean Thermohaline Circulation). In paleoclimate studies, one major problem with the simulation of regional climate changes is that boundary conditions are not available from observations or data reconstruction to drive high-resolution regional models. One consistent way to advance paleoclimate modelling is to use a comprehensive global to regional approach. However, this approach needs long-term integration to reach equilibrium (hundreds of years), implying enormous computational resources. To tackle this issue, a sequential architecture of a global-regional modelling platform has been developed for the first time and is described in detail in this paper. First of all, the platform is validated for the historical period. It is then used to investigate the climate and in particular, the oceanic circulation, during the Early Holocene. This period was characterised by a large reorganisation of the MTC that strongly affected oxygen supply to the intermediate and deep waters, which ultimately led to an anoxic crisis (called sapropel). Beyond the case study shown here, this platform may be applied to a large number of paleoclimate contexts from the Quaternary to the Pliocene, as long as regional tectonics remain mostly unchanged. For example, the climate responses of the Mediterranean basin during the last interglacial (LIG), the last glacial maximum (LGM) and the Late Pliocene, all present interesting scientific challenges which may be addressed using this numerical platform.

1 Framework of the study

1.1. Introduction

The Mediterranean basin is a key region for the global climate system. It is considered to be a climate "hotspot" (Giorgi, 2006), due to its high sensitivity to global warming. In the past, it has been the seat

of important human civilisations, and it continues to play a very important role in international geopolitics with a dense population along its coasts. There is great diversity in the Mediterranean ecosystems, both marine and terrestrial. The Mediterranean region is also rich in paleoclimate records with a variety of proxies. Indeed, this area experienced major changes during the glacial-interglacial cycles (Jost et al., 2005; Ludwig et al., 2018; Ramstein et al., 2007). Another long-term cycle of changes due to high-frequency precession which drastically modified the hydrological patterns of this area (monsoon, sapropels) is also superimposed.

Due to the peculiarities of both the atmospheric and oceanic circulation in the region, high-quality climate modelling of the Mediterranean region needs to have high spatial resolution (Li et al., 2006). Indeed, the presence of strong gusts of wind in winter are essential to trigger oceanic convection and these can only be correctly represented in high-resolution models. Limited area models (LAM), or regional climate models (RCM), present some advantages in this regard, since they generally demand less computing resources, allowing them to be run at high spatial resolution for a given region. However, their usefulness for paleoclimate purposes is limited because of the lack of adequate lateral boundary conditions to drive the RCMs. The main reason why few comprehensive modelling exercises to explain paleoclimate changes around the Mediterranean have been performed is that the level of computing resources required for high resolution and long simulations is inaccessible. This is especially true in the case of the Mediterranean Thermohaline Circulation (MTC), which has significantly changed in the past, at both centennial and millennial scales.

Here we describe a modelling suite to define high-resolution atmospheric conditions over the Mediterranean basin from global ESM (Earth System Model) paleoclimate simulations. This atmospheric forcing can then be used to run a highly resolved ocean model (NEMOMED8 1/8°) to accurately simulate ocean dynamics. This tool allows us to achieve a high spatial resolution and equilibrated simulations with a run time of 100 years. The objective of this study is to develop a modelling platform sufficiently comprehensive to conduct paleoclimate studies of the Mediterranean basin. The potential of this platform is illustrated by investigating climate situations from the present period and from the Early Holocene that is supposed to generate sapropel events.

The sapropel events provide excellent case studies on the impact of global changes on the Mediterranean basin. These periodic events are related to a long period of anoxia of the deep and bottom waters triggered by an enhancement of the African monsoon caused by periodicities of the orbital precession. However, the localisation of the forcing source caused by orbital variability is still a subject of debate. This is especially true for the last sapropel, denoted S1, which occurred during the early Holocene (between 10500 and 6800 ka BP) (De Lange et al., 2008). Reproducing past climate variations over the

Mediterranean basin, including the sapropel events, is therefore a challenge for the modelling community.

The paper is organised as follows: In the first section, we briefly review the different approaches used to simulate the Mediterranean climate and sea conditions, and we also present the concept of the sequential procedure that we propose. Section 2 presents in detail the model architecture we developed. Finally, we present applications with simulations of the historical period (1970-1999) in Section 3 and the Early Holocene (around 9.5 ka) in Section 4.

1.2. Overview of current Mediterranean Sea modelling

The Mediterranean Sea, due to its limited size and its semi-enclosed configuration, has a faster equilibrium response (10^2 years) than the global ocean (10^3 years). Because of this semi-enclosed configuration, there are a few requirements that modelling of the Mediterranean Sea needs to satisfy so that its evolution can be properly represented. High resolution in both the atmospheric forcing and the oceanic configuration is necessary to correctly simulate the convection areas and the associated thermohaline circulation (Lebeaupin Brossier et al., 2011; Li et al., 2006). Depending on the mechanism studied, the resolution of the ocean model used by the research community ranges from ¼° (e.g. for paleo-climatic simulation), to 1/75° (for hourly description of the mixed layer, tide-based investigation). The results for oceanic convection are highly dependent on the flux of heat, flux of water, and the wind stress at the air-sea interface especially the seasonal variability and intensity. There are many modelling configurations in the scientific literature making it impossible to provide an exhaustive review of all of them. We can summarise them by presenting the different approaches used to drive the Mediterranean oceanic model, along with their advantages and drawbacks. We underline our new, coherent method, which captures the changes in ocean dynamics in the Mediterranean basin derived from global paleoclimate simulations.

Observations and reanalysis

The most common way to simulate the general circulation of the Mediterranean Sea is to run a regional oceanic general circulation model forced by surface fluxes and wind stresses derived from observations and reanalyses. In this way, an oceanic model can be driven by realistic fluxes. In most cases, this implies an observation-based reconstruction of relevant variables with a spatial atmospheric resolution of less than 50 km and a daily temporal resolution, at a minimum, in order to simulate the formation of dense water (Artale, 2002). This approach is adapted to simulate the present-day Mediterranean Sea and to explore the complexity of its sub-basin circulation and water mass formation (Millot and Taupier-Letage, 2005). However, it is not well adapted to the study of past and future climate, partly due to the excessive computing resources needed.

Atmospheric model

A second method consists of forcing a regional oceanic model with simulations from an atmospheric model, AGCM (Atmospheric Global Climate Model) or ARCM (Atmospheric Regional Climate Model). Since the AGCM resolution (typically 100 to 300 km horizontally) is coarse, statistical and/or dynamical downscaling is usually needed, especially for wind-stress so that the ORCM (Ocean Regional Circulation Model) can be correctly forced (Béranger et al., 2010). Currently, dynamical downscaling with ARCM is the preferred option because it generally improves simulations of the climate in the Mediterranean region and especially of the hydrological cycle (Li et al., 2012).

This configuration is broadly used to assess anthropogenic climate changes (Adloff et al., 2015; Macias et al., 2015; Somot et al., 2006). In these studies, the Mediterranean Sea simulations are generally driven by the outputs of an ARCM, which is, in turn, driven by the GCM or observation-based reanalysis. It should be noted that biases in oceanic variables can be reduced through constant flux correction (Somot et al., 2006). This configuration is suitable for high-resolution simulation of the past Mediterranean Sea (Mikolajewicz, 2011 for the LGM; Adloff et al., 2011 for the Early Holocene among others).

Regional coupled model

Although the majority of the Mediterranean Sea models are ocean-alone models, some of them use a coupled configuration between the Mediterranean Sea and the atmosphere. Such a coupled configuration generally improves the simulation of the air-sea fluxes, including their annual cycle (de Zolt et al., 2003), but may show climate drifts in key parameters such as the SST. Regional coupled models are now emerging as a tool in Mediterranean climate modelling (Artale et al., 2010; Dell'Aquila et al., 2012; Drobinski et al., 2012; Sevault et al., 2014; Somot et al., 2008). However, this full-coupling configuration is currently not possible for high-resolution paleoclimate issues requiring long simulation for hundreds or thousands of years.

Importance of boundary conditions

The boundary conditions applied to the Mediterranean Sea domain, in particular, the exchanges of water, salt and heat with the Atlantic Ocean through the Strait of Gibraltar modulate significantly the Mediterranean circulation (Adloff et al., 2015). This is especially true at the millennial scale where deglaciation episodes and fluctuations of the AMOC (Atlantic Meridional Overturning Circulation) and the Mediterranean Sea affect each other (Swingedouw et al., 2019). The level of discharge from the main rivers is also crucial as is illustrated by the sapropel episodes, where an increase in freshwater input drastically slowed down the MTC. Most of current models impose prescribed (observed when possible) conditions in the near Atlantic zone, including temperature and salinity. The same methodology can be used to prescribe river discharges. However, it must be acknowledged that

144 determining inputs from rivers into the Mediterranean Sea, either of water or other materials, still
145 presents serious challenges for modelling.

146 **1.3. Concepts for a sequential procedure to perform global-to-regional modelling**

147 In this paper, a new architecture for high-resolution modelling of the climate of the Mediterranean basin
148 for past, present and future conditions is proposed. This architecture is based on a method that provides
149 as much compatibility as possible amongst the models used and high consistency with data~~This~~
150 ~~architecture is based on a method as much consistency among the models as possible and high~~
151 ~~congruency with data~~.
152
153 *Step 1: Global climate*
154 Our goal is to simulate different climate conditions for the Mediterranean basin. The first step of any
155 relevant procedure should be to simulate the global climate conditions from which the simulation of the
156 regional climate is driven. These may be already available in simulations from previous PMIP exercises
157 for various periods (e.g. mid-Holocene, Last Glacial Maximum, Last Interglacial and mid-Pliocene) as
158 well as for different sapropel events and interglacials (e.g. MIS11, MIS13 and MIS19). However, this
159 is not always possible due to the large volume of high-frequency 3-D atmospheric circulation variables
160 involved. An alternative approach, used in some regional climate simulations (Chen et al., 2011;
161 Goubanova and Li, 2007; Krinner et al., 2014), consists of using an AGCM (either an independent one
162 or the same one used for the global climate simulation) run with appropriate values for global Sea
163 Surface Temperature (SST) and Sea Ice cover (SIC), derived from PMIP global simulations. SST is
164 crucial to determine atmospheric features and responses, while SIC plays a key role in determining the
165 global albedo. Monthly SST and SIC are necessary and sufficient to drive an AGCM. They can be
166 acquired from global climate simulations or through a bias-correction procedure.
167
168 *Step 2: Regional climate*
169 After running an AGCM, regional climate can be now reproduced with an ARCM nested into the high-
170 frequency outputs from the AGCM. Of course, the ARCM can be run in parallel to the AGCM, or with
171 a small time delay. Thus, we avoid a large accumulation of intermediate information between the AGCM
172 and the ARCM. In our study, we assume that there would be no feedback from the regional scale to the
173 global scale, so only a "one-way" transfer of information (from global to regional) is considered. In our
174 case, the ARCM is a strongly zoomed-in version of the AGCM and is also driven by monthly SST and
175 SIC values, as used for AGCM. The higher resolution of the ARCM allows the synoptic variability and
176 seasonality of the Mediterranean region to be depicted so that a realistic wind pattern and hydrological
177 cycle may be reproduced. This approach provides a general framework for use in many different

paleoclimate periods from the Pliocene to the Pleistocene, as long as the basin tectonics remain unchanged.

Step 3: Mediterranean Sea Circulation

Daily air-sea fluxes and wind stress provided by the ARCM are used as surface boundary conditions to drive the ORCM to investigate the oceanic dynamics of the Mediterranean. It is reasonable to assume that the boundary conditions of these air-sea fluxes represent the long-term trends of the oceanic dynamics. Rivers may be considered interactive or not depending on the investigative objectives: runoff can be prescribed from climatology or obtained from the hydrological component of the surface model. Again, we highlight that our architecture does not include any feedback, between either the regional ocean and the regional atmosphere, or the regional ocean and the global ocean. This configuration means that we can avoid dealing with certain issues, for example, the influence of the Mediterranean Outflow Water on the North Atlantic Ocean but is well adapted to provide consistent river runoff associated with changes in continental precipitation.

2 Model architecture

An ensemble of modelling tools that includes two atmospheric models and a regional oceanic model is used. Figure 1 summarises the configuration and shows the experimental flowchart.

2.1. The atmospheric models (AGCM and ARCM)

LMDZ4 (Hourdin et al., 2006; Li, 1999) is the atmospheric general circulation model developed and maintained by IPSL (Institut Pierre Simon Laplace). It has been widely used in previous phases of CMIP and PMIP projects. The resolution of the model is variable. Its global version used here (referred to as LMDZ4-global) is 3.75° in longitude and 2.5° in latitude with 19 layers in the vertical. It provides the boundary conditions to drive LMDZ4-regional. LMDZ4-regional (Li et al., 2012) is a regionally-oriented version of LMDZ4 with the same physics and same vertical discretisation, dedicated to the Mediterranean region. The zoomed-in model covers an effective domain of 13°W to 43°E and 24°N to 56°N with a horizontal resolution of about 30 km inside the zoom. The rest of the globe outside this domain is considered to be the buffer-zone for LMDZ4-regional where a relaxation operation is performed to nudge the model with variables from the AGCM, at a 2-hour frequency. The resolution of LMDZ4-regional decreases rapidly outside its effective domain. In both LMDZ4-global and LMDZ4-regional, land-surface processes, including the hydrological cycle, are taken into account through a full coupling with the surface model, ORCHIDEE (Krinner et al., 2005).

2.2 The regional oceanic model (ORCM)

NEMOMED8 (Beuvier et al., 2010; Herrmann et al., 2010) is the regional Mediterranean configuration of the NEMO oceanic modelling platform (Madec, 2008). The horizontal domain includes the Mediterranean Sea and the nearby Atlantic Ocean which serves as a buffer zone (from 11°W to 7.5°W). The horizontal resolution is 1/8° in longitude and 1/8°cosφ in latitude, i.e. 9km to 12km from the north to the south. The model has 43 layers of inhomogeneous thickness (from 7 m at the surface to 200 m in the depths) in the vertical. River discharges are accounted for as freshwater fluxes in the grids corresponding to the river mouths. A dataset of climatological river discharges ~~is~~ was proposed by default to cover the entire Mediterranean draining basin with 33 river mouths. It is of course switched off when rivers are interactive in the platform. The interactive calculation of freshwater discharges from rivers by the land-surface model, ORCHIDEE, includes 192 river mouths that~~to~~ cover the Mediterranean draining basin. The Black Sea, not included in NEMOMED8, counts as a river dumping freshwater into the Aegean. The Black Sea fresh water assumption comes from NEMOMED modeling community that consider it as a yearly source of freshwater .The deposit rate is calculated based on total runoff into the Black Sea, plus the net budget of precipitation (P) minus evaporation (E) over the Black Sea.

When the oceanic model NEMO is used alone, with prescribed surface fluxes, it is indispensable to implement a restoring term with a constant coefficient of 40 $W.m^{-2}.K^{-1}$ ~~.~~(as defined in Barnier et al. 1995) . This is a standard procedure for NEMO to prevent eventual run-away cases. In our modelling chain, the target temperature for the restoration is the surface air temperature from the regional atmospheric model LMDZ4-regional.

2.3 Modelling Sequence

As shown in Fig. 1, the first step in our modelling chain is to obtain SST and SIC values from an Earth System Model simulation able to reproduce global climate (for the past, present or future). We can reasonably hypothesise that major global climate information can transit from global SST and SIC. This hypothesis was deemed legitimate for climate downscaling purposes for Antarctic and Africa, in Krinner et al. (2014) and Hernández-Díaz et al. (2017) respectively. In the present work we use IPSL-CM5A (Dufresne et al., 2013) to extract relevant SST and SIC values to drive the AGCM (LMDZ4-global) and the ARCM (LMDZ4-regional). The next step is to run the two atmospheric models, LMDZ4-global and LMDZ4-regional, in the usual way as proposed by the AMIP community. This is the most expensive step, as atmospheric models are the most demanding in terms of computing resources. Fortunately, it is not necessary to run them for a long time as the atmosphere reaches equilibrium quickly. We applied 30 years of simulation to both models. We consider this duration to be long enough to depict climate variability for the simulation of past events. The AGCM nudges the ARCM in the conventional way of one-way nesting for temperature, humidity, meridional and zonal wind every two hours. The nudging is

done using an exponential relaxation procedure with a timescale of half an hour outside the zoom and 10 days inside the zoom. Table S2 in the SOM summarises the forcings used, especially the orbital forcing and atmospheric CO_2.

The necessary variables (surface air temperature, wind stress, P-E over the sea, heat fluxes) are provided by ARCM to NEMOMED8 (ORCM) at daily frequency. The salinity and temperature conditions are provided in three dimensions in the Atlantic buffer zone, near the Gibraltar Strait, and updated every month. River runoff, updated every month, depends on the configuration used (prescribed climatological rivers, or interactive rivers). Table S3 in SOM details these boundary conditions.

It is worthy to mention the work of Mikolajewicz (2011) who used a similar modelling chain (from a coarse-resolution earth system model to a high-resolution regional oceanic model) to simulate the Mediterranean Sea climate during the last glacial maximum. However, Mikolajewicz (2011) used only an AGCM (ECHAM5) as the intermediate step. In our case, we found that the use of ARCM was indispensable to produce high-quality forcing to correctly simulate the oceanic convection in NEMOMED8.

2.4 Bias correction

The sequential modelling chain, despite the lack of interactivity and feedback at interfaces, allows for error removal and bias correction at each step of the methodology. This adjustment is sometimes crucial, especially when model outputs need to be of very high quality to be incorporated into impact studies. This concept was further described in Krinner et al. (2019), as illustrated in Fig. 16 of their paper. Therefore, to enhance our confidence in the realism of the simulation results, bias-correction may be introduced when necessary. The correction method used in the present work generally follows the conventional procedure, which is based on the difference between the model outputs for present day simulations and actual observations. Biases corrected in this way, theoretically only valid for the historical simulation (named HIST hereafter), are assumed to remain unchanged for past and future simulation scenarios. However, the transferability between past and future periods is questionable. There is no guarantee that the model error for one period is the same for other periods, even though the model physics may be the same. In addition, paleodata are often rare and incomplete, and so, are unsuitable for evaluation and correction of model errors. The most reliable basis is that established for the present day. The reader can find a full description of the bias corrections and their eventual use in our applications in the supplementary online material, “Text S2: Bias correction”.

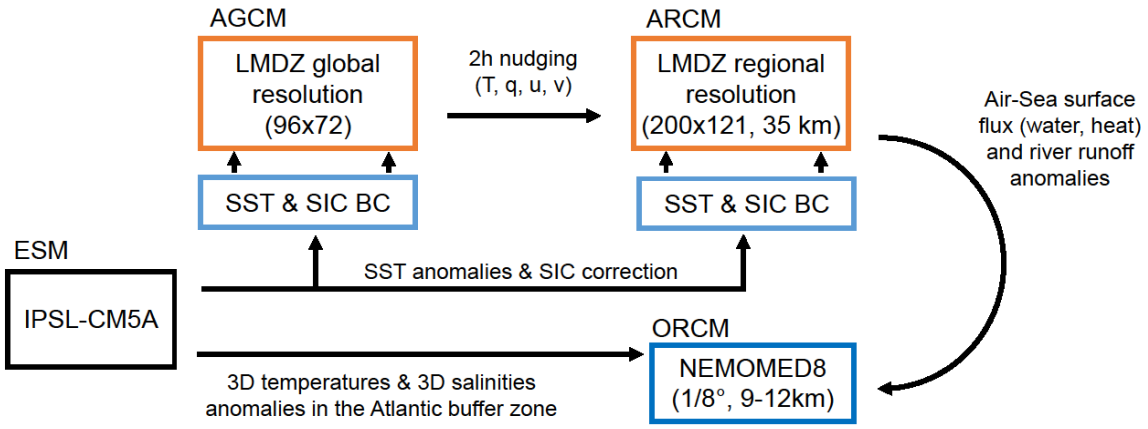

Figure 1: Flowchart of the modelling chain including the four main components generally represented by ESM, AGCM, ARCM and ORCM, respectively, and actually implemented in our platform by IPSL-CM5A, LMDZ-global, LMDZ-regional and NEMOMED8. BC: boundary condition, u: zonal wind, v: meridional wind, q: specific humidity, T: temperature, S: salinity, SST: sea surface temperature, SIC: sea-ice concentration.

3 Validation of the modelling chain for present-day climate 1970-1999

In this section, the capacity of the model to reproduce the climate of the recent past is evaluated, in particular, its ability to simulate sea surface characteristics as well as the Mixed Layer Depth (MLD) and oceanic convection patterns as these are key elements to reproduce the evolution of the Mediterranean Sea in past climate conditions.

3. 1 Experimental design

For the HIST experiment, SST and SIC observations (ERA-Interim, Dee et al., 2011) are used to force the AGCM. River runoff is from the climatology of Ludwig et al., (2009). Monthly mean climatological sea temperatures and salinities (World Ocean Atlas database from Locarnini et al., 2013, Zweng et al., 2013) are used for the Atlantic boundary zone. HIST atmospheric simulations for both global and regional simulations have a duration of 30 years. The length of the HIST oceanic simulation is also 30 years, but obtained after a 150-year spin-up. The forcings for each experiment are detailed in “Tables S2 and S3” in the supplementary online material. Spin-up phases for each simulation are also shown from “Figure S4” to “Figure S8” for the overturning stream function and the index of stratification.

3.2 Evolution of temperatures

Figure 2 depicts the temporal evolution, between 1970 and 1999, of annual mean surface air temperatures at two metres in the atmospheric simulations (global and regional) compared to observations for the whole globe and over the Mediterranean region. The two models reproduce a range of temperatures similar to the observations, with the Mediterranean temperatures warmer than the global temperatures. The global simulation (continued red curve in Fig. 2), after SST bias correction, is very close to the observation (continued black curve), with a tremendous improvement compared to IPSLCM5A (green curve in Figure 2)~~The global simulation, after SST bias correction, ranged with the observation, compared to IPSLCM5A (Figure 2).~~ The regional model reproduces the warming trend and aspects of the interannual variability ~~which are quite~~ close to observations, but with a mean cold shift of about -0.6°C.

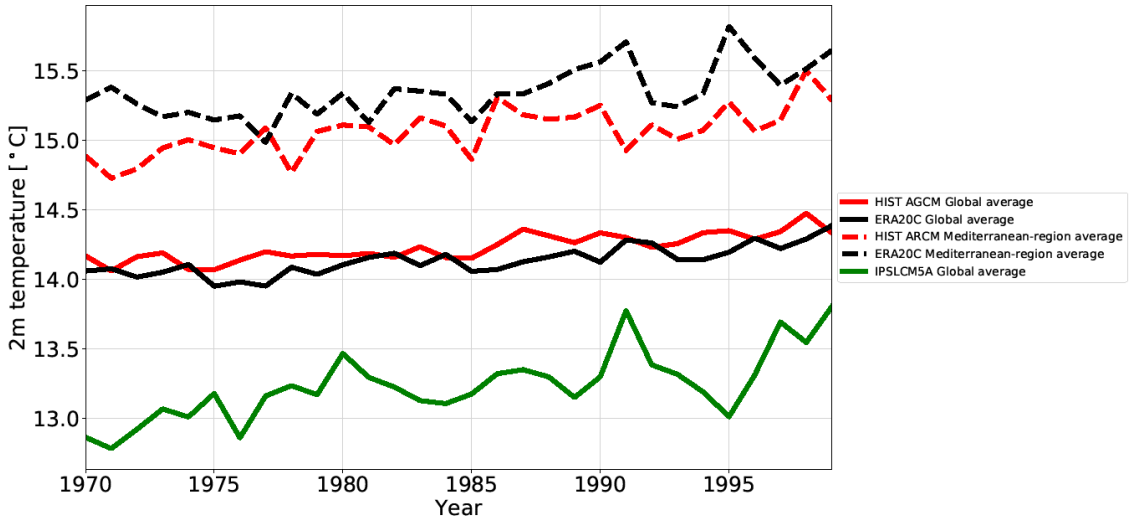

Figure 2: Time series of annual mean surface air temperatures at 2 m in HIST (red) and ERA20C (black, ref: Stickler et al., 2014) and IPSLCM5A (green) for global average (solid lines) and Mediterranean-region (10°W- 35°E, 20°N-50°N) average (dashed lines).

~~**Figure 2: Time series of annual mean surface air temperatures at 2 m in HIST (red) and ERA20C (black, ref: Stickler et al., 2014) and IPSLCM5A (green) for global average (solid lines) and Mediterranean region (ocean and continent) average (dashed lines).**~~

3.3 Precipitation and freshwater budget

Figure 3 a and b show the average annual precipitation for 1970-1999 in HIST over the Mediterranean region and the differences with observations. The main features of the distribution of precipitation over the Mediterranean region are simulated, in particular the distinct contrast between the very low

precipitation in the southern region and higher precipitation in the north. The ARCM tends to generate higher precipitation than the AGCM due to the resolution refinement. Compared to observation, AGCM is closer to ERA20C (Stickler et al., 2014), whereas ARCM is closer to GPCP data (Adler et al., 2018). However, the regional model still overestimates the amount of precipitation, especially at 42°N, from 45° to 50° N, at 8°E and 20°E. It corresponds to most of Europe, especially over the Alps, the Pyrenees, the Balkans and other mountainous regions. The freshwater budget over the Mediterranean Sea from observations (a synthesis from Sanchez-Gomez et al., 2011 and from other sources) and in the various simulations conducted in this study are summed up in Table 1. The simulated continental precipitation is overestimated, but both the precipitation and evaporation over the Mediterranean Sea in HIST are~~is~~ very close to the observations, with 10 mm.yr^{-1} of oceanic precipitation difference between HIST and the mean observation value (by taking the upper and the lower value), and 18 mm.yr^{-1} for the oceanic evaporation~~.~~ The two other simulations included in Table 1, PICTRL and EHOL, are those designed to investigates the Early Holocene climate (see Section 4)~~Two other simulations, PICTRL and EHOL, are those designed in Section 4 to investigate the Early Holocene climate~~.

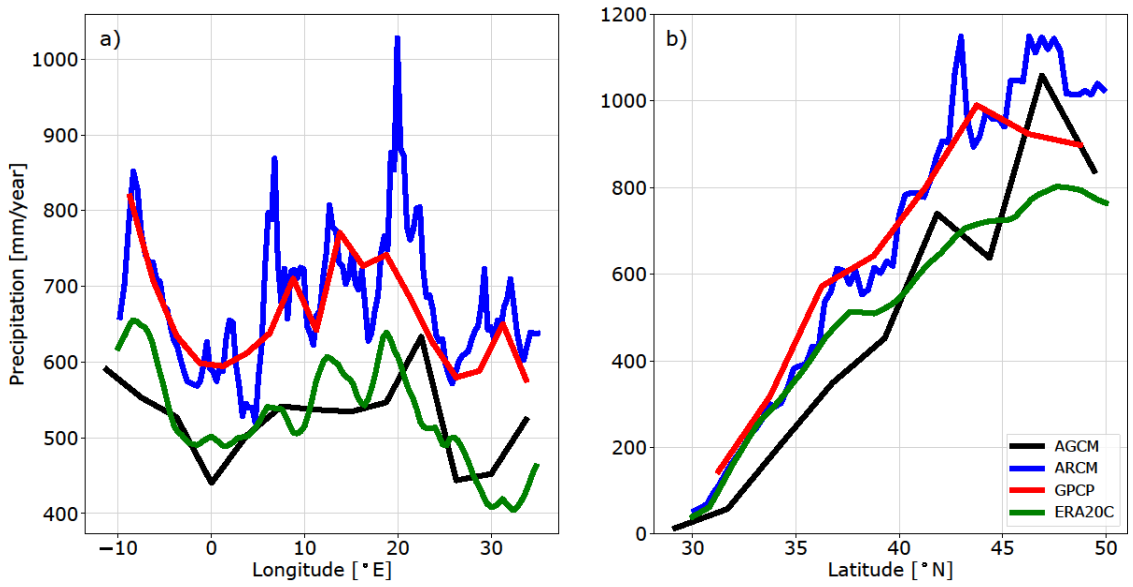

Figure 3: Annual mean precipitation, a) meridionally averaged (30 to 50°N), b) zonally averaged (-10 to 35°E), in the historical simulations with AGCM (LMDZ-global) and ARCM (LMDZ-regional). Observation comes from GPCP (Global Precipitation Climatology Project, 1979 to 1999, blue line, ref: Adler et al., 2018). and ERA20C (green line, ref: Stickler et al., 2014).

Dataset or experiment	E	P	R	B	E – P – R - B

OBS	1096-1136	256-595	102-142	73-121	238-705
HIST	1106	443	74	104	485
PICTRL	1031	451	98	104	378
EHOL	1094	460	225	104	305

Table 1: The Mediterranean Sea freshwater budget, expressed as mm.y~~ea~~r^{-1} for the whole water area (about 2.5 million of km^2). E, evaporation, P, precipitation, R, river runoff, B, Black Sea discharge into the Mediterranean Sea. OBS is a summary from Sanchez-Gomez et al., (2011) for P, E and P-E, from Ludwig et al., (2009) for R, from Lacombe and Tchernia, (1972), Stanev et al., (2000) and Kourafalou and Barbopoulos, (2003) for B. River discharges in HIST are from the climatology of Ludwig et al., (2009). PICTRL uses the Nile of its pre-industrial (pre-damming) value, 2930 m^3.s^{-1}, annually (Rivdis database, Vorosmarty et al., 1998). River discharges in EHOL are deduced from the difference between EHOL and PICTRL.

3.4 Mediterranean Sea surface characteristics

Figure 4 displays the temperatures and salinities of the Mediterranean Sea simulated in HIST and the deviations from observations. The model is able to capture the main characteristics of the pronounced west-east gradient of SSS in the Mediterranean Sea (Figure 4 a). Values are within the range of observations (mean bias = 0.32 PSU, error = 0.37 PSU, table 2). In the simulation, the Aegean Sea is not salty enough (about -1.5 PSU) and the Adriatic/Ionian Sea is too salty (+1 PSU).

The model reproduced the northwest to southeast temperature gradient, as shown in Figure 4b. However, the model shows a general cold bias (from -0.5 to -1.5 °C) over the entire Mediterranean (Figure 4e), due to the cold bias already observed for the air temperature at 2m in the regional atmospheric forcing (cf Figure 2).

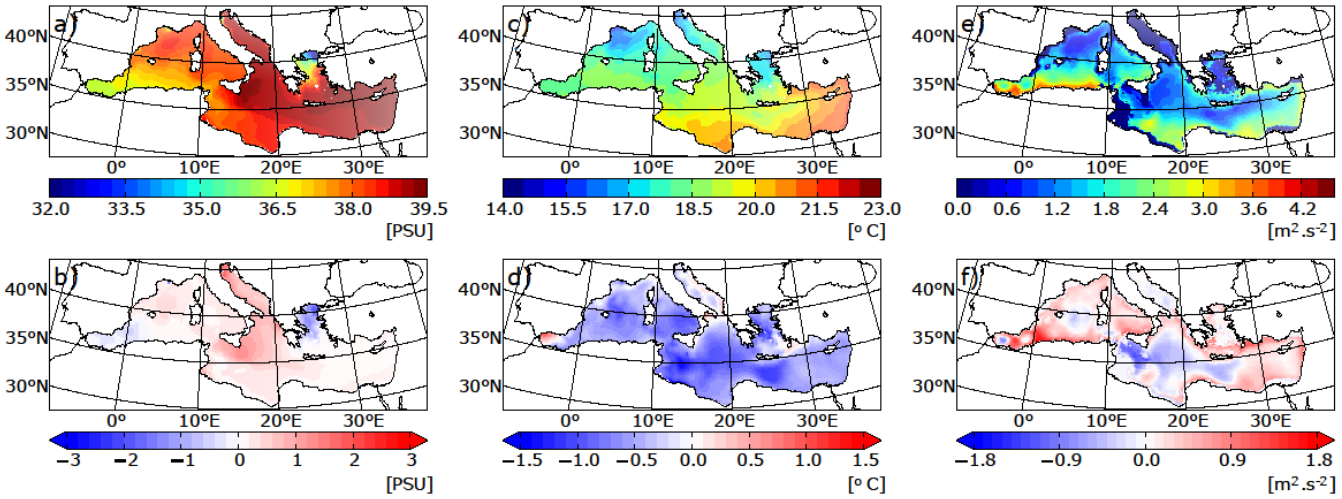

Figure 4: Annual mean sea-surface salinity (left panels, SSS in PSU), sea-surface temperature (middle panels, SST in °C) and index of water column stratification (right panels, winter IS in $m^2.s^{-2}$) simulated in HIST (top panels) and the HIST deviation (model – obs) from the observation-based MEDATLAS data (averaged over the entire simulation).

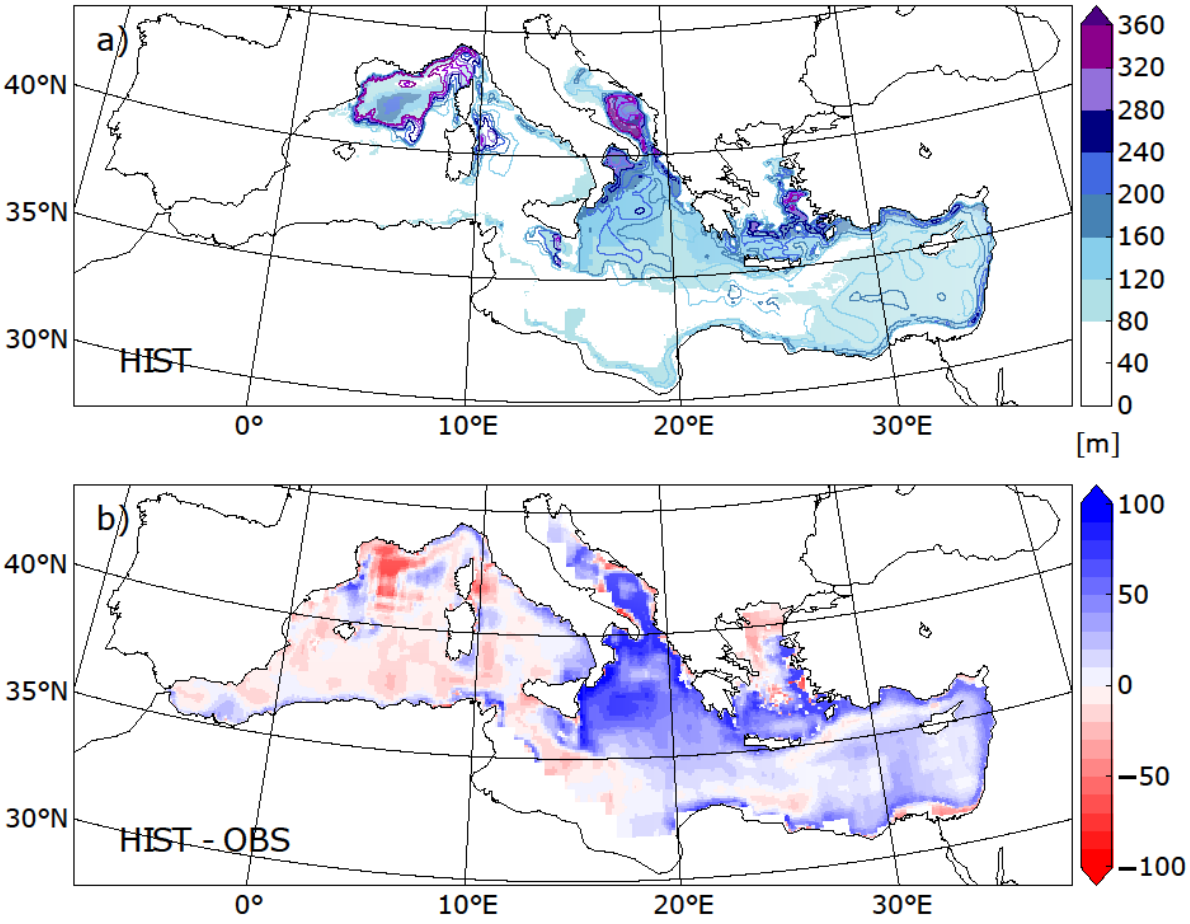

Figure 5: a) Mixed layer depth simulated in HIST (panel a, in m) and as deviation (b) of HIST from observations of Houpert et al., (2015) averaged over the entire simulation for JFM (January February March). Contour lines in the upper panel a) represents the maximum of MLD throughout the HIST simulation.

	SST (°C)	SSS (PSU)	IS ($m^2.s^{-2}$)
Mean bias (model – obs)	**-0.64**	**0.32**	**0.91**
RMS error	**0.45**	**0.37**	**0.29**

Table 2: Mean biases of sea surface temperature (SST), sea surface salinity (SSS) and index of stratification (IS) in the HIST simulation, expressed as the deviation from observations (MEDATLAS-II), and associated root mean square errors.

3.4 Mediterranean Thermohaline circulation

Here, the general characteristics of the simulated thermohaline circulation is evaluated in regions where deep and intermediate water formation occurs. Figure 4c displays the stratification index (IS[1]) for HIST. IS is a vertical integration of the Brunt-Vaisala frequency. A lower IS implies that convection is more likely. The range of IS biases (Figure 4f), is from -1 to 1 $m^2.s^{-2}$ (mean bias = 0.91 $m^2.s^{-2}$, error = 0.29 $m^2.s^{-2}$). The model satisfactorily reproduces the convection in known intermediate and deep-water formation areas, namely the Gulf of Lions, the Adriatic Sea, the Ionian Sea, the Aegean Sea and the North Levantine.

Comparison with observations of the mixed-layer depth (Houpert et al., 2015) confirms that the model reproduces realistic intermediate and deep-water formation patterns, with a thicker MLD in the eastern basin, due to salty condition (Figure 4a and e), and a shallower MLD in the Gulf of Lions (figure 5b).

The simulated Mediterranean overturning circulation is analysed (figure 6). The Zonal Overturning stream Function (ZOF[2]) in figure 6a depicts the surface and intermediate circulation and the

[1] $IS(x,y,h) = \int_0^h N^2(x,y)zdz$. N^2 is the Brunt-Väisälä frequency. IS is calculated at each model grid (x,y) for a given depth h (set as the bottom of the sea, or as 1000 m when the depth is greater than 1000 m).

[2] $ZOF(x,z) = \int_h^z \int_{ys}^{yn} u(x,y,z)dydz$. u is the zonal currents, h is the depth of the bottom, yn and ys are the north and south coordinates respectively.

intermediate/deep circulation. The surface current from the Strait of Gibraltar flows up to 30°E and back to the Atlantic Ocean in the intermediate layers, through the Levantine Intermediate Water (LIW) outflow. Figure 6 c, e, and g represents the Meridional Overturning stream Function (MOF[3]) in the Gulf of Lions, the Adriatic Sea and the Aegean Sea, respectively. The surface cell in the longitude-depth plan is comparable to previous studies done with the same regional oceanic model, but with different forcings (Adloff et al., 2015; Somot et al., 2006): the mean strength of the surface cell ranges from 0.8 to 1.0 Sv, and the longitudinal extension is from 5°W to 30°E. The simulated intermediate and deep cells are recognized in existing studies as having different characteristics. Our simulated pattern is very close to a similar historical run in Adloff et al., (2015), but is weaker than a historical run in Somot et al., (2006), and a second historical configuration (with refined air-sea flux) in Adloff et al., (2015). The ZOF in HIST depicted in figure 6)~~HIST~~ is consistent with the reanalyses (1987-2013) of Pinardi et al. (2019) over the Western basin, but shows a weaker Eastern deep cell compared to the reconstruction.

[3] $MOF(y,z) = \int_h^z \int_{xe}^{xw} v(x,y,z)dxdz$. v is the meridional currents, h is the depth of the bottom, xw and xe are the west and east coordinates respectively.

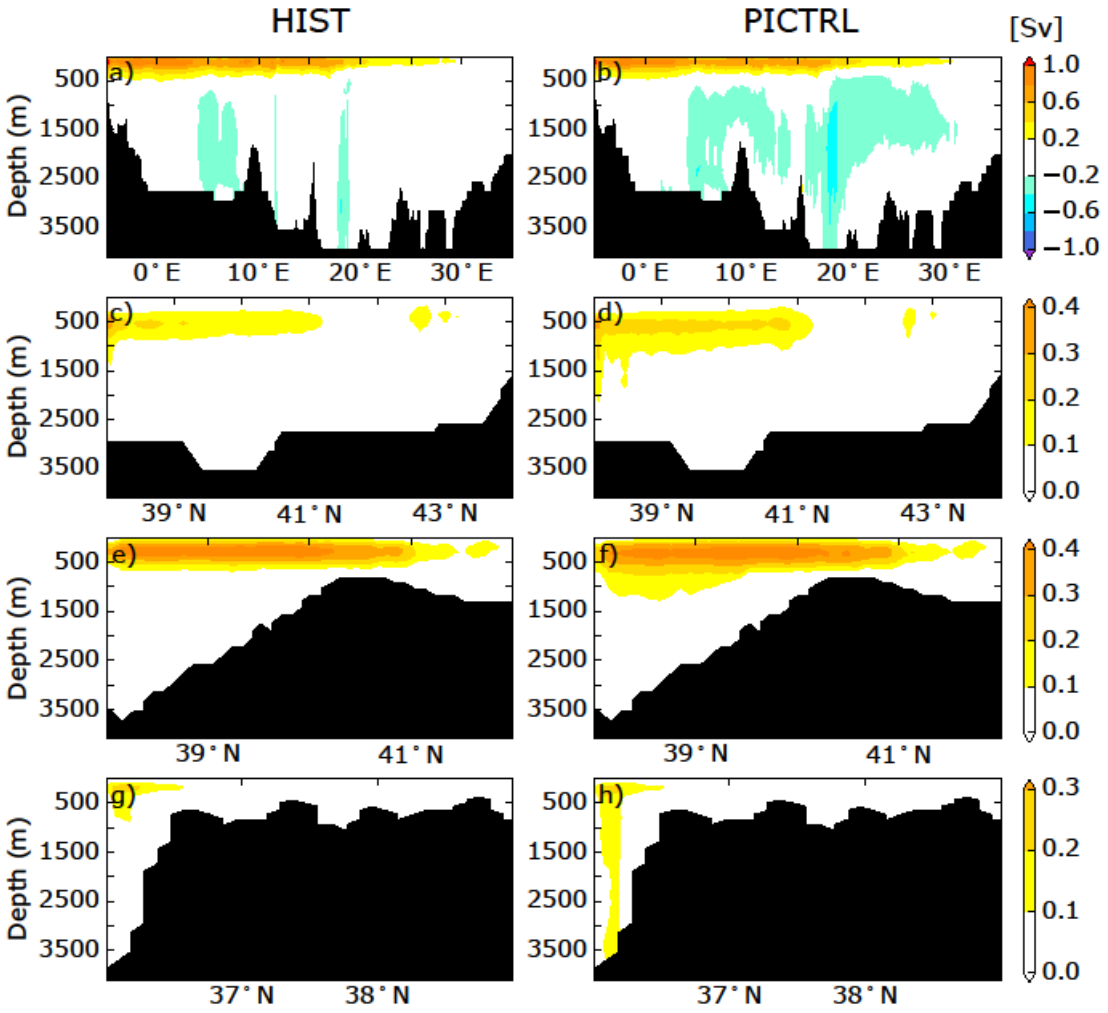

Figure 6: a, b, Zonal Overturning stream-Function (ZOF~~, first row , panels a, and b~~) integrated from north to south and shown as a longitude-depth section for the whole Mediterranean Sea, for HIST, and PICTRL simulations (from top to bottom), respectively. Other panels show Meridional Overturning stream-Function (MOF) shown as a latitude-depth section, integrated west/east for the Gulf of Lion (~~second row~~c and d, longitudinal extent: 4.5° to 8°E), the Adriatic/Ionian Sea (~~third row~~e and f, 12° to 21°E), and the Aegean Sea (~~fourth row~~g and h, 24° to 28°E) averaged over the entire simulation for HIST and over the last 30 years of simulation for PICTRL.

3.5 Summary of Validation

Validation of our platform was based on the historical period from1970 to 1999. after bias correction of global SST, the 2-m surface air temperature in the HIST global simulation is comparable to the observational counterpart. However, the simulated surface air temperature within the regional model is

colder (as shown in Figure2), which implies SST cold biases for the Mediterranean Sea~~Validation of our platform was based on the historical period, 1970 to 1999. The atmospheric simulation is acceptable compared with observations for the air temperature at 2m at both global and regional scales.~~ The simulated precipitation from the atmospheric models produces a signal that has the same range of variability as the observations~~ranges with the observation~~, but there is significant overestimation of precipitation over the mountainous area and over the land surrounding the Mediterranean Sea. However, the freshwater budget over the sea is close to observations for both evaporation and precipitation. The areas of intermediate and deep convection produced by the model are realistic, and the simulation of the thermohaline circulation is well captured by the oceanic model and in the range of the state-of-the-art existing Mediterranean regional models (compared to the simulations of Adloff et al., 2015 and Somot et al., 2006 for instance) and reanalysis as well (Pinardi et al., 2019). These features inspire confidence in our modelling platform for the investigations of past climate.

4 Application of the modelling chain to the Early Holocene

In this section, results obtained when our sequential modelling chain is applied in a paleoclimate context are presented, which was our initial motivation for developing this modelling tool. We chose to test the performance of our tool on the Early Holocene, a period marked by significant changes in climate and ocean dynamics over the Mediterranean basin, when the last sapropel event, S1, occurred in the Mediterranean Sea. Our experimental design relies on the comparison of two simulations: the Early Holocene (EHOL) with PICTRL based on pre-industrial conditions, the latter acting as a reference.

4.1 Experimental design

As indicated in the general flowchart of our modelling platform, global SST and SIC are required to initiate our sequential modelling. The basic assumption is that the climate change signal can be reconstructed from global SST and SIC, an accepted practice within the climate modelling community. In this study, two existing long-term coupled simulations from IPSL-CM5A is used, one covering the pre-industrial period and the other covering the Early Holocene (around 9.5 ka). Taking the last 100 years of each simulation, a climatological SST and SIC is constructed. After conducting bias-correction, these outputs from IPSL-CM5A are then used to drive the AGCM (LMDZ-global) and the ARCM (LMDZ-regional) in a further step. The duration of the PICTRL and EHOL atmospheric simulations is 30 years (both global and regional models).

Oceanic temperature and salinity in the Atlantic buffer-zone, as well as freshwater discharges from Mediterranean rivers, are all bias-corrected for NEMOMED8, as described in the general methodology. However, it needs to be pointed out that the reference point for the Nile river discharge is not modern observations but is set at pre-industrial values (2930 $m^3.s^{-1}$ for annual mean, Vorosmarty et al., 1998)

corresponding to a period before construction of the Aswan dam. For this part, the water budget over the Black Sea is calculated from the ARCM output. The oceanic simulation is 90 years for EHOL and 30 years for PICTRL, performed after a 200-year spin-up of PICTRL.

4.2 Climate features depicted in LMDZ-global (AGCM)

Because Early Holocene simulations are mainly driven by insolation forcing, an important feature is the model response to seasonal temperatures. Figure 7 shows the difference between EHOL and PICTRL, as reproduced in the AGCM, LMDZ-global, for the summer/winter temperature, JJAS precipitation and JAS surface runoff. The atmospheric model imprints a stronger seasonality due to the increased Early Holocene summer insolation. Warmer summer temperatures over Europe and North Africa (+ 6 °C, figure 7b) and lower winter temperatures over Africa (-2 °C, figure 7a) reflect this feature. Variations of the precession also trigger an enhancement of the African Monsoon (+ 10 $mm.day^{-1}$ over the Ethiopian region, figure 7c). The main consequence of this increase in precipitation is an enhanced surface runoff over the Ethiopian region. This hydrological state is similar to the African Humid Period caused by the enhanced African Monsoon and the resultant increase in surface runoff, as shown in Rossignol-Strick et al. (1982).

Our results are similar to those of previous modelling exercises for the Early- and Mid-Holocene (e.g. Adloff et al., 2011; Bosmans et al., 2012; Braconnot et al., 2007; Marzin and Braconnot, 2009). They are also consistent with various reconstructions of mid-Holocene precipitation (Harrison et al., 2014). A detailed comparison can be made with the Early Holocene simulation reported in Marzin and Braconnot (2009) which used for their experiment the same orbital parameters and the same atmospheric model as EHOL. However, their model was coupled to an oceanic model, while an atmospheric model and prescribed SST and SIC as boundary conditions are used in this study. Generally speaking, our results for both surface air temperature and precipitation are very similar to those of Marzin and Braconnot (2009), attesting to the validity of our approach using a simple atmospheric model constrained by boundary conditions. In the ensemble of PMIP simulations, available for the Early Holocene and mid-Holocene, there are some robust outputs for the climate response to orbital forcing but there are also some weaknesses common to most of the models (Braconnot et al., 2007; Kageyama et al., 2013). One of these weaknesses is the underestimation of the spread of the African monsoon towards North Africa. However, the increased discharge from the Nile river, induced by the enhanced monsoon is well supported by data (Adamson et al., 1980; Revel et al., 2014; Williams, 2000).

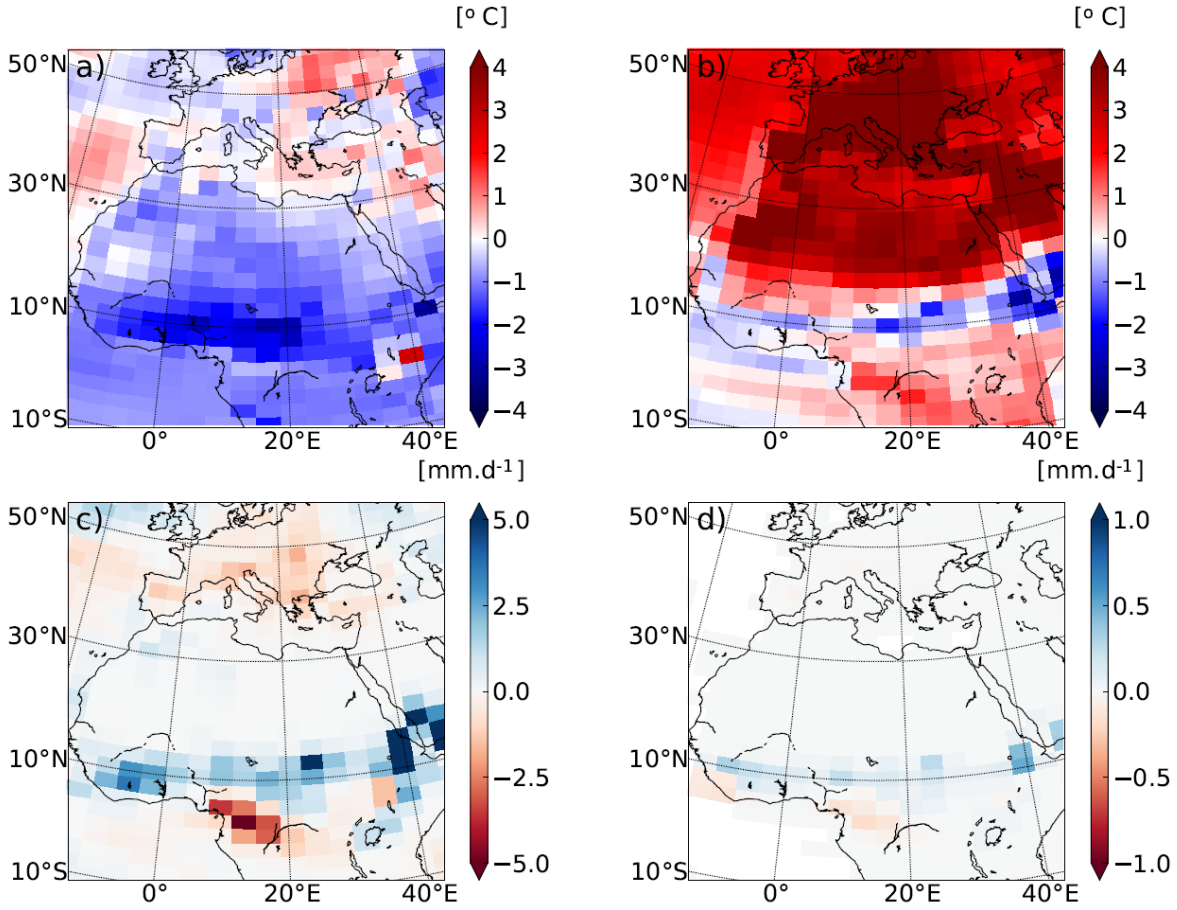

Figure 7: Temperature and precipitation deviations of EHOL from PICTRL in LMDZ-global, the AGCM for a) winter surface air temperatures at 2 m, b) summer surface air temperatures at 2 m, c) June to August precipitation, and d) July to September surface runoff (averaged over the entire simulation).

4.3 Mediterranean climate features with dynamical downscaling refinement

Figures 8, 9 and 10 show the results from the regional atmospheric model (LMDZ-regional), compared to those from LMDZ-global for PICTRL and EHOL over the Mediterranean region. In both the global and regional simulations, an increased seasonality is depicted, with warmer summer (+2 to +6 °C) and colder winter, especially over land (-3 to -1 °C, Figure 8). Downscaling with LMDZ-regional slightly reduces the amplitude of the summer warming and shows a more homogenous signal in winter over land. The general circulation of the surface wind in PICTRL is west to east (Figure 9b), in line with the dominant winter regime of westerlies in the region. This important feature is almost missed in the global model (Figure 9a) which reproduces a lower intensity than the regional model. The winter precipitation in EHOL, for ARCM (LMDZ-regional), increases over land in the Balkans and Italy and over the Adriatic, Ionian and Aegean Seas (Figure 10b). These changes are also present in the AGCM (LMDZ-

global) that, furthermore, shows an increase in Spain and Portugal (Figure 10a). It is in summer that the two models show the largest differences. In ARCM (LMDZ-regional), the Mediterranean basin experiences drier conditions, except in Italy and the North of the Balkans. Over the sea, precipitations slightly increase in EHOL (Figure 10). However, the AGCM (LMDZ-global) shows drier conditions in the northern two thirds of the Mediterranean domain, with more humid conditions in the southern third (Figure 10c). Changes in precipitation lead to unavoidable modifications in the runoff and river discharge into the Mediterranean Sea.

Although it is not straightforward to compare our "snapshot" simulations against environmental records (often used to reconstruct a timeline), our results compare well with the available data for this area (see supplementary online material, "Text S3: Comparison of model simulation outputs and reconstructed data for the Mediterranean basin"). Numerous proxies provide information on lake levels, paleo fires, pollen, isotopic signals recovered from speleothems which together describe the Mediterranean climate in the past. All of these proxies need to be brought together to provide a clear impression of the Mediterranean climate for this period (Magny et al., 2013; Peyron et al., 2011). Magny et al. (2007), based on records from Lake Acessa (Italy), suggested that aridification took place around 9200–7700 cal BP. Zanchetta et al. (2007), based on data recovered from speleothems in Italy, conclude that the Western Mediterranean basin experienced enhanced rainfall during the S1 (10000-7000 cal BP). Jalut et al. (2009), using pollen data, suggest that the summers were short and dry and that there was abundant rainfall in winter (autumn and spring as well) and remarked that these wetter conditions favoured broad-leaf tree vegetation. Different proxies seem to provide contradictory information and therefore, seasonality must be introduced to reconcile them. Peyron et al., (2011) mentioned wet winters and dry summers during the 'Holocene optimum'. Magny et al., (2013) support the hypothesis of seasonal contrast based on the analysis of multi-proxies.

Our EHOL simulation successfully depicts this temperature contrast between winter and summer. Precipitation is enhanced in winter. In summer, the Mediterranean region is globally drier, except over Northern Italy and the northern Balkans. As explained above, there is no precipitation signal over Northern Africa, although evidence of paleo-lakes has been found in Algeria (Callot and Fontugne, 1992; Petit-Maire et al., 1991), Tunisia (Fontes and Gasse, 1991) and Libya (Gaven et al., 1981; Lézine and Casanova, 1991) during the Early Holocene indicating increased rainfall in this area. In the supplementary material, a comparison between simulated continental precipitation outputs and pollen reconstruction data is provided. This comparison shows that the winter precipitation anomalies are consistent in both cases but that there is a distinct difference in summer values due to the more contrasted summer in the EHOL simulation.

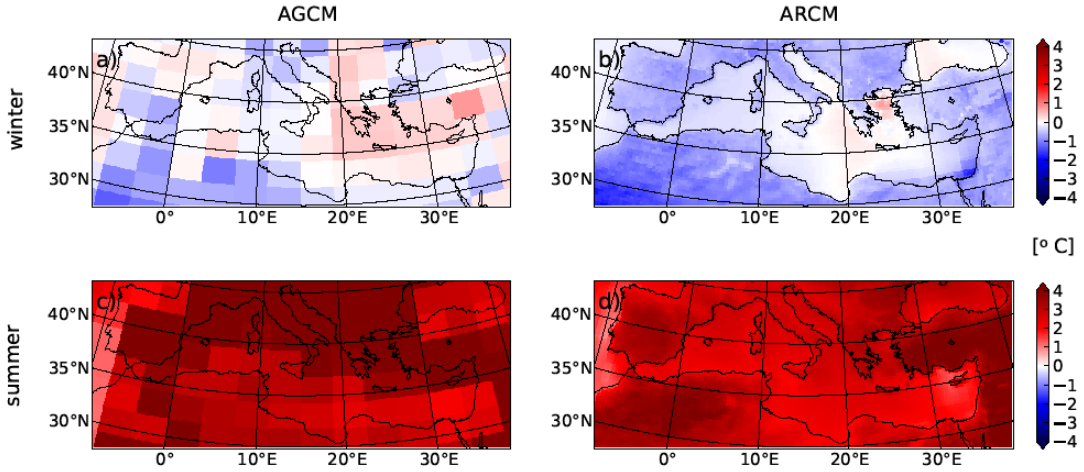

Figure 8: Deviations (EHOL – PICTRL, averaged over the entire simulation) of surface air temperature at 2 m for winter (upper panels) and summer (lower panels), respectively. AGCM (LMDZ-global) is displayed on the left and ARCM (LMDZ-regional) on the right.

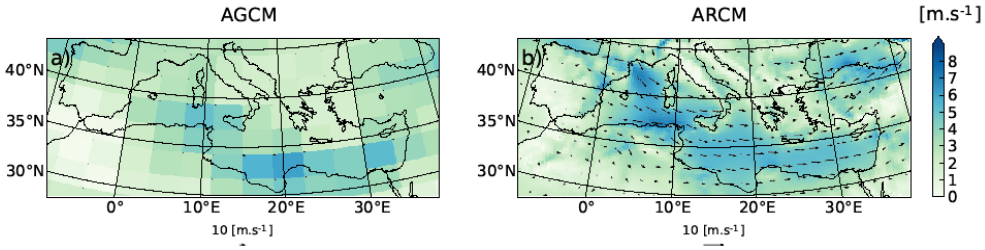

Figure 9: Winter wind-speed in PICTRL for a) the AGCM and b) the ARCM.

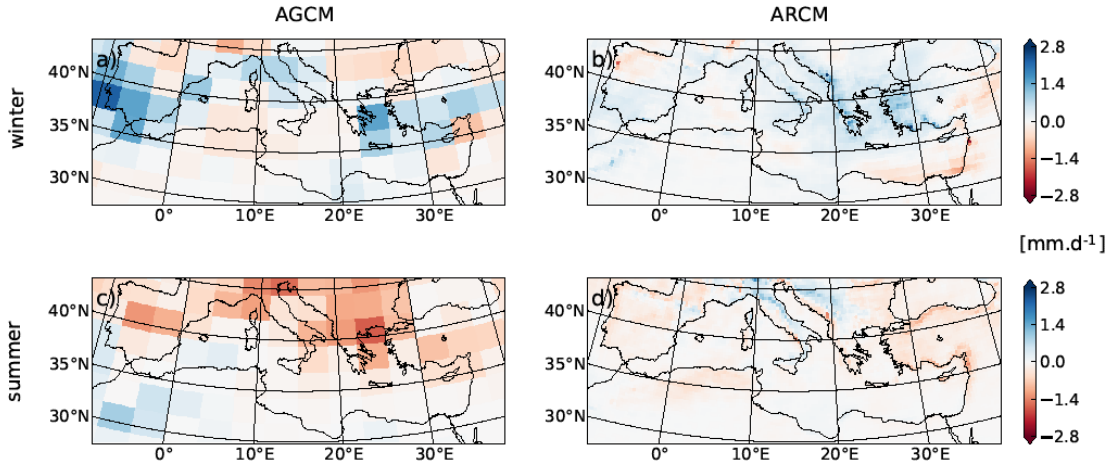

552

553 **Figure 10: Same as in Figure 8, but for precipitation rate (mm/day).**

554 ## 4.4 Hydrological changes

555

556

557 Figure 11 shows anomalies (EHOL – PICTRL) of river freshwater supplies into the Mediterranean basin
558 as simulated by the ARCM (LMDZ-regional). Bars are displayed for each calendar month to show the
559 strong seasonal variation, and for the western and eastern basins separately. Due to their particular role
560 and their specific treatment in our current modelling practice, the Nile and the Black Sea are also shown
561 for the eastern basin, but not accounted in the sum. The North African rivers are not displayed since
562 they don't show much changes for their catchment area. The Nile River shows important seasonal
563 variation, with increase in summer and autumn and decrease in winter and spring. The Albanian rivers
564 (Drini, Mat, Dures, Shkumbin and Vjosa) as well as the Vardar and the Buyukmenderes, produce
565 positive anomalies in EHOL in winter, due to enhanced winter land precipitation in this simulation
566 (Figure 10 b and d). The Black Sea net freshwater supply also changes in EHOL with important
567 decreases in January, February, March and July, but increase in April. In EHOL, the supplementary
568 winter freshwater input is less pronounced for the western basin than for the eastern basin (Figure 11b),
569 but major rivers, such as Rhone and Ebro, do show a strong seasonal cycle. As a whole the western basin
570 sees an increase of river discharges from March to June.
571 In terms of areal means for the entire Mediterranean draining basin, the different components of the
572 freshwater budget are shown in Table 1 (bottom) for both PICTRL and EHOL, to be compared to the
573 observation-based estimation OBS and the historical simulation HIST. From PICTRL to EHOL, the
574 annual precipitation over the Mediterranean Sea itself does not change much, but the annual evaporation
575 amount shows a slight increase (from 1031 to 1094 mm.year^{-1}). However, the most remarkable feature

is the increase of river discharges: 98 mm.year^{-1} in PICTRL to 225 mm.year^{-1} in EHOL. The total water deficit finally decreases from 378 to 305 mm.year^{-1}.

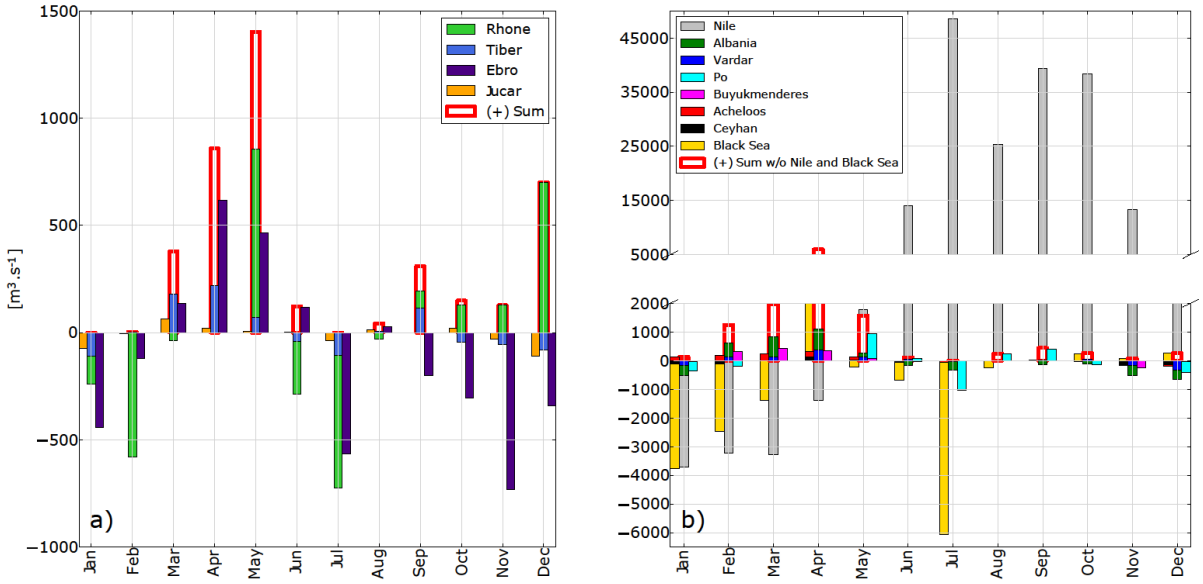

Figure 11: Monthly anomalies (EHOL – PICTRL, with seasonal variation) of fresh water discharges (m^3.s^{-1}) for major rivers flowing into the western basin (left panel) and the eastern basin (right panel). The sum of all rivers for each basin is also plotted. The Nile and the Black Sea are also shown as rivers of the eastern basin, but not accounted into the basin-scale sum.

4.5 Changes in water properties of the Mediterranean Sea

At the end of our modelling chain, changes in the properties of the Mediterranean seawater produced by NEMOMED8 for PICTRL and EHOL are examined. It is important to mention at this stage, that for the correction of the river runoff the reference is the pre-industrial state, and not the historical simulation (as is the case for SST and SIC). Our aim was to keep river runoff anomalies free of anthropogenic influence. In addition, the fact that the "pre-industrial" Nile river runoff (in other words before damming) is well known influenced this choice. The procedure of river runoff correction is detailed in the supplementary material (Text S2: Bias correction) . Figure 12 shows changes (EHOL minus PICTRL) for sea surface salinities, index of stratification and MLD for the last 30 years of simulation. The EHOL simulation reasonably reaches the steady state in terms of IS, ZOF and SSS, as shown in

Figures S6 to S8 of the supplementary material. The freshwater inputs from the Nile and the north-eastern margin imply a lower salinity in the eastern basin. This decrease in salinity enhances stratification throughout the Mediterranean Sea (with the exception of the Sicily Sea) and affects the convection areas by decreasing the MLD, especially in the Gulf of Lions, in the Adriatic and Ionian Seas and in the Aegean. Such a situation is expected and consistent with the basic climatology of MLD, shown in Figure 5. This global stratification in EHOL is followed by a general reduction in the thermohaline circulation compared to PICTRL (ZOF and MOF, Figure 13).

Numerous studies have documented the sapropel event S1 and the state of the Mediterranean Sea that caused it. Emeis et al. (2000) mentioned a decreased SSS during this period in both the eastern and western basins (as did Kallel et al., 1997 in the Tyrrhenian basin). In the subsection "*Sea Surface Temperatures*" and "*Sea Surface Salinity*" of the section "Text S3"in the supplementary online material, simulated SST and SSS to reconstructions are compared. Although simulated SST is in good agreement with the reconstructed data, there is a gap between the simulated SSS and reconstructions. This discrepancy is not surprising. Indeed, there are many explanations for the underestimation in our model of the salinity. One of them is a common weakness in Early to Mid-Holocene simulations, namely, the underestimation of the northward spread of the African monsoon and therefore, the underestimation of the freshwater flow from North Africa. Adloff (2011), already pointed to a shortfall in freshwater input to reconcile the simulated and observed SSS during the Early Holocene. Our oceanic simulation depicts these behaviours well and is overall similar to previous modelling studies with lower resolution (Adloff et al., 2011; Bosmans et al., 2015; Myers et al., 1998).

Two other issues need to be discussed for the Early Holocene. The first one is sea level, which was 20 metres lower than the present day (Peltier et al., 2015). For the sake of simplicity, this difference of sea level is not taken into account in the EHOL simulation. The second issue is the timing of the (re)connection between the Black Sea and the Aegean Sea. This topic is still being debated. Sperling et al. (2003) suggested this reconnection occurred around 8.4 ka BP, while by the calculations of Soulet et al. (2011) it happened around 9 ka BP. Other studies found that an overflow from the Black Sea likely occurred before this reconnection due to Fennoscandian ice-sheet melting during the deglaciation (Chepalyga, 2007; Major et al., 2002; Soulet et al., 2011). For the purposes of this work, the Bosphorus is maintened open in EHOL simulation, with the water exchange set at its modern value.

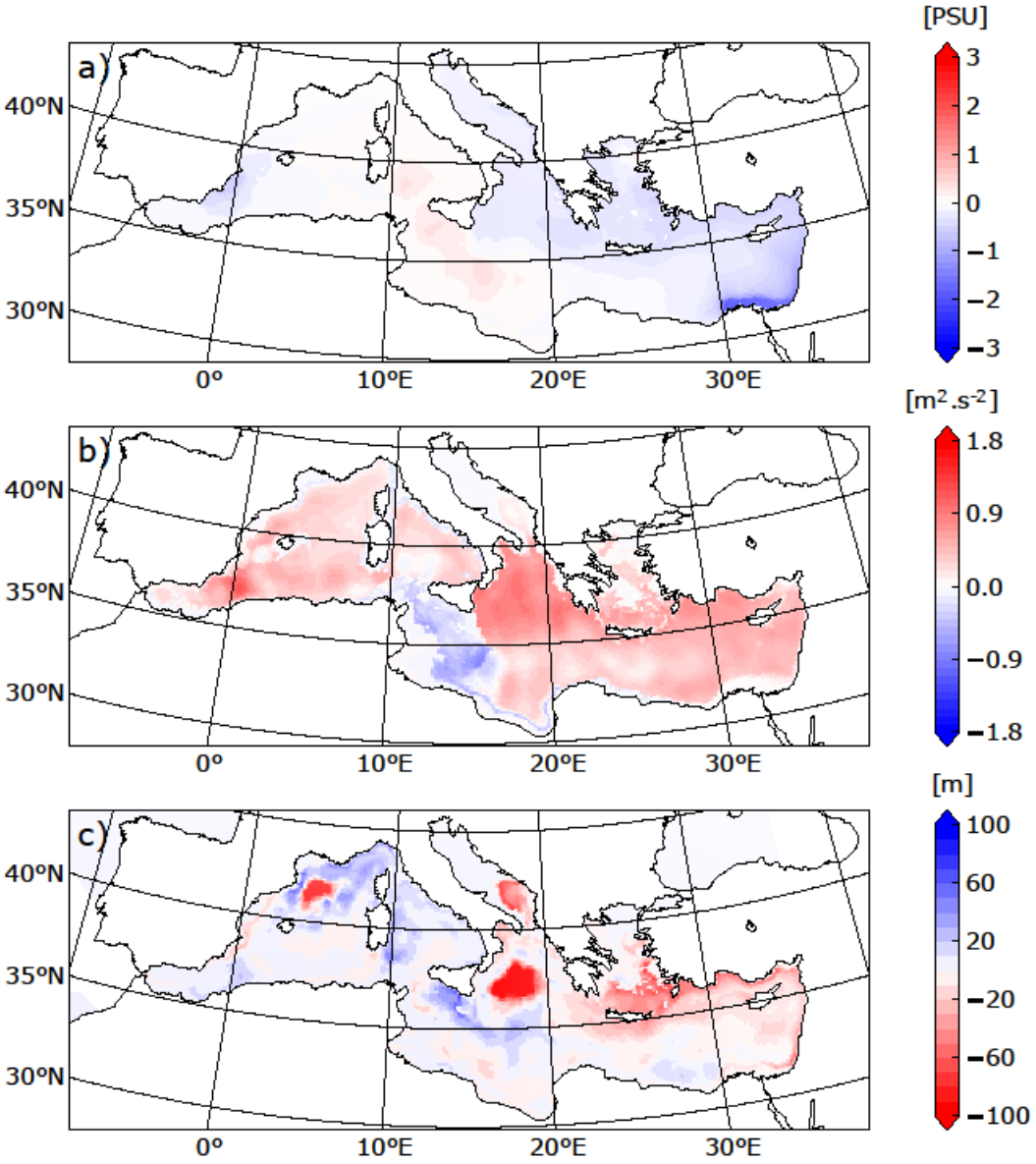

Figure 12: Deviations between EHOL and PICTRL in a) sea surface salinity, b) index of stratification, c) mixed-layer depth, averaged over the last 30 years of simulation

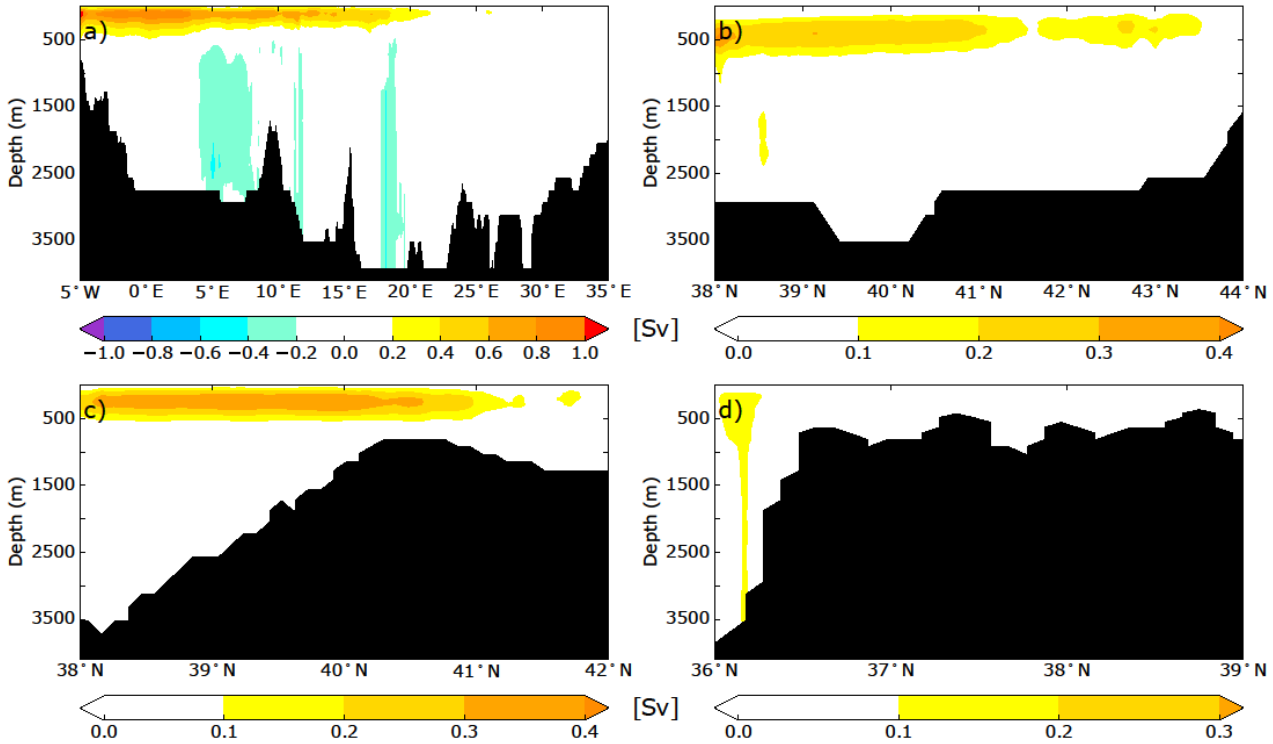

Figure 13: ZOF (a) and MOF (b, Gulf of Lion, c, Adriatic/Ionian Sea, d, Aegean Sea) for EHOL experiment, averaged over the last 30 years of simulation. These overturning stream-functions were calculated in the same way as in Fig. 6, providing a strict comparison with the experiments HIST and PICTRL.

5 Conclusion and perspectives for the modelling platform

This study aimed to develop a modelling platform to simulate different climatic conditions of the Mediterranean basin. We developed a useful regional climate investigation platform with high spatial resolution over the Mediterranean region. This is particularly relevant for the study of impacts on the circulation of the Mediterranean Sea. The model chain has been evaluated for the historical period. We have presented Early Holocene simulations as an example of the potential of this platform to simulate past climate. For the Early Holocene, our model reproduced satisfactorily the global and regional climate features, compared to the observed data. Our platform allowed, for the first time, the generation of a high-resolution freshwater budget for this period, with a particular focus on continental precipitation, a key factor for the Mediterranean Sea in the assessment of its impact on circulation during the onset of the sapropel event, S1. An important limitation of our sequential approach is the fact that it does not take account of feedback of ocean changes on atmospheric circulation. However, this architecture allows eventual bias correction, conducted at different levels of the platform if needed. One way to overcome

this problem of interactive ocean would be to consider an "asynchronous mode", namely, to take account of feedback from the ocean component to the atmosphere at a yearly or decadal frequency.

The modelling sequence, moving from global simulation at low resolution to high-resolution regional ocean modelling, avoids the problem of boundary conditions, and provides a fully consistent platform that may be used for many paleoclimate studies. We focused here on the Early Holocene period but this architecture could be used to study other periods investigated in MIPs, such as the Last Glacial Maximum or the deposition of older sapropels, from the Pliocene to the Quaternary, as long as the tectonics remain mainly unchanged (PMIP, PlioMIP).

Code and data availability. The current version of LMDZ and NEMO are available from the project website: https://forge.ipsl.jussieu.fr/igcmg_doc/wiki/DocImodelBlmdz and http://forge.ipsl.jussieu.fr/nemo/wiki/Users under the terms of the CeCill license for LMDZ and NEMO both. The exact version of the model used to produce the results used in this paper is archived on Zenodo (Vadsaria et al., 2019), as are input data and scripts to run the model and produce the plots for all the simulations presented in this paper.

Author's contribution. This study was co-designed and approved by all co-authors. The simulation protocol was constructed by TV and LL from a modelling architecture provided by LL. TV conducted the numerical simulations and drafted the first version of the manuscript. All co-authors are largely involved in the writing and revision of the manuscript.

Acknowledgments. We thank Mary Minnock for her professional English revision. This work was supported by the French National program LEFE "HoMoSapIENS". This work was granted access to the HPC resources of TGCC under the allocation 2017-A0010102212, 2018-A0030102212 and 2018-A004-01-00239 made by GENCI.

References

Adamson, D. A., Gasse, F., Street, F. A. and Williams, M. A. J.: Late Quaternary history of the Nile, Nature, 288(5786), 50–55, doi:10.1038/288050a0, 1980.

Adler, R., Sapiano, M., Huffman, G., Wang, J.-J., Gu, G., Bolvin, D., Chiu, L., Schneider, U., Becker, A., Nelkin, E., Xie, P., Ferraro, R. and Shin, D.-B.: The Global Precipitation Climatology Project (GPCP) Monthly Analysis (New Version 2.3) and a Review of 2017 Global Precipitation, Atmosphere (Basel)., 9(4), 138, doi:10.3390/atmos9040138, 2018.

Adloff, F., Mikolajewicz, U., Kučera, M., Grimm, R., Maier-Reimer, E., Schmiedl, G. and Emeis, K.-C.: Upper ocean climate of the Eastern Mediterranean Sea during the Holocene Insolation Maximum – a model study" published in Clim. Past, 7, 1103–1122, 2011, Clim. Past, 7(4), 1149–1168, doi:10.5194/cp-7-1149-2011, 2011.

Adloff, F., Somot, S., Sevault, F., Jordà, G., Aznar, R., Déqué, M., Herrmann, M., Marcos, M., Dubois, C., Padorno, E., Alvarez-Fanjul, E. and Gomis, D.: Mediterranean Sea response to climate change in an ensemble of twenty first century scenarios, Clim. Dyn., 45(9–10), 2775–2802, doi:10.1007/s00382-015-2507-3, 2015.

Artale, V.: Role of surface fluxes in ocean general circulation models using satellite sea surface temperature: Validation of and sensitivity to the forcing frequency of the Mediterranean thermohaline circulation, J. Geophys. Res., 107(C8), 3120, doi:10.1029/2000JC000452, 2002.

Artale, V., Calmanti, S., Carillo, A., Dell'Aquila, A., Herrmann, M., Pisacane, G., Ruti, P. M., Sannino, G., Struglia, M. V., Giorgi, F., Bi, X., Pal, J. S. and Rauscher, S.: An atmosphere–ocean regional climate model for the Mediterranean area: assessment of a present climate simulation, Clim. Dyn., 35(5), 721–740, doi:10.1007/s00382-009-0691-8, 2010.

Barnier, B., Siefridt, L. and Marchesiello, P.: Thermal forcing for a global ocean circulation model using a three-year climatology of ECMWF analyses, J. Mar. Syst., 6(4), 363–380, doi:10.1016/0924-7963(94)00034-9, 1995.

Béranger, K., Drillet, Y., Houssais, M.-N., Testor, P., Bourdallé-Badie, R., Alhammoud, B., Bozec, A., Mortier, L., Bouruet-Aubertot, P. and Crépon, M.: Impact of the spatial distribution of the atmospheric forcing on water mass formation in the Mediterranean Sea, J. Geophys. Res., 115(C12), C12041, doi:10.1029/2009JC005648, 2010.

Beuvier, J., Sevault, F., Herrmann, M., Kontoyiannis, H., Ludwig, W., Rixen, M., Stanev, E., Béranger, K. and Somot, S.: Modeling the Mediterranean Sea interannual variability during 1961–2000: Focus on the Eastern Mediterranean Transient, J. Geophys. Res., 115(C8), C08017, doi:10.1029/2009JC005950, 2010.

Bosmans, J. H. C., Drijfhout, S. S., Tuenter, E., Lourens, L. J., Hilgen, F. J. and Weber, S. L.: Monsoonal response to mid-holocene orbital forcing in a high resolution GCM, Clim. Past, 8(2), 723–740, doi:10.5194/cp-8-723-2012, 2012.

Bosmans, J. H. C., Drijfhout, S. S., Tuenter, E., Hilgen, F. J., Lourens, L. J. and Rohling, E. J.: Precession and obliquity forcing of the freshwater budget over the Mediterranean, Quat. Sci. Rev., 123, 16–30, doi:10.1016/j.quascirev.2015.06.008, 2015.

Braconnot, P., Otto-Bliesner, B., Harrison, S., Joussaume, S., Peterchmitt, J., Abe-Ouchi, A., Crucifix, M., Driesschaert, E., Fichefet, T., Hewitt, C. D., Kageyama, M., Kitoh, A., Laîné, A., Loutre, M., Marti, O., Merkel, U., Ramstein, G., Valdes, P., Weber, S. L., Yu, Y. and Zhao, Y.: Results of PMIP2 coupled simulations of the Mid-Holocene and Last Glacial Maximum – Part 1: experiments and large-scale features, Clim. Past, 3(2), 261–277, doi:10.5194/cp-3-261-2007, 2007.

Callot, Y. and Fontugne, M.: Les étagements de nappes dans les paléolacs holocènes du nord-est du Grand Erg Occidental (Algérie)., 1992.

Chen, J., Brissette, F. P. and Leconte, R.: Uncertainty of downscaling method in quantifying the impact of climate change on hydrology, J. Hydrol., 401(3–4), 190–202, doi:10.1016/j.jhydrol.2011.02.020, 2011.

Chepalyga, A. L.: The late glacial great flood in the Ponto-Caspian basin, in The Black Sea Flood Question: Changes in Coastline, Climate, and Human Settlement, pp. 119–148, Springer Netherlands., 2007.

Dee, D. P., Uppala, S. M., Simmons, A. J., Berrisford, P., Poli, P., Kobayashi, S., Andrae, U., Balmaseda, M. A., Balsamo, G., Bauer, P., Bechtold, P., Beljaars, A. C. M., van de Berg, L., Bidlot, J., Bormann, N., Delsol, C., Dragani, R., Fuentes, M., Geer, A. J., Haimberger, L., Healy, S. B., Hersbach, H., Hólm, E. V., Isaksen, L., Kållberg, P., Köhler, M., Matricardi, M., McNally, A. P., Monge-Sanz, B. M., Morcrette, J.-J., Park, B.-K., Peubey, C., de Rosnay, P., Tavolato, C., Thépaut, J.-N. and Vitart, F.: The ERA-Interim reanalysis: configuration and performance of the data assimilation system, Q. J. R. Meteorol. Soc., 137(656), 553–597, doi:10.1002/qj.828, 2011.

Dell'Aquila, A., Calmanti, S., Ruti, P., Struglia, M., Pisacane, G., Carillo, A. and Sannino, G.: Effects of seasonal cycle fluctuations in an A1B scenario over the Euro-Mediterranean region, Clim. Res., 52(1), 135–157, doi:10.3354/cr01037, 2012.

765
766 Drobinski, P., Anav, A., Lebeaupin Brossier, C., Samson, G., Stéfanon, M., Bastin, S., Baklouti, M.,
767 Béranger, K., Beuvier, J., Bourdallé-Badie, R., Coquart, L., D'Andrea, F., de Noblet-Ducoudré, N.,
768 Diaz, F., Dutay, J.-C., Ethe, C., Foujols, M.-A., Khvorostyanov, D., Madec, G., Mancip, M., Masson,
769 S., Menut, L., Palmieri, J., Polcher, J., Turquety, S., Valcke, S. and Viovy, N.: Model of the Regional
770 Coupled Earth system (MORCE): Application to process and climate studies in vulnerable regions,
771 Environ. Model. Softw., 35, 1–18, doi:10.1016/j.envsoft.2012.01.017, 2012.
772
773 Dufresne, J.-L., Foujols, M.-A., Denvil, S., Caubel, A., Marti, O., Aumont, O., Balkanski, Y., Bekki, S.,
774 Bellenger, H., Benshila, R., Bony, S., Bopp, L., Braconnot, P., Brockmann, P., Cadule, P., Cheruy, F.,
775 Codron, F., Cozic, A., Cugnet, D., de Noblet, N., Duvel, J.-P., Ethé, C., Fairhead, L., Fichefet, T.,
776 Flavoni, S., Friedlingstein, P., Grandpeix, J.-Y., Guez, L., Guilyardi, E., Hauglustaine, D., Hourdin, F.,
777 Idelkadi, A., Ghattas, J., Joussaume, S., Kageyama, M., Krinner, G., Labetoulle, S., Lahellec, A.,
778 Lefebvre, M.-P., Lefevre, F., Levy, C., Li, Z. X., Lloyd, J., Lott, F., Madec, G., Mancip, M., Marchand,
779 M., Masson, S., Meurdesoif, Y., Mignot, J., Musat, I., Parouty, S., Polcher, J., Rio, C., Schulz, M.,
780 Swingedouw, D., Szopa, S., Talandier, C., Terray, P., Viovy, N. and Vuichard, N.: Climate change
781 projections using the IPSL-CM5 Earth System Model: from CMIP3 to CMIP5, Clim. Dyn., 40(9–10),
782 2123–2165, doi:10.1007/s00382-012-1636-1, 2013.
783
784 Emeis, K.-C., Struck, U., Schulz, H.-M., Rosenberg, R., Bernasconi, S., Erlenkeuser, H., Sakamoto, T.
785 and Martinez-Ruiz, F.: Temperature and salinity variations of Mediterranean Sea surface waters over
786 the last 16,000 years from records of planktonic stable oxygen isotopes and alkenone unsaturation ratios,
787 Palaeogeogr. Palaeoclimatol. Palaeoecol., 158(3–4), 259–280, doi:10.1016/S0031-0182(00)00053-5,
788 2000.
789
790 Fontes, J. C. and Gasse, F.: PALHYDAF (Palaeohydrology in Africa) program: objectives, methods,
791 major results, Palaeogeogr. Palaeoclimatol. Palaeoecol., 84(1–4), 191–215, doi:10.1016/0031-
792 0182(91)90044-R, 1991.
793
794 Gaven, C., Hillaire-Marcel, C. and Petit-Maire, N.: A Pleistocene lacustrine episode in southeastern
795 Libya, Nature, 290(5802), 131–133, doi:10.1038/290131a0, 1981.
796
797 Giorgi, F.: Climate change hot-spots, Geophys. Res. Lett., 33(8), L08707, doi:10.1029/2006GL025734,
798 2006.
799
800 Goubanova, K. and Li, L.: Extremes in temperature and precipitation around the Mediterranean basin
801 in an ensemble of future climate scenario simulations, Glob. Planet. Change, 57(1–2), 27–42,

doi:10.1016/j.gloplacha.2006.11.012, 2007.

Harrison, S. P., Bartlein, P. J., Brewer, S., Prentice, I. C., Boyd, M., Hessler, I., Holmgren, K., Izumi, K. and Willis, K.: Climate model benchmarking with glacial and mid-Holocene climates, Clim. Dyn., 43(3–4), 671–688, doi:10.1007/s00382-013-1922-6, 2014.

Hernández-Díaz, L., Laprise, R., Nikiéma, O. and Winger, K.: 3-Step dynamical downscaling with empirical correction of sea-surface conditions: application to a CORDEX Africa simulation, Clim. Dyn., 48(7–8), 2215–2233, doi:10.1007/s00382-016-3201-9, 2017.

Herrmann, M., Sevault, F., Beuvier, J. and Somot, S.: What induced the exceptional 2005 convection event in the northwestern Mediterranean basin? Answers from a modeling study, J. Geophys. Res., 115(C12), C12051, doi:10.1029/2010JC006162, 2010.

Houpert, L., Testor, P., Durrieu de Madron, X., Somot, S., D'Ortenzio, F., Estournel, C. and Lavigne, H.: Seasonal cycle of the mixed layer, the seasonal thermocline and the upper-ocean heat storage rate in the Mediterranean Sea derived from observations, Prog. Oceanogr., 132, 333–352, doi:10.1016/j.pocean.2014.11.004, 2015.

Hourdin, F., Musat, I., Bony, S., Braconnot, P., Codron, F., Dufresne, J.-L., Fairhead, L., Filiberti, M.-A., Friedlingstein, P., Grandpeix, J.-Y., Krinner, G., LeVan, P., Li, Z.-X. and Lott, F.: The LMDZ4 general circulation model: climate performance and sensitivity to parametrized physics with emphasis on tropical convection, Clim. Dyn., 27(7–8), 787–813, doi:10.1007/s00382-006-0158-0, 2006.

Jalut, G., Dedoubat, J. J., Fontugne, M. and Otto, T.: Holocene circum-Mediterranean vegetation changes: Climate forcing and human impact, Quat. Int., 200(1–2), 4–18, doi:10.1016/j.quaint.2008.03.012, 2009.

Jost, A., Lunt, D., Kageyama, M., Abe-Ouchi, A., Peyron, O., Valdes, P. J. and Ramstein, G.: High-resolution simulations of the last glacial maximum climate over Europe: a solution to discrepancies with continental palaeoclimatic reconstructions?, Clim. Dyn., 24(6), 577–590, doi:10.1007/s00382-005-0009-4, 2005.

Kageyama, M., Braconnot, P., Bopp, L., Caubel, A., Foujols, M.-A., Guilyardi, E., Khodri, M., Lloyd, J., Lombard, F., Mariotti, V., Marti, O., Roy, T. and Woillez, M.-N.: Mid-Holocene and Last Glacial Maximum climate simulations with the IPSL model—part I: comparing IPSL_CM5A to IPSL_CM4, Clim. Dyn., 40(9–10), 2447–2468, doi:10.1007/s00382-012-1488-8, 2013.

Kallel, N., Paterne, M., Labeyrie, L., Duplessy, J.-C. and Arnold, M.: Temperature and salinity records of the Tyrrhenian Sea during the last 18,000 years, Palaeogeogr. Palaeoclimatol. Palaeoecol., 135(1–4), 97–108, doi:10.1016/S0031-0182(97)00021-7, 1997.

Kourafalou, V. H. and Barbopoulos, K.: High resolution simulations on the North Aegean Sea seasonal circulation, Ann. Geophys., 21(1), 251–265, doi:10.5194/angeo-21-251-2003, 2003.

Krinner, G., Viovy, N., de Noblet-Ducoudré, N., Ogée, J., Polcher, J., Friedlingstein, P., Ciais, P., Sitch, S. and Prentice, I. C.: A dynamic global vegetation model for studies of the coupled atmosphere-biosphere system, Global Biogeochem. Cycles, 19(1), 1–33, doi:10.1029/2003GB002199, 2005.

Krinner, G., Largeron, C., Ménégoz, M., Agosta, C. and Brutel-Vuilmet, C.: Oceanic Forcing of Antarctic Climate Change: A Study Using a Stretched-Grid Atmospheric General Circulation Model, J. Clim., 27(15), 5786–5800, doi:10.1175/JCLI-D-13-00367.1, 2014.

Krinner, G., Beaumet, J., Favier, V., Déqué, M. and Brutel-Vuilmet, C.: Empirical Run-Time Bias Correction for Antarctic Regional Climate Projections With a Stretched-Grid AGCM, J. Adv. Model. Earth Syst., 11(1), 64–82, doi:10.1029/2018MS001438, 2019.

Lacombe, H. and Tchernia, P.: Caractères hydrologiques et circulation des eaux enMéditerranée., in The Mediterranean Sea: A natural sedimentation laboratory, edited by D. . Stanley, pp. 25–36, Dowden, Hutchinson & Ross, Stroudsburg., 1972.

De Lange, G. J., Thomson, J., Reitz, A., Slomp, C. P., Speranza Principato, M., Erba, E. and Corselli, C.: Synchronous basin-wide formation and redox-controlled preservation of a Mediterranean sapropel, Nat. Geosci., 1(9), 606–610, doi:10.1038/ngeo283, 2008.

Lebeaupin Brossier, C., Béranger, K., Deltel, C. and Drobinski, P.: The Mediterranean response to different space–time resolution atmospheric forcings using perpetual mode sensitivity simulations, Ocean Model., 36(1–2), 1–25, doi:10.1016/j.ocemod.2010.10.008, 2011.

Lézine, A.-M. and Casanova, J.: Correlated oceanic and continental records demonstrate past climate and hydrology of North Africa (0-140 ka), Geology, 19(4), 307–310, doi:10.1130/0091-7613(1991)019<0307:COACRD>2.3.CO;2, 1991.

Li, L., Bozec, A., Somot, S., Bouruet-Aubertot, P. and Crepon, M.: Regional atmospheric, marine

processes and climate modelling, in Mediterranean climate variability and predictability, edited by P. Lionello, P. Malanotte-Rizzoli, and R. Boscolo, Elsevier., 2006.

Li, L., Casado, A., Congedi, L., Dell'Aquila, A., Dubois, C., Elizalde, A., L'Hévéder, B., Lionello, P., Sevault, F., Somot, S., Ruti, P. and Zampieri, M.: Modeling of the mediterranean climate system, in The Climate of the Mediterranean Region, pp. 419–448, Elsevier Inc., 2012.

Li, Z.-X.: Ensemble Atmospheric GCM Simulation of Climate Interannual Variability from 1979 to 1994, J. Clim., 12(4), 986–1001, doi:10.1175/1520-0442(1999)012<0986:EAGSOC>2.0.CO;2, 1999.

Locarnini, R. A., Mishonov, A. V., Antonov, J. I., Boyer, T. P., Garcia, H. E., Baranova, O. K., Zweng, M. M., Paver, C. R., Reagan, J. R., Johnson, D. R., Hamilton, M. and Seidov, D.: World Ocean Atlas 2013. Vol. 1: Temperature., S. Levitus, Ed.; A. Mishonov, Tech. Ed.; NOAA Atlas NESDIS, 73(September), 40, doi:10.1182/blood-2011-06-357442, 2013.

Ludwig, P., Shao, Y., Kehl, M. and Weniger, G.-C.: The Last Glacial Maximum and Heinrich event I on the Iberian Peninsula: A regional climate modelling study for understanding human settlement patterns, Glob. Planet. Change, 170, 34–47, doi:10.1016/j.gloplacha.2018.08.006, 2018.

Ludwig, W., Dumont, E., Meybeck, M. and Heussner, S.: River discharges of water and nutrients to the Mediterranean and Black Sea: Major drivers for ecosystem changes during past and future decades?, Prog. Oceanogr., 80(3–4), 199–217, doi:10.1016/j.pocean.2009.02.001, 2009.

Macias, D. M., Garcia-Gorriz, E. and Stips, A.: Productivity changes in the Mediterranean Sea for the twenty-first century in response to changes in the regional atmospheric forcing, Front. Mar. Sci., 2, doi:10.3389/fmars.2015.00079, 2015.

Madec, G.: NEMO ocean engine-version 3.0-Laboratoire d'Océanographie et du Climat: Expérimentation et Approches Numériques, 2008.

Magny, M., de Beaulieu, J.-L., Drescher-Schneider, R., Vannière, B., Walter-Simonnet, A.-V., Miras, Y., Millet, L., Bossuet, G., Peyron, O., Brugiapaglia, E. and Leroux, A.: Holocene climate changes in the central Mediterranean as recorded by lake-level fluctuations at Lake Accesa (Tuscany, Italy), Quat. Sci. Rev., 26(13–14), 1736–1758, doi:10.1016/j.quascirev.2007.04.014, 2007.

Magny, M., Combourieu-Nebout, N., de Beaulieu, J. L., Bout-Roumazeilles, V., Colombaroli, D., Desprat, S., Francke, A., Joannin, S., Ortu, E., Peyron, O., Revel, M., Sadori, L., Siani, G., Sicre, M. A., Samartin, S., Simonneau, A., Tinner, W., Vannière, B., Wagner, B., Zanchetta, G., Anselmetti, F.,

Brugiapaglia, E., Chapron, E., Debret, M., Desmet, M., Didier, J., Essallami, L., Galop, D., Gilli, A., Haas, J. N., Kallel, N., Millet, L., Stock, A., Turon, J. L. and Wirth, S.: North–south palaeohydrological contrasts in the central Mediterranean during the Holocene: tentative synthesis and working hypotheses, Clim. Past, 9(5), 2043–2071, doi:10.5194/cp-9-2043-2013, 2013.

Major, C., Ryan, W., Lericolais, G. and Hajdas, I.: Constraints on Black Sea outflow to the Sea of Marmara during the last glacial–interglacial transition, Mar. Geol., 190(1–2), 19–34, doi:10.1016/S0025-3227(02)00340-7, 2002.

Marzin, C. and Braconnot, P.: Variations of Indian and African monsoons induced by insolation changes at 6 and 9.5 kyr BP, Clim. Dyn., 33(2–3), 215–231, doi:10.1007/s00382-009-0538-3, 2009.

Mikolajewicz, U.: Modeling Mediterranean Ocean climate of the Last Glacial Maximum, Clim. Past, 7(1), 161–180, doi:10.5194/cp-7-161-2011, 2011.

Millot, C. and Taupier-Letage, I.: Circulation in the Mediterranean Sea, pp. 29–66., 2005.

Myers, P. G., Haines, K. and Rohling, E. J.: Modeling the paleocirculation of the Mediterranean: The Last Glacial Maximum and the Holocene with emphasis on the formation of sapropel S 1, Paleoceanography, 13(6), 586–606, doi:10.1029/98PA02736, 1998.

Peltier, W. R., Argus, D. F. and Drummond, R.: Space geodesy constrains ice age terminal deglaciation: The global ICE-6G_C (VM5a) model, J. Geophys. Res. Solid Earth, 120(1), 450–487, doi:10.1002/2014JB011176, 2015.

Petit-Maire, N., Fontugne, M. and Rouland, C.: Atmospheric methane ratio and environmental change in the Sahara an Sahel during the last 130 kyrs, Palaeogeogr. Palaeoclimatol. Palaeoecol., 86(1–2), 197–206, doi:10.1016/0031-0182(91)90009-G, 1991.

Peyron, O., Goring, S., Dormoy, I., Kotthoff, U., Pross, J., de Beaulieu, J.-L., Drescher-Schneider, R., Vannière, B. and Magny, M.: Holocene seasonality changes in the central Mediterranean region reconstructed from the pollen sequences of Lake Accesa (Italy) and Tenaghi Philippon (Greece), The Holocene, 21(1), 131–146, doi:10.1177/0959683610384162, 2011.

Pinardi, N., Cessi, P., Borile, F. and Wolfe, C. L. P.: The Mediterranean sea overturning circulation, J. Phys. Oceanogr., 49(7), 1699–1721, doi:10.1175/JPO-D-18-0254.1, 2019.

Ramstein, G., Kageyama, M., Guiot, J., Wu, H., Hély, C., Krinner, G. and Brewer, S.: How cold was Europe at the Last Glacial Maximum? A synthesis of the progress achieved since the first PMIP model-

data comparison, Clim. Past, 3(2), 331–339, doi:10.5194/cp-3-331-2007, 2007.

Revel, M., Colin, C., Bernasconi, S., Combourieu-Nebout, N., Ducassou, E., Grousset, F. E., Rolland, Y., Migeon, S., Bosch, D., Brunet, P., Zhao, Y. and Mascle, J.: 21,000 Years of Ethiopian African monsoon variability recorded in sediments of the western Nile deep-sea fan, Reg. Environ. Chang., 14(5), 1685–1696, doi:10.1007/s10113-014-0588-x, 2014.

Rossignol-Strick, M., Nesteroff, W., Olive, P. and Vergnaud-Grazzini, C.: After the deluge: Mediterranean stagnation and sapropel formation, Nature, 295(5845), 105–110, doi:10.1038/295105a0, 1982.

Sanchez-Gomez, E., Somot, S., Josey, S. A., Dubois, C., Elguindi, N. and Déqué, M.: Evaluation of Mediterranean Sea water and heat budgets simulated by an ensemble of high resolution regional climate models, Clim. Dyn., 37(9–10), 2067–2086, doi:10.1007/s00382-011-1012-6, 2011.

Sevault, F., Somot, S., Alias, A., Dubois, C., Lebeaupin-Brossier, C., Nabat, P., Adloff, F., Déqué, M. and Decharme, B.: A fully coupled Mediterranean regional climate system model: design and evaluation of the ocean component for the 1980–2012 period, Tellus A Dyn. Meteorol. Oceanogr., 66(1), 23967, doi:10.3402/tellusa.v66.23967, 2014.

Somot, S., Sevault, F. and Déqué, M.: Transient climate change scenario simulation of the Mediterranean Sea for the twenty-first century using a high-resolution ocean circulation model, Clim. Dyn., 27(7–8), 851–879, doi:10.1007/s00382-006-0167-z, 2006.

Somot, S., Sevault, F., Déqué, M. and Crépon, M.: 21st century climate change scenario for the Mediterranean using a coupled atmosphere–ocean regional climate model, Glob. Planet. Change, 63(2–3), 112–126, doi:10.1016/j.gloplacha.2007.10.003, 2008.

Soulet, G., Ménot, G., Garreta, V., Rostek, F., Zaragosi, S., Lericolais, G. and Bard, E.: Black Sea "Lake" reservoir age evolution since the Last Glacial — Hydrologic and climatic implications, Earth Planet. Sci. Lett., 308(1–2), 245–258, doi:10.1016/j.epsl.2011.06.002, 2011.

Sperling, M., Schmiedl, G., Hemleben, C., Emeis, K. ., Erlenkeuser, H. and Grootes, P. .: Black Sea impact on the formation of eastern Mediterranean sapropel S1? Evidence from the Marmara Sea, Palaeogeogr. Palaeoclimatol. Palaeoecol., 190, 9–21, doi:10.1016/S0031-0182(02)00596-5, 2003.

Stanev, E. V., Le Traon, P.-Y. and Peneva, E. L.: Sea level variations and their dependency on

meteorological and hydrological forcing: Analysis of altimeter and surface data for the Black Sea, J. Geophys. Res. Ocean., 105(C7), 17203–17216, doi:10.1029/1999JC900318, 2000.

Stickler, A., Brönnimann, S., Valente, M. A., Bethke, J., Sterin, A., Jourdain, S., Roucaute, E., Vasquez, M. V., Reyes, D. A., Allan, R. and Dee, D.: ERA-CLIM: Historical Surface and Upper-Air Data for Future Reanalyses, Bull. Am. Meteorol. Soc., 95(9), 1419–1430, doi:10.1175/BAMS-D-13-00147.1, 2014.

Swingedouw, D., Colin, C., Eynaud, F., Ayache, M. and Zaragosi, S.: Impact of freshwater release in the Mediterranean Sea on the North Atlantic climate, Clim. Dyn., 53(7–8), 3893–3915, doi:10.1007/s00382-019-04758-5, 2019.

Vadsaria, T., Li, L., Ramstein, G. and Dutay, J.-C.: Model and output for Vadsaria et al, "Development of a sequential tool LMDZ-NEMO-med-V1 for global to regional past climate simulation over the Mediterranean basin: an early Holocene case study", GMD publication, , doi:10.5281/ZENODO.3258410, 2019.

Vorosmarty, C. J., Feteke, B. M. and Tucker, B. A.: Global River Discharge, 1807-1991, V. 1.1 (RivDIS), , doi:https://doi.org/10.3334/ORNLDAAC/199, 1998.

Williams, M.: Late Quaternary environments in the White Nile region, Sudan, Glob. Planet. Change, 26(1–3), 305–316, doi:10.1016/S0921-8181(00)00047-3, 2000.

Zanchetta, G., Drysdale, R. N., Hellstrom, J. C., Fallick, A. E., Isola, I., Gagan, M. K. and Pareschi, M. T.: Enhanced rainfall in the Western Mediterranean during deposition of sapropel S1: stalagmite evidence from Corchia cave (Central Italy), Quat. Sci. Rev., 26(3–4), 279–286, doi:10.1016/j.quascirev.2006.12.003, 2007.

de Zolt, S., Lionello, P. and Malguzzi, P.: Implementation of an aorcm in the mediterranean sea, 2003.

Zweng, M. M., Reagan, J. R., Antonov, J. I., Mishonov, A. V., Boyer, T. P., Garcia, H. E., Baranova, O. K., Johnson, D. R., Seidov, D. and Bidlle, M. M.: World Ocean Atlas 2013, Volume 2: Salinity, NOAA Atlas NESDIS, 2(1), 39, doi:10.1182/blood-2011-06-357442, 2013.